Structurally Diverse Covalent Triazine-based Framework Materials for Photocatalytic Hydrogen Evolution from Water

Christian B. Meier,[‡] Rob Clowes,[‡] Enrico Berardo,[Δ] Kim E. Jelfs,[Δ] Martijn A. Zwijnenburg,*[‖] Reiner Sebastian Sprick,*[‡] and Andrew I. Cooper*[‡]

[‡]*Department of Chemistry and Materials Innovation Factory, 51 Oxford Street, Liverpool L7 3NY, U.K.*

[‖]*Department of Chemistry, University College London, 20 Gordon Street, London WC1H 0AJ, U.K.*

[Δ]*Department of Chemistry, Molecular Sciences Research Hub, Imperial College London, White City Campus, Wood Lane, London, W12 0BZ, U.K.*

1. Experimental methods

All reagents were obtained from Sigma-Aldrich, Fluorochem, TCI, Alfa Aesar or Howin Consultancy Limited (P. R. China) and used as received, except for 2,4,6-tris-[4-(4,4,5,5-tetramethyl-1,3,2-dioxaborolan-2-yl)phenyl]-1,3,5-triazine,[1] 3,7-dibromo dibenzo[*b*,*d*]thiophene-*S,S*-dioxide,[2] and CTF-2/CTF-3 Suzuki[1] which were synthesized based on literature procedures. Nicanite was purchased from Carbodeon Ltd Oy (Finland).

Analytical methods: UV-Visible absorption spectra of the polymers were recorded on a Shimadzu UV-2550 UV-Vis spectrometer as powders in the solid state. The fluorescence spectra of the polymer powders were measured with a Shimadzu RF-5301PC fluorescence spectrometer at room temperature. Transmission FT-IR spectra were recorded on a Bruker Tensor 27 at room temperature; samples were prepared as KBr pellets. Thermogravimetric analysis was performed on a TA instruments Q5000IR analyzer by heating samples at 10 °C min^{-1} in air in open aluminium pans from room temperature to 600 °C and holding at 600 °C for 30 minutes. CHN Analysis was performed on a Thermo EA1112 Flash CHNS-O Analyzer using standard microanalytical procedures. The porosity to nitrogen was tested on Micromeritics 2420 instruments at a temperature of 77 K. Light obscuration were tested by average transmission on a Turbiscan AGS with a NIR light source (λ = 880 nm). Palladium content was determined by ICP-OES by Exeter Analytical Service (Coventry, United Kingdom). Water contact angles were measured using pressed pellets and a drop-shape analysis apparatus (Krüss DSA100). The contact angles were analyzed by the Young-Laplace fitting method. TCSPC experiments were performed on an Edinburgh Instruments LS980-D2S2-STM spectrometer equipped with picosecond pulsed LED excitation sources and a R928 detector, with a stop count rate below 3%. Pulsed diode lasers were used to excite the polymers in the solid state with optical pulses between 50-200 ps FWHM (EPL-375 diode - λ = 370.5 nm, EPL-445 - λ = 441.2 nm, EPL-475 - λ = 472.8 nm) The instrument response function was measured with colloidal silica (LUDOX® HS-40, Sigma-Aldrich) at the excitation wavelength without filter. Decay times were fitted in the FAST software using three decay exponents.

2. Polymer synthesis

CTF-5: 2,4,6-Tris[4-(4,4,5,5-tetramethyl-1,3,2-dioxaborolan-2-yl)phenyl]-1,3,5-triazine (500 mg, 728 µmol), 1,3-dibromobenzene (257 mg, 1.09 mmol), *N,N*-dimethylformamide (10.9 mL), aqueous K_2CO_3 (2.0 M, 2.18 mL) and $[Pd(PPh_3)_4]$ (10.1 mg, 1.2 mol %) were used in the polymerization. After work-up, the product was obtained as a grey powder in 92% yield (283 mg). CHN analysis calc. for $(C_{20}H_{12}N_2)_n$: C, 85.69; H, 4.31; N, 9.99%, found: C, 78.75; H, 4.24; N 8.22%.

CTF-6: 2,4,6-Tris[4-(4,4,5,5-tetramethyl-1,3,2-dioxaborolan-2-yl)phenyl]-1,3,5-triazine (500 mg, 728 µmol), 2,4-dibromo-1,1'-biphenyl (340 mg, 1.09 mmol), *N,N*-dimethylformamide (10.9 mL), aqueous K_2CO_3 (2.0 M, 2.18 mL) and [$Pd(PPh_3)_4$] (10.1 mg, 1.2 mol %) were used in the polymerisation. After work-up, the product was obtained as a brown solid in 96% yield (376 mg). CHN analysis calc. for $(C_{26}H_{16}N_2)_n$: C, 87.62; H, 4.52; N, 7.86%, found: C, 78.37; H, 4.30; N 6.59%.

CTF-7: 2,4,6-Tris[4-(4,4,5,5-tetramethyl-1,3,2-dioxaborolan-2-yl)phenyl]-1,3,5-triazine (500 mg, 728 µmol), 3,5-dibromo-1,1'-biphenyl (340 mg, 1.09 mmol), *N,N*-dimethylformamide (10.9 mL), aqueous K_2CO_3 (2.0 M, 2.18 mL) and [$Pd(PPh_3)_4$] (10.1 mg, 1.2 mol %) were used in the polymerisation. After work-up, the product was obtained as a grey powder in 97% yield (381 mg). CHN analysis calc. for $(C_{26}H_{16}N_2)_n$: C, 87.62; H, 4.52; N, 7.86%, found: C, 74.53; H, 4.23; N 6.11%.

CTF-8: 2,4,6-Tris[4-(4,4,5,5-tetramethyl-1,3,2-dioxaborolan-2-yl)phenyl]-1,3,5-triazine (500 mg, 728 µmol), 2,7-dibromotriphenylene (421 mg, 1.09 mmol), *N,N*-dimethylformamide (10.9 mL), aqueous K_2CO_3 (2.0 M, 2.18 mL) and [$Pd(PPh_3)_4$] (10.1 mg, 1.2 mol %) were used in the polymerisation. After work-up, the product was obtained as a pale green powder in 99% yield (468 mg). CHN analysis calc. for $(C_{32}H_{18}N_2)_n$: C, 89.28; H, 4.21; N, 6.51%, found: C, 64.52; H, 3.40; N 4.43%.

CTF-9: 2,4,6-Tris[4-(4,4,5,5-tetramethyl-1,3,2-dioxaborolan-2-yl)phenyl]-1,3,5-triazine (500 mg, 728 µmol), 9,10-dibromoanthracene (367 mg, 1.09 mmol), *N,N*-dimethylformamide (10.9 mL), aqueous K_2CO_3 (2.0 M, 2.18 mL) and [$Pd(PPh_3)_4$] (10.1 mg, 1.2 mol %) were used in the polymerisation. After work-up, the product was obtained as a bright yellow powder in 85% yield (356 mg). CHN analysis calc. for $(C_{28}H_{16}N_2)_n$: C, 88.40; H, 4.24; N, 7.36%, found: C, 82.15; H, 4.16; N 6.74%.

CTF-10: 2,4,6-Tris[4-(4,4,5,5-tetramethyl-1,3,2-dioxaborolan-2-yl)phenyl]-1,3,5-triazine (500 mg, 728 µmol), 2,5-dibromofuran (246 mg, 1.09 mmol), *N,N*-dimethylformamide (10.9 mL), aqueous K_2CO_3 (2.0 M, 2.18 mL) and [$Pd(PPh_3)_4$] (10.1 mg, 1.2 mol %) were used in the polymerisation. After work-up, the product was obtained as a bright yellow powder in 79% yield (234 mg). CHN analysis calc. for $(C_{18}H_{10}N_2O)_n$: C, 79.99; H, 3.73; N, 10.36%, found: C, 75.75; H, 3.79; N 9.48%.

CTF-11: 2,4,6-Tris[4-(4,4,5,5-tetramethyl-1,3,2-dioxaborolan-2-yl)phenyl]-1,3,5-triazine (500 mg, 728 µmol), 2,5-dibromothiophene (264 mg, 1.09 mmol), *N,N*-dimethylformamide (10.9 mL), aqueous K_2CO_3 (2.0 M, 2.18 mL) and [$Pd(PPh_3)_4$] (10.1 mg, 1.2 mol %) were used in the polymerisation. After work-up, the product was obtained as an orange powder in 95% yield (297 mg). CHN analysis calc. for $(C_{18}H_{10}N_2S)_n$: C, 75.50; H, 3.52; N, 9.87%, found: C, 68.07; H, 3.69; N 8.10%.

CTF-12: 2,4,6-Tris[4-(4,4,5,5-tetramethyl-1,3,2-dioxaborolan-2-yl)phenyl]-1,3,5-triazine (500 mg, 728 µmol), 2,5-dibromoselenophene (315 mg, 1.09 mmol), *N,N*-dimethylformamide (10.9 mL),

aqueous K_2CO_3 (2.0 M, 2.18 mL) and [$Pd(PPh_3)_4$] (10.1 mg, 1.2 mol %) were used in the polymerisation. After work-up, the product was obtained as a yellow powder in 75% yield (276 mg). CHN analysis calc. for $(C_{18}H_{10}N_2Se)_n$: C, 64.88; H, 3.02; N, 8.41%, found: C, 62.72; H, 3.17; N 8.48%.

CTF-13: 2,4,6-Tris[4-(4,4,5,5-tetramethyl-1,3,2-dioxaborolan-2-yl)phenyl]-1,3,5-triazine (500 mg, 728 µmol), 2,5-dibromothiazole (265 mg, 1.09 mmol), *N,N*-dimethylformamide (10.9 mL), aqueous K_2CO_3 (2.0 M, 2.18 mL) and [$Pd(PPh_3)_4$] (10.1 mg, 1.2 mol %) were used in the polymerisation. After work-up, the product was obtained as a grey powder in 37% yield (118 mg). CHN analysis calc. for $(C_{17}H_9N_3S)_n$: C, 71.06; H, 3.16; N, 14.62%, found: C, 73.18; H, 4.20; N 12.10%.

CTF-14: 2,4,6-Tris[4-(4,4,5,5-tetramethyl-1,3,2-dioxaborolan-2-yl)phenyl]-1,3,5-triazine (500 mg, 728 µmol), 2,5-dibromothiophene dioxide (299 mg, 1.09 mmol), *N,N*-dimethylformamide (10.9 mL), aqueous K_2CO_3 (2.0 M, 2.18 mL) and [$Pd(PPh_3)_4$] (10.1 mg, 1.2 mol %) were used in the polymerisation. After work-up, the product was obtained as a brown powder in 51% yield (177 mg). CHN analysis calc. for $(C_{18}H_{10}N_2S)_n$: C, 75.50; H, 3.52; N, 9.78%, found: C, 67.91; H, 3.87; N 6.4%.

CTF-15: 2,4,6-Tris[4-(4,4,5,5-tetramethyl-1,3,2-dioxaborolan-2-yl)phenyl]-1,3,5-triazine (500 mg, 728 µmol), 2,5-dibromobenzonitrile (285 mg, 1.09 mmol), *N,N*-dimethylformamide (10.9 mL), aqueous K_2CO_3 (2.0 M, 2.18 mL) and [$Pd(PPh_3)_4$] (10.1 mg, 1.2 mol %) were used in the polymerisation. After work-up, the product was obtained as a pale brown powder in 82% yield (309 mg). CHN analysis calc. for $(C_{21}H_{11}N_3)_n$: C, 82.61; H, 3.63; N, 13.76%, found: C, 75.36; H, 3.58; N 12.23%.

CTF-16: 2,4,6-Tris[4-(4,4,5,5-tetramethyl-1,3,2-dioxaborolan-2-yl)phenyl]-1,3,5-triazine (500 mg, 728 µmol), 2,5-dibromo-1,4-benzenedicarbonitrile (312 mg, 1.09 mmol), *N,N*-dimethylformamide (10.9 mL), aqueous K_2CO_3 (2.0 M, 2.18 mL) and [$Pd(PPh_3)_4$] (10.1 mg, 1.2 mol %) were used in the polymerisation. After work-up, the product was obtained as a dark yellow powder in 98% yield (355 mg). CHN analysis calc. for $(C_{22}H_{10}N_4)_n$: C, 79.99; H, 3.05; N, 16.96%, found: C, 70.42; H, 3.79; N 14.14%.

CTF-17: 2,4,6-Tris[4-(4,4,5,5-tetramethyl-1,3,2-dioxaborolan-2-yl)phenyl]-1,3,5-triazine (500 mg, 728 µmol), 2,5-dibromoaniline (274 mg, 1.09 mmol), *N,N*-dimethylformamide (10.9 mL), aqueous K_2CO_3 (2.0 M, 2.18 mL) and [$Pd(PPh_3)_4$] (10.1 mg, 1.2 mol %) were used in the polymerisation. After work-up, the product was obtained as a yellow powder in 94% yield (305 mg). CHN analysis calc. for $(C_{20}H_{13}N_3)_n$: C, 81.34; H, 4.44; N, 14.23%, found: C, 72.90; H, 4.24; N 11.51%.

CTF-18: 2,4,6-Tris[4-(4,4,5,5-tetramethyl-1,3,2-dioxaborolan-2-yl)phenyl]-1,3,5-triazine (500 mg, 728 µmol), 1,4-dibromo-2-nitrobenzene (307 mg, 1.09 mmol), *N,N*-dimethylformamide (10.9 mL), aqueous K_2CO_3 (2.0 M, 2.18 mL) and [$Pd(PPh_3)_4$] (10.1 mg, 1.2 mol %) were used in the polymerisation.

After work-up, the product was obtained as a grey powder in 76% yield (270 mg). CHN analysis calc. for $(C_{20}H_{15}N_3O_2)_n$: C, 73.84; H, 3.41; N, 12.92%, found: C, 42.49; H, 2.65; N 6.20%.

CTF-19: 2,4,6-Tris[4-(4,4,5,5-tetramethyl-1,3,2-dioxaborolan-2-yl)phenyl]-1,3,5-triazine (1.00 g, 1.46 mmol), 1,4-dibromotetrafluorobenzene (672 mg, 2.18 mmol), *N,N*-dimethylformamide (21.8 mL), aqueous K_2CO_3 (2.0 M, 4.36 mL) and $[Pd(PPh_3)_4]$ (20.2 mg, 1.2 mol %) were used in the polymerisation. After work-up, the product was obtained as a grey powder in 67% yield (521 mg). CHN analysis calc. for $(C_{20}H_8F_4N_2)_n$: C, 68.19; H, 2.29; N, 7.95%, found: C, 45.79; H, 2.13; N 5.19%.

CTF-20: 2,4,6-Tris[4-(4,4,5,5-tetramethyl-1,3,2-dioxaborolan-2-yl)phenyl]-1,3,5-triazine (500 mg, 728 µmol), 1,4-dibromo-2,5-difluorobenzene (297 mg, 1.09 mmol), *N,N*-dimethylformamide (10.9 mL), aqueous K_2CO_3 (2.0 M, 2.18 mL) and $[Pd(PPh_3)_4]$ (10.1 mg, 1.2 mol %) were used in the polymerisation. After work-up, the product was obtained as a grey powder in 94% yield (325 mg). CHN analysis calc. for $(C_{20}H_{10}F_2N_2)_n$: C, 75.94; H, 3.19; N, 12.01%, found: C, 66.32; H, 3.22; N 6.99%.

CTF-21: 2,4,6-Tris[4-(4,4,5,5-tetramethyl-1,3,2-dioxaborolan-2-yl)phenyl]-1,3,5-triazine (1.00 g, 1.46 mmol), 1,4-dibromo-2,3-difluorobenzene (593 mg, 2.18 mmol), *N,N*-dimethylformamide (21.8 mL), aqueous K_2CO_3 (2.0 M, 4.36 mL) and $[Pd(PPh_3)_4]$ (20.2 mg, 1.2 mol %) were used in the polymerisation. After work-up, the product was obtained as a grey powder in 70% yield (353 mg). CHN analysis calc. for $(C_{20}H_{10}F_2N_2)_n$: C, 75.94; H, 3.19; N, 8.86%, found: C, 65.09; H, 2.96; N 6.78%.

CTF-22: 2,4,6-Tris[4-(4,4,5,5-tetramethyl-1,3,2-dioxaborolan-2-yl)phenyl]-1,3,5-triazine (500 mg, 728 µmol), 1,4-dibromo-2-fluorobenzene (277 mg, 1.09 mmol), *N,N*-dimethylformamide (10.9 mL), aqueous K_2CO_3 (2.0 M, 2.18 mL) and $[Pd(PPh_3)_4]$ (10.1 mg, 1.2 mol %) were used in the polymerisation. After work-up, the product was obtained as a grey powder in 86% yield (283 mg). CHN analysis calc. for $(C_{20}H_{11}FN_2)_n$: C, 80.52; H, 3.72; N, 9.39%, found: C, 72.95; H, 3.63; N 7.96%.

CTF-23: 2,4,6-Tris[4-(4,4,5,5-tetramethyl-1,3,2-dioxaborolan-2-yl)phenyl]-1,3,5-triazine (1.00 g, 1.46 mmol), 2,5-dibromo-1,4-benzoquinone (580 mg, 2.18 mmol), *N,N*-dimethylformamide (21.8 mL), aqueous K_2CO_3 (2.0 M, 4.36 mL) and $[Pd(PPh_3)_4]$ (20.2 mg, 1.2 mol %) were used in the polymerisation. After work-up, the product was obtained as a black powder in 21% yield (146 mg). CHN analysis calc. for $(C_{20}H_{10}N_2O_2)_n$: C, 77.41; H, 3.25; N, 9.03%, found: C, 55.07; H, 3.04; N 5.33%.

CTF-24: 2,4,6-Tris[4-(4,4,5,5-tetramethyl-1,3,2-dioxaborolan-2-yl)phenyl]-1,3,5-triazine (1.00 g, 1.46 mmol), 2,5-dibromobenzene-1,4-diol (307 mg, 2.18 mmol), *N,N*-dimethylformamide (21.8 mL), aqueous K_2CO_3 (2.0 M, 4.36 mL) and $[Pd(PPh_3)_4]$ (20.2 mg, 1.2 mol %) were used in the polymerisation. After work-up, the product was obtained as a black powder in 11% yield (77 mg). CHN analysis calc. for $(C_{20}H_{12}N_2O_2)_n$: C, 76.91; H, 3.87; N, 8.97%, found: C, 46.78; H, 2.86; N 4.82%.

CTF-25: 2,4,6-Tris[4-(4,4,5,5-tetramethyl-1,3,2-dioxaborolan-2-yl)phenyl]-1,3,5-triazine (500 mg, 728 µmol), 1,4-dibromo-2,5-dimethoxybenzene (323 mg, 1.09 mmol), *N,N*-dimethylformamide (10.9 mL), aqueous K_2CO_3 (2.0 M, 2.18 mL) and [$Pd(PPh_3)_4$] (10.1 mg, 1.2 mol %) were used in the polymerisation. After work-up, the product was obtained as a pale yellow powder in 98% yield (364 mg). CHN analysis calc. for $(C_{22}H_{16}N_2O_2)_n$: C, 77.63; H, 4.74; N, 8.23%, found: C, 73.95; H, 4.74; N 7.92%.

CTF-26: 2,4,6-Tris[4-(4,4,5,5-tetramethyl-1,3,2-dioxaborolan-2-yl)phenyl]-1,3,5-triazine (500 mg, 728 µmol), 6,6'-dibromo-2,2'-bipyridine (343 mg, 1.09 mmol), *N,N*-dimethylformamide (10.9 mL), aqueous K_2CO_3 (2.0 M, 2.18 mL) and [$Pd(PPh_3)_4$] (10.1 mg, 1.2 mol %) were used in the polymerisation. After work-up, the product was obtained as a white powder in 99% yield (389 mg). CHN analysis calc. for $(C_{24}H_{14}N_4)_n$: C, 80.43; H, 3.94; N, 15.63%, found: C, 75.02; H, 3.83; N 14.42%.

CTF-27: 2,4,6-Tris[4-(4,4,5,5-tetramethyl-1,3,2-dioxaborolan-2-yl)phenyl]-1,3,5-triazine (500 mg, 728 µmol), 5,5'-dibromo-2,2'-bipyridine (343 mg, 1.09 mmol), *N,N*-dimethylformamide (10.9 mL), aqueous K_2CO_3 (2.0 M, 2.18 mL) and [$Pd(PPh_3)_4$] (10.1 mg, 1.2 mol %) were used in the polymerisation. After work-up, the product was obtained as a pale yellow powder in 90% yield (352 mg). CHN analysis calc. for $(C_{24}H_{14}N_4)_n$: C, 80.43; H, 3.94; N, 15.63%, found: C, 69.48; H, 3.68; N 12.75%.

CTF-28: 2,4,6-Tris[4-(4,4,5,5-tetramethyl-1,3,2-dioxaborolan-2-yl)phenyl]-1,3,5-triazine (500 mg, 728 µmol), 4,4'-dibromo-2,2'-bipyridine (343 mg, 1.09 mmol), *N,N*-dimethylformamide (10.9 mL), aqueous K_2CO_3 (2.0 M, 2.18 mL) and [$Pd(PPh_3)_4$] (10.1 mg, 1.2 mol %) were used in the polymerisation. After work-up, the product was obtained as a grey powder in 70% yield (276 mg). CHN analysis calc. for $(C_{24}H_{14}N_4)_n$: C, 80.43; H, 3.94; N, 15.63%, found: C, 70.24; H, 4.17; N 12.68%.

CTF-29: 2,4,6-Tris[4-(4,4,5,5-tetramethyl-1,3,2-dioxaborolan-2-yl)phenyl]-1,3,5-triazine (500 mg, 728 µmol), 3,8-dibromo-1,10-phenanthroline (369 mg, 1.09 mmol), *N,N*-dimethylformamide (10.9 mL), aqueous K_2CO_3 (2.0 M, 2.18 mL) and [$Pd(PPh_3)_4$] (10.1 mg, 1.2 mol %) were used in the polymerisation. After work-up, the product was obtained as a brown powder in 53% yield (225 mg). CHN analysis calc. for $(C_{26}H_{14}N_4)_n$: C, 81.66; H, 3.69; N, 14.65%, found: C, 73.83; H, 3.98; N 12.93%.

CTF-30: 2,4,6-Tris[4-(4,4,5,5-tetramethyl-1,3,2-dioxaborolan-2-yl)phenyl]-1,3,5-triazine (500 mg, 728 µmol), 2,5-dibromopyrazine (260 mg, 1.09 mmol), *N,N*-dimethylformamide (10.9 mL), aqueous K_2CO_3 (2.0 M, 2.18 mL) and [$Pd(PPh_3)_4$] (10.1 mg, 1.2 mol %) were used in the polymerisation. After work-up, the product was obtained as a grey powder in 61% yield (188 mg). CHN analysis calc. for $(C_{18}H_{10}N_4)_n$: C, 76.58; H, 3.57; N 19.85%, found: C, 65.12; H, 3.61; N 15.31%.

CTF-31: 2,4,6-Tris[4-(4,4,5,5-tetramethyl-1,3,2-dioxaborolan-2-yl)phenyl]-1,3,5-triazine (500 mg, 728 µmol), 2,5-dibromopyrimidine (260 mg, 1.09 mmol), *N,N*-dimethylformamide (10.9 mL), aqueous K_2CO_3 (2.0 M, 2.18 mL) and $[Pd(PPh_3)_4]$ (10.1 mg, 1.2 mol %) were used in the polymerisation. After work-up, the product was obtained as a pale brown powder in 80% yield (248 mg). CHN analysis calc. for $(C_{18}H_{10}N_4)_n$: C, 76.58; H, 3.57; N 19.85%, found: C, 66.33; H, 3.51; N 17.09%.

CTF-32 2,4,6-Tris[4-(4,4,5,5-tetramethyl-1,3,2-dioxaborolan-2-yl)phenyl]-1,3,5-triazine (500 mg, 728 µmol), 2,5-dibromopyridine (259 mg, 1.09 mmol), *N,N*-dimethylformamide (10.9 mL), aqueous K_2CO_3 (2.0 M, 2.18 mL) and $[Pd(PPh_3)_4]$ (10.1 mg, 1.2 mol %) were used in the polymerisation. After work-up, the product was obtained as a yellow powder in 99% yield (305 mg). CHN analysis calc. for $(C_{19}H_{11}N_3)_n$: C, 81.12; H, 3.94; N, 14.94%, found: C, 70.97; H, 3.74; N 12.63%.

CTF-33: 2,4,6-Tris[4-(4,4,5,5-tetramethyl-1,3,2-dioxaborolan-2-yl)phenyl]-1,3,5-triazine (500 mg, 728 µmol), 2,6-dibromopyridine (259 mg, 1.09 mmol), *N,N*-dimethylformamide (10.9 mL), aqueous K_2CO_3 (2.0 M, 2.18 mL) and $[Pd(PPh_3)_4]$ (10.1 mg, 1.2 mol %) were used in the polymerisation. After work-up, the product was obtained as a pale 305yellow powder in 99% yield (304 mg). CHN analysis calc. for $(C_{19}H_{11}N_3)_n$: C, 81.12; H, 3.94; N, 14.94%, found: C, 63.19; H, 3.51; N 10.21%.

CTF-34: 2,4,6-Tris[4-(4,4,5,5-tetramethyl-1,3,2-dioxaborolan-2-yl)phenyl]-1,3,5-triazine (500 mg, 728 µmol), 3,7-dibromo dibenzo[*b*,*d*]thiophene-*S,S*-dioxide (408 mg, 1.09 mmol), *N,N*-dimethylformamide (10.9 mL), aqueous K_2CO_3 (2.0 M, 2.18 mL) and $[Pd(PPh_3)_4]$ (10.1 mg, 1.2 mol %) were used in the polymerisation. After work-up, the product was obtained as a pale yellow powder in 98% yield (452 mg). CHN analysis calc. for $(C_{26}H_{14}N_2O_2S)_n$: C, 74.63; H, 3.37; N, 6.69%, found: C, 66.00; H, 3.49; N 5.55%.

CTF-35: 2,4,6-Tris[4-(4,4,5,5-tetramethyl-1,3,2-dioxaborolan-2-yl)phenyl]-1,3,5-triazine (500 mg, 728 µmol), 3,7-dibromo dibenzo[*b*,*d*]thiophene (373 mg, 1.09 mmol), *N,N*-dimethylformamide (10.9 mL), aqueous K_2CO_3 (2.0 M, 2.18 mL) and $[Pd(PPh_3)_4]$ (10.1 mg, 1.2 mol %) were used in the polymerisation. After work-up, the product was obtained as a pale yellow powder in 99% yield (420 mg). CHN analysis calc. for $(C_{26}H_{14}N_2S)_n$: C, 80.80; H, 3.65; N, 7.25%, found: C, 73.42; H, 3.64; N 6.29%.

CTF-36: 2,4,6-Tris[4-(4,4,5,5-tetramethyl-1,3,2-dioxaborolan-2-yl)phenyl]-1,3,5-triazine (500 mg, 728 µmol), 2,7-dibromo-9*H*-fluorene (354 mg, 1.09 mmol), *N,N*-dimethylformamide (10.9 mL), aqueous K_2CO_3 (2.0 M, 2.18 mL) and $[Pd(PPh_3)_4]$ (10.1 mg, 1.2 mol %) were used in the polymerisation. After work-up, the product was obtained as an orange powder in 99% yield (399 mg). CHN analysis calc. for $(C_{27}H_{16}N_2)_n$: C, 80.43; H, 3.94; N, 15.63%, found: C, 74.23; H, 3.75; N 6.13%.

CTF-37: 2,4,6-Tris[4-(4,4,5,5-tetramethyl-1,3,2-dioxaborolan-2-yl)phenyl]-1,3,5-triazine (500 mg, 728 µmol), 2,7-dibromo-9*H*-carbazole (354 mg, 1.09 mmol), *N,N*-dimethylformamide (10.9 mL), aqueous K_2CO_3 (2.0 M, 2.18 mL) and [$Pd(PPh_3)_4$] (10.1 mg, 1.2 mol %) were used in the polymerisation. After work-up, the product was obtained as a yellow powder in 99% yield (402 mg). CHN analysis calc. for $(C_{26}H_{15}N_3)_n$: C, 84.53; H, 4.09; N, 11.37%, found: C, 73.80; H, 4.01; N 9.32%.

CTF-38: 2,4,6-Tris[4-(4,4,5,5-tetramethyl-1,3,2-dioxaborolan-2-yl)phenyl]-1,3,5-triazine (500 mg, 728 µmol), 2,7-dibromo-9-fluorenone (369 mg, 1.09 mmol), *N,N*-dimethylformamide (10.9 mL), aqueous K_2CO_3 (2.0 M, 2.18 mL) and [$Pd(PPh_3)_4$] (10.1 mg, 1.2 mol %) were used in the polymerisation. After work-up, the product was obtained as a grey powder in 95% yield (400 mg). CHN analysis calc. for $(C_{27}H_{14}N_2O)_n$: C, 84.80; H, 3.69; N, 7.33%, found: C, 73.97; H, 3.66; N 5.61%.

CTF-39: 2,4,6-Tris[4-(4,4,5,5-tetramethyl-1,3,2-dioxaborolan-2-yl)phenyl]-1,3,5-triazine (500 mg, 728 µmol), 4,7-dibromo-2,1,3-benzo[*c*]thiadiazole (321 mg, 1.09 mmol), *N,N*-dimethylformamide (10.9 mL), aqueous K_2CO_3 (2.0 M, 2.18 mL) and [$Pd(PPh_3)_4$] (10.1 mg, 1.2 mol %) were used in the polymerisation. After work-up, the product was obtained as a bright orange powder in 90% yield (333 mg). CHN analysis calc. for $(C_{20}H_{10}N_4S)_n$: C, 70.99; H, 2.98; N, 16.56%, found: C, 65.81; H, 3.17; N 14.58%.

CTF-40: 2,4,6-Tris[4-(4,4,5,5-tetramethyl-1,3,2-dioxaborolan-2-yl)phenyl]-1,3,5-triazine (500 mg, 728 µmol), 4,7-dibromobenzo[*c*][1,2,5]oxadiazole (303 mg, 1.09 mmol), *N,N*-dimethylformamide (10.9 mL), aqueous K_2CO_3 (2.0 M, 2.18 mL) and [$Pd(PPh_3)_4$] (10.1 mg, 1.2 mol %) were used in the polymerisation. After work-up, the product was obtained as a brown powder in 90% yield (318 mg). CHN analysis calc. for $(C_{20}H_{10}N_4O)_n$: C, 74.53; H, 3.13; N, 17.38%, found: C, 68.02; H, 3.64; N 15.13%.

CTF-41: 2,4,6-Tris[4-(4,4,5,5-tetramethyl-1,3,2-dioxaborolan-2-yl)phenyl]-1,3,5-triazine (500 mg, 728 µmol), 4,7-dibromo-2,1,3-benzo[*c*]selenadiazole (372 mg, 1.09 mmol), *N,N*-dimethylformamide (10.9 mL), aqueous K_2CO_3 (2.0 M, 2.18 mL) and [$Pd(PPh_3)_4$] (10.1 mg, 1.2 mol %) were used in the polymerisation. After work-up, the product was obtained as an orange powder in 99% yield (418 mg). CHN analysis calc. for $(C_{20}H_{10}N_4Se)_n$: C, 62.35; H, 2.62; N, 14.54%, found: C, 55.40; H, 2.90; N 12.27%.

CTF-42: 2,4,6-Tris[4-(4,4,5,5-tetramethyl-1,3,2-dioxaborolan-2-yl)phenyl]-1,3,5-triazine (500 mg, 728 µmol), 4,7-dibromo-5,6-difluorobenzo[*c*][1,2,5]thiadiazole (360 mg, 1.09 mmol), *N,N*-dimethylformamide (10.9 mL), aqueous K_2CO_3 (2.0 M, 2.18 mL) and [$Pd(PPh_3)_4$] (10.1 mg, 1.2 mol %) were used in the polymerisation. After work-up, the product was obtained as a brown powder in 70% yield (364 mg). CHN analysis calc. for $(C_{20}H_8F_2N_2S)_n$: C, 64.17; H, 2.15; N, 14.97%, found: C, 49.90; H, 2.70; N 10.77%.

CTF-43: 2,4,6-Tris[4-(4,4,5,5-tetramethyl-1,3,2-dioxaborolan-2-yl)phenyl]-1,3,5-triazine (500 mg, 728 µmol), 4,7-dibromo-5-fluoro-2,1,3-benzo[*c*]thiadiazole (340 mg, 1.09 mmol), *N,N*-dimethylformamide (10.9 mL), aqueous K_2CO_3 (2.0 M, 2.18 mL) and $[Pd(PPh_3)_4]$ (10.1 mg, 1.2 mol %) were used in the polymerisation. After work-up, the product was obtained as a grey powder in 87% yield (340 mg). CHN analysis calc. for $(C_{20}H_9FN_4S)_n$: C, 67.41; H, 2.55; N, 15.72%, found: C, 61.61; H, 2.83; N 13.33%.

CTF-44: 2,4,6-Tris[4-(4,4,5,5-tetramethyl-1,3,2-dioxaborolan-2-yl)phenyl]-1,3,5-triazine (500 mg, 728 µmol), 5,8-dibromoquinoxaline (314 mg, 1.09 mmol), *N,N*-dimethylformamide (10.9 mL), aqueous K_2CO_3 (2.0 M, 2.18 mL) and $[Pd(PPh_3)_4]$ (10.1 mg, 1.2 mol %) were used in the polymerisation. After work-up, the product was obtained as a grey powder in 99% yield (360 mg). CHN analysis calc. for $(C_{22}H_{12}N_4)_n$: C, 79.50; H, 3.64; N, 16.86%, found: C, 68.12; H, 3.60; N 13.84%.

3. Analysis of polymers

FT-IR spectra showed strong vibrational bands around 1510 and 1360 cm^{-1} that can be assigned to aromatic C=C bending modes. CTF-15 and CTF-16 show aryl nitrile bands at 2226 cm^{-1} and 2228 cm^{-1}, respectively, and CTF-23 has a broad peak at ~3430 cm^{-1} arising from the phenol linker. CTF-38 shows a strong vibration at 1710 cm^{-1} that could be assigned to the carbonyl bridge head.

TGA Most polymers were even stable up to 450 °C, with three exceptions: CTF-23 and CTF-24 degraded rapidly under combustion in air, leading to a weight loss of 40% and 37% at 300 °C, which might indicate a low degree of polymerization. Polymer CTF-25 showed a weight loss of 29% between 381-394 °C, which could be due to the thermal cleavage of the methyl or methoxy-group.

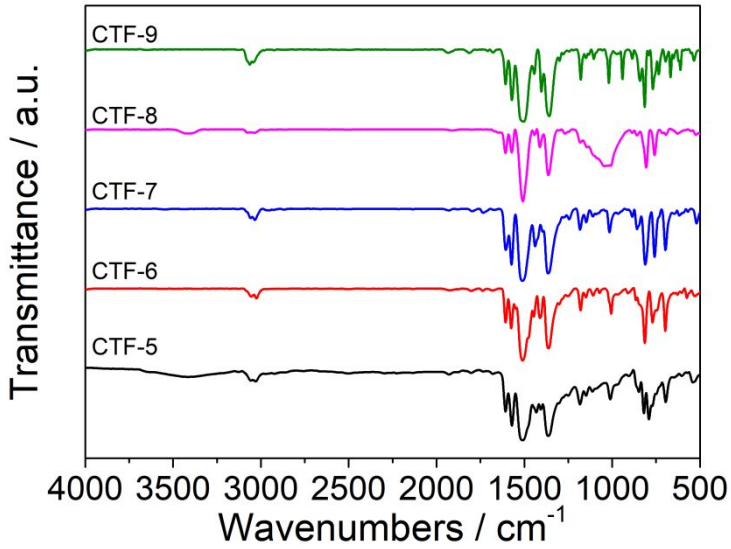

Figure S-1: FT-IR spectra for polymers CTF-5 to CTF-9 (KBr-pellets).

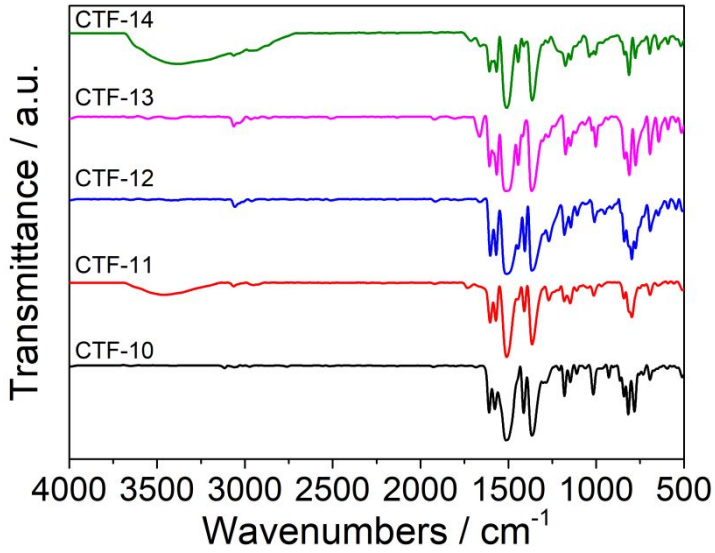

Figure S-2: FT-IR spectra for polymers CTF-10 to CTF-14 (KBr-pellets).

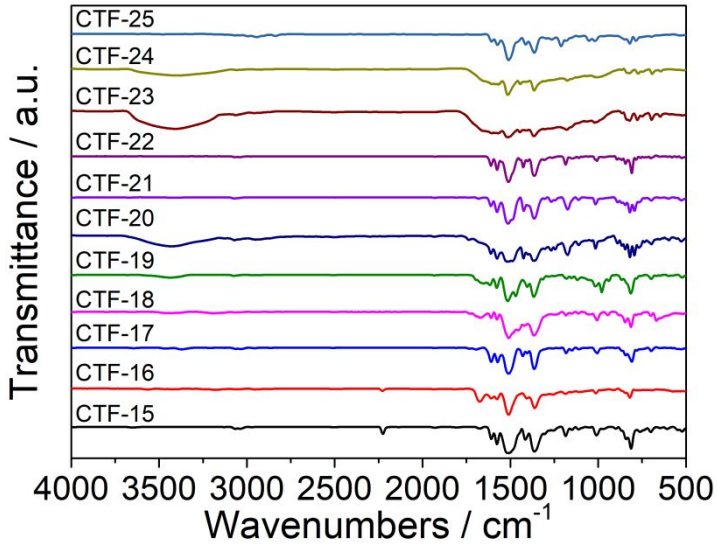

Figure S-3: FT-IR spectra for polymers CTF-15 to CTF-25 (KBr-pellets).

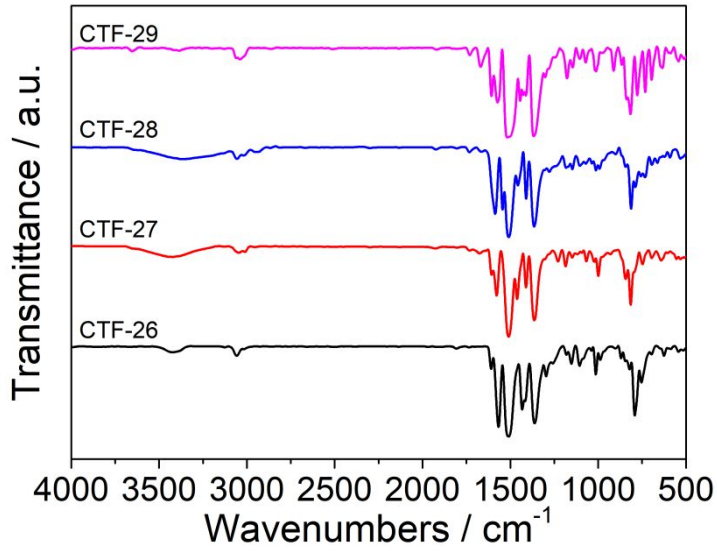

Figure S-4: FT-IR spectra for polymers CTF-26 to CTF-29 (KBr-pellets).

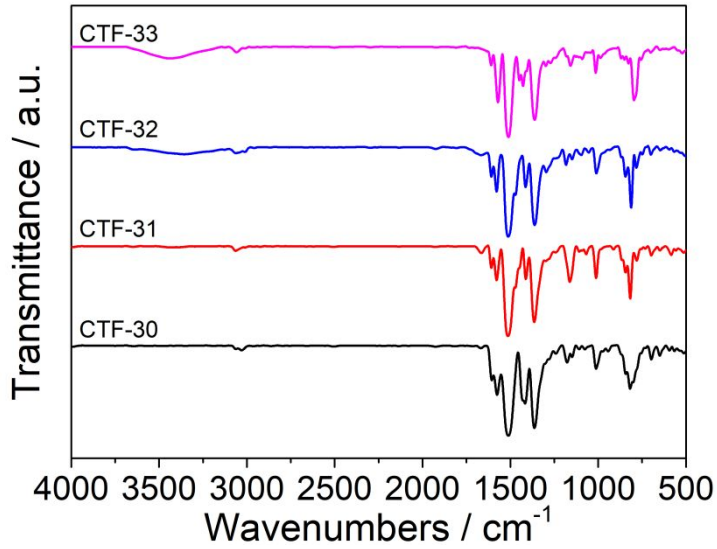

Figure S-5: FT-IR spectra for polymers CTF-30 to CTF-33 (KBr-pellets).

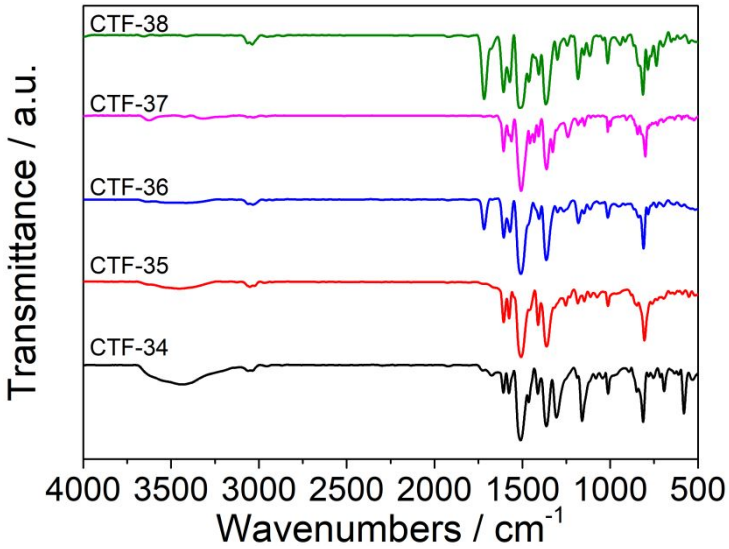

Figure S-6: FT-IR spectra for polymers CTF-34 to CTF-38 (KBr-pellets).

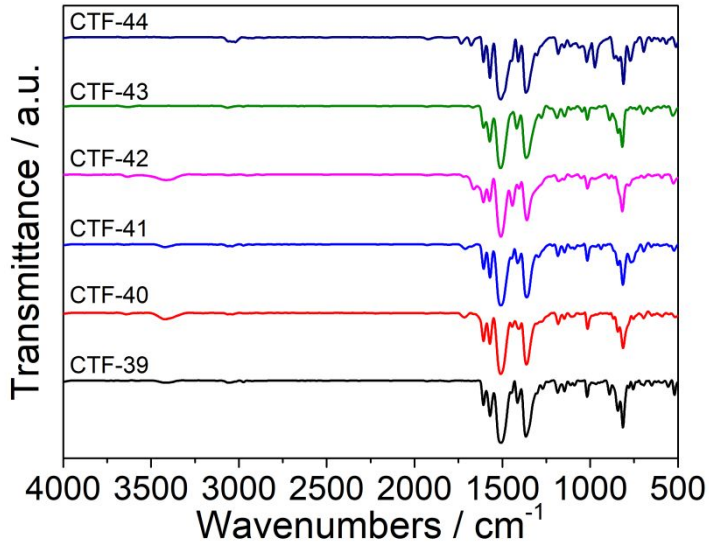

Figure S-7: FT-IR spectra for polymers CTF-39 to CTF-44 (KBr-pellets).

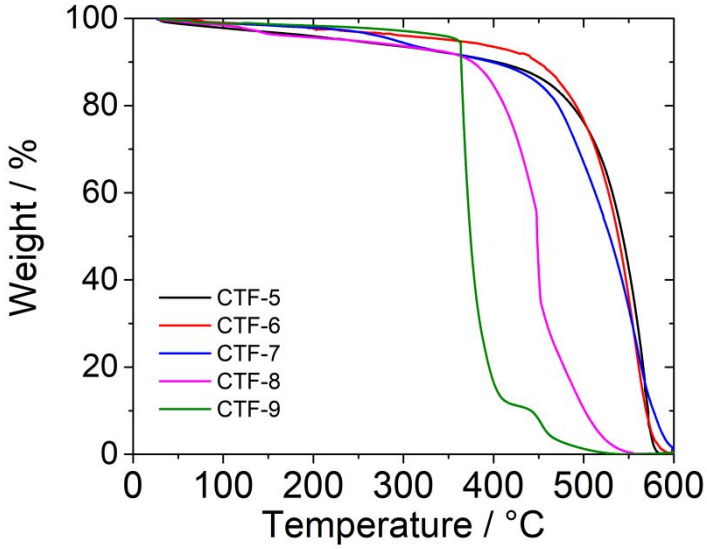

Figure S-8: Thermogravimetric analysis curves for the polymers CTF-5 to CTF-9 in air with a heating rate of 10 °C min^{-1}.

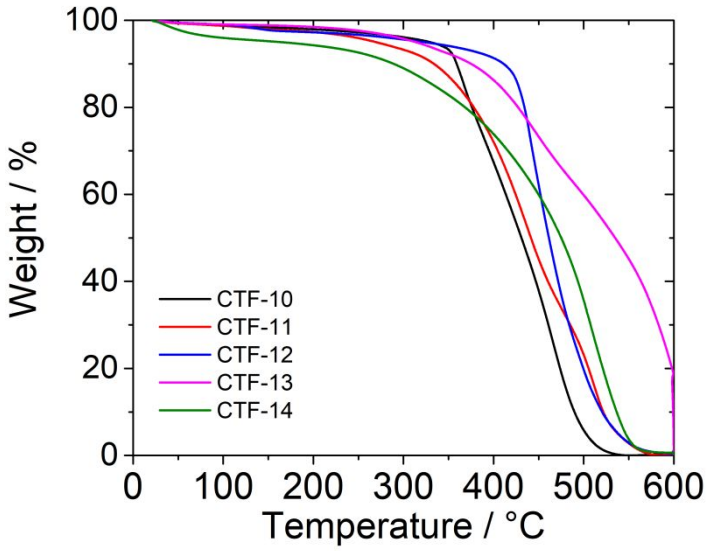

Figure S-9: Thermogravimetric analysis curves for the polymers CTF-10 to CTF-14 in air with a heating rate of 10 °C min^{-1}.

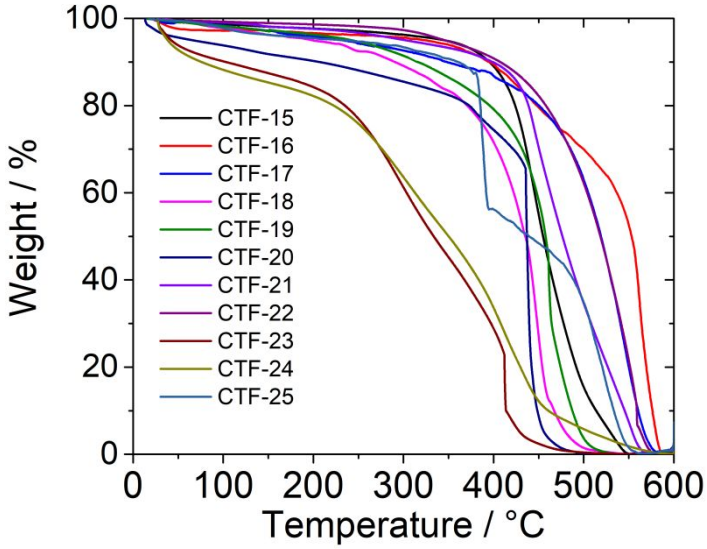

Figure S-10: Thermogravimetric analysis curves for the polymers CTF-15 to CTF-25 in air with a heating rate of 10 °C min^{-1}.

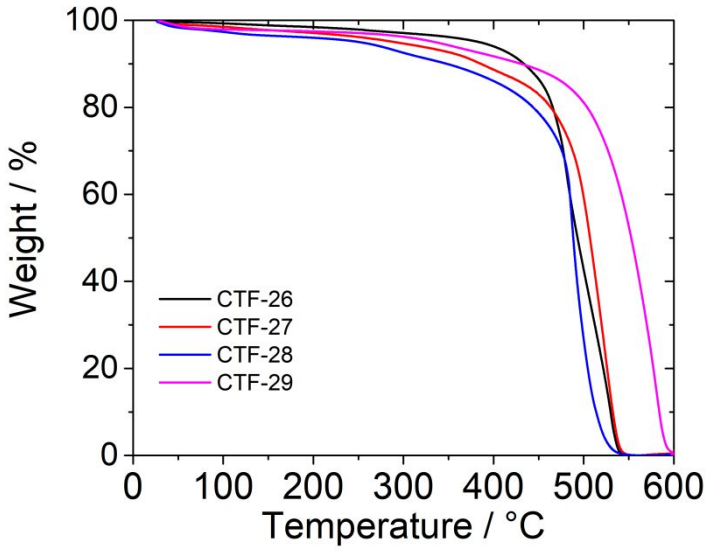

Figure S-11: Thermogravimetric analysis curves for the polymers CTF-26 to CTF-29 in air with a heating rate of 10 °C min^{-1}.

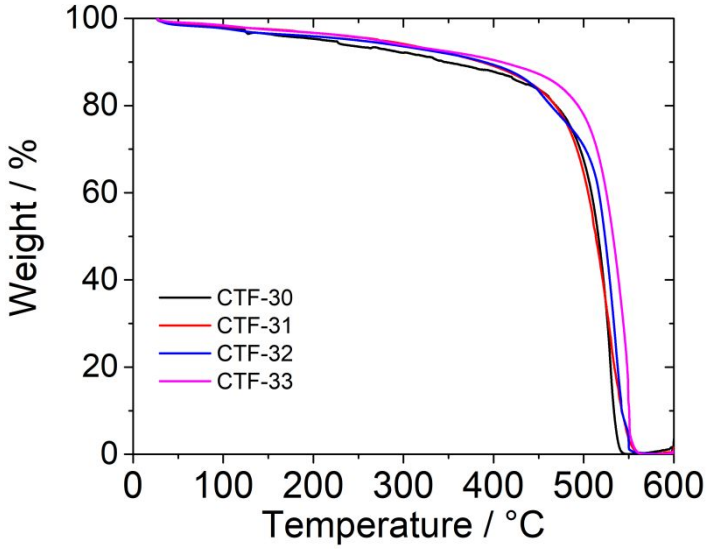

Figure S-12: Thermogravimetric analysis curves for the polymers CTF-30 to CTF-33 in air with a heating rate of 10 °C min^{-1}.

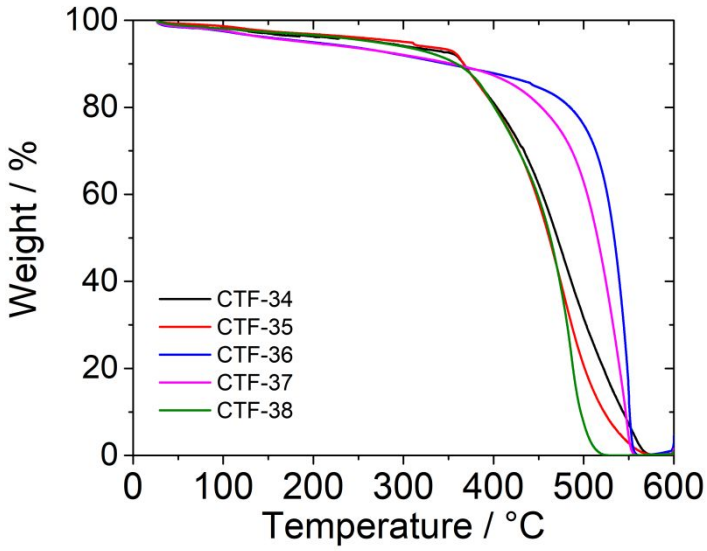

Figure S-13: Thermogravimetric analysis curves for the polymers CTF-34 to CTF-38 in air with a heating rate of 10 °C min^{-1}.

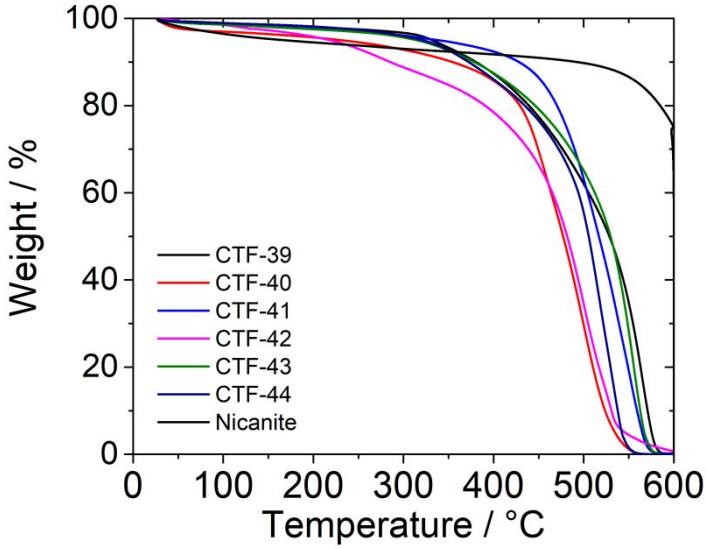

Figure S-14: Thermogravimetric analysis curves for the polymers CTF-39 to CTF-44 and Nicanite in air with a heating rate of 10 °C min^{-1}.

Table S-1: Brunauer-Emmett-Teller surface areas for CTF-5 to CTF-44, measured at 77.3 K. Reference materials CTF-2, CTF-3 Suzuki, and Nicanite are listed for comparison.

Polymer	SA_{BET} ($m^2 g^{-1}$)	Polymer	SA_{BET} ($m^2 g^{-1}$)	Polymer	SA_{BET} ($m^2 g^{-1}$)
CTF-5	168	**CTF-20**	244	**CTF-35**	446
CTF-6	10	**CTF-21**	482	**CTF-36**	175
CTF-7	121	**CTF-22**	338	**CTF-37**	48
CTF-8	24	**CTF-23**	14	**CTF-38**	91
CTF-9	708	**CTF-24**	7	**CTF-39**	536
CTF-10	597	**CTF-25**	488	**CTF-40**	412
CTF-11	184	**CTF-26**	242	**CTF-41**	106
CTF-12	134	**CTF-27**	166	**CTF-42**	13
CTF-13	29	**CTF-28**	76	**CTF-43**	281
CTF-14	10	**CTF-29**	365	**CTF-44**	66
CTF-15	383	**CTF-30**	25		
CTF-16	278	**CTF-31**	33		
CTF-17	326	**CTF-32**	160	**CTF-2**	560
CTF-18	136	**CTF-33**	99	**CTF-3 Suzuki**	380
CTF-19	461	**CTF-34**	397	**Nicanite**	23

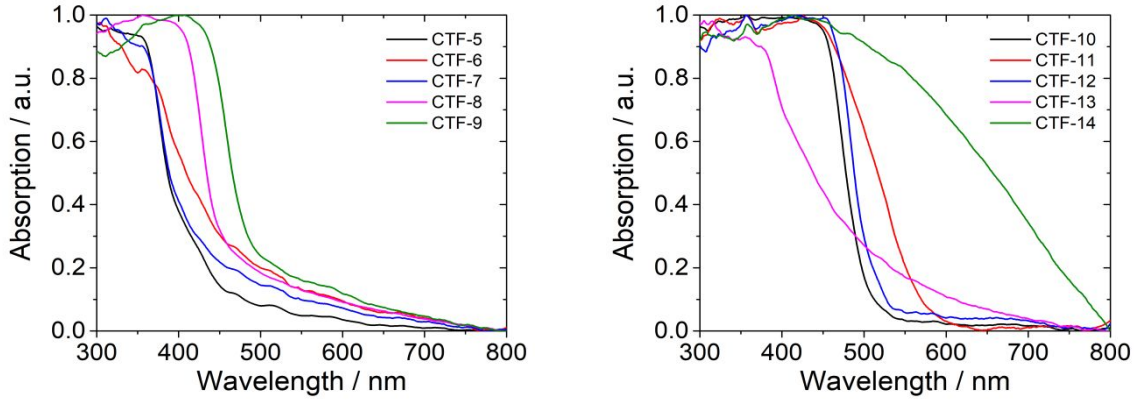

Figure S-15: Solid-state UV-Vis spectra of CTF-5 to CTF-9 and CTF-10 to CTF-14.

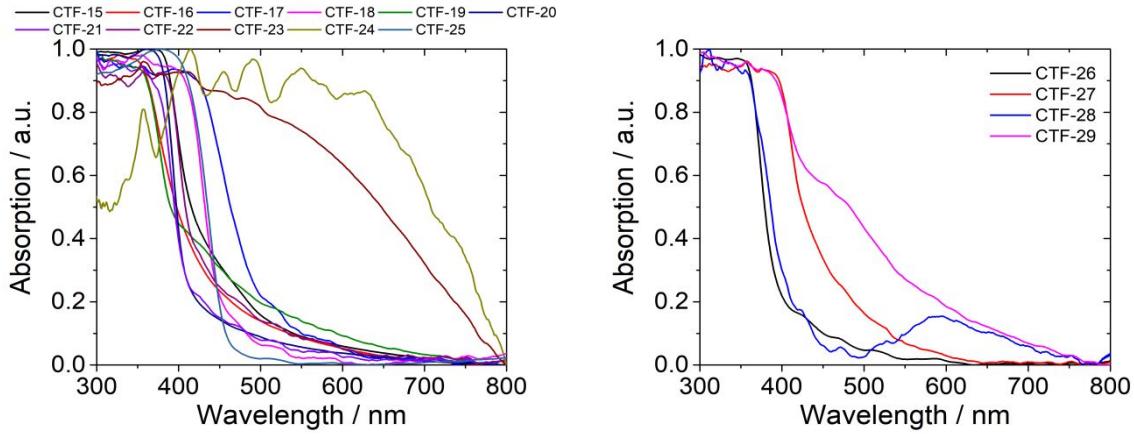

Figure S-16: Solid-state UV-Vis spectra of CTF-15 to CTF-25 and CTF-26 to CTF-29.

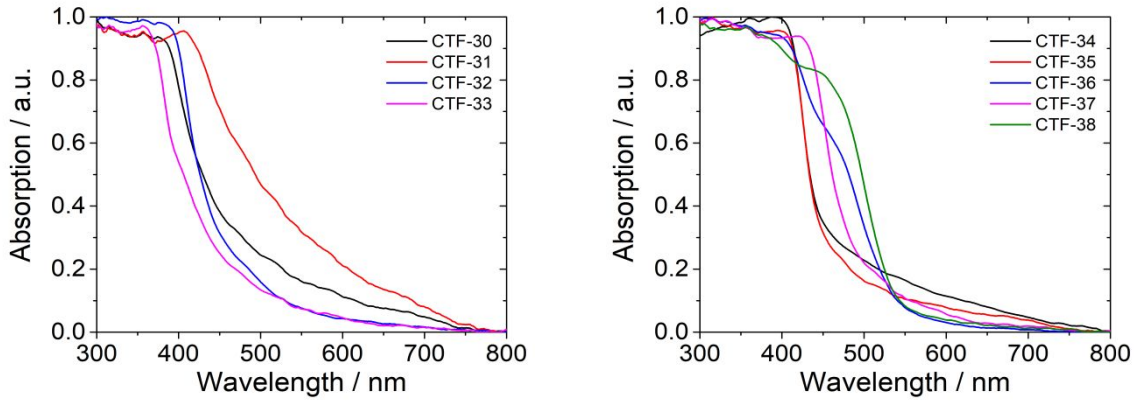

Figure S-17: Solid-state UV-Vis spectra of CTF-30 to CTF-33 and CTF-34 to CTF-38.

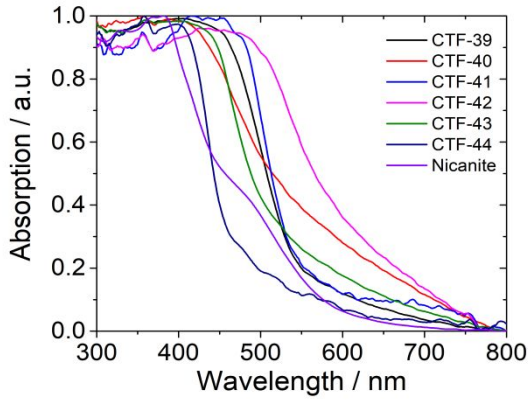

Figure S-18: Solid-state UV-Vis spectra of CTF-39 to CTF-44 and Nicanite.

Table S-2: Overview of the optical properties for the polymers.

Polymer	Optical-gap[a] / eV	λ_{max}[b] / nm	λ_{max}[b] / eV	λ_{exc}[d] / nm	λ_{em}[d] / nm	HER λ > 420 nm[e] / µmol g^{-1} h^{-1}
CTF-5	2.93	318	3.90	280	464	20 ± 2
CTF-6	2.58	356	3.48	280	468	8 ± 1
CTF-7	2.90	355	3.49	280	465	20 ± 6
CTF-8	2.51	376	3.30	280	481	571 ± 37
CTF-9	2.49	407	3.05	360	563	63 ± 3
CTF-10	2.25	409	3.03	360	537	1412 ± 63
CTF-11	2.15	426	2.91	360	576	1151 ± 29
CTF-12	2.41	451	2.75	280	435	1515 ± 66
CTF-13	2.57	374	3.32	280	435	72 ± 3
CTF-14	1.55	479	2.59	280	463	16 ± 2
CTF-15	2.58	374	3.32	280	461	2946 ± 381
CTF-16	2.60	359	3.45	280	462	1354 ± 133
CTF-17	2.42	397	3.12	360	530	537 ± 30
CTF-18	2.71	386	3.21	280	468	5 ± 1
CTF-19	2.91	349	3.55	280	433	1158 ± 78
CTF-20	2.71	362	3.43	280	434	87 ± 2
CTF-21	2.95	355	3.49	280	435	550 ± 28
CTF-22	2.86	379	3.27	280	437	413 ± 39
CTF-23	1.56	413	3.00	280	433	5 ± 1
CTF-24	1.52	626	1.98	280	400	0[f]
CTF-25	2.69	381	3.25	280	485	548 ± 97
CTF-26	3.08	345	3.59	280	420	67 ± 1
CTF-27	2.70	378	3.28	280	519	911 ± 37
CTF-28	2.96	355	3.49	280	427	119 ± 2
CTF-29	2.68	374	3.32	280	470	371 ± 39
CTF-30	2.62	375	3.31	280	473	1561 ± 150
CTF-31	2.21	406	3.05	360	560	650 ± 45
CTF-32	2.69	375	3.31	280	460	1041 ± 70
CTF-33	2.86	355	3.49	280	468	260 ± 20
CTF-34	2.69	392	3.16	280	474	2373 ± 25
CTF-35	2.70	398	3.12	280	471	600 ± 22
CTF-36	2.28	374	3.32	360	579	160 ± 13
CTF-37	2.50	418	2.97	280	501	507 ± 33
CTF-38	2.28	374	3.32	360	581	150 ± 15
CTF-39	2.21	403	3.08	360	567	1151 ± 75
CTF-40	2.07	409	3.03	280	435	33 ± 3
CTF-41	2.24	455	2.72	360	564	0[f]
CTF-42	1.91	455	2.72	280	436	100 ± 2
CTF-43	2.30	406	3.05	360	548	652 ± 45
CTF-44	2.60	399	3.10	280	493	44 ± 1
CTF-2	2.58	398	3.12	280	441	358 ± 21
CTF-3 Suzuki	2.90	377	3.29	280	440	158 ± 56
Nicanite	2.51	383	3.24	280	522	59 ± 3

[a] The optical gap was calculated from the on-set of absorption in the solid-state UV-vis spectrum; [b] λ_{max} was determined from the peak maximum of the most red-shifted peak in the solid state UV-Vis spectrum; [c] The predicted λ_{max} were obtained from TD-B3LYP calculations on TPhLPhT cluster models of the CTFs (T = triazine, Ph = *para*-phenyl, L = linker, T = triazine); [d] Spectra see section 4. Time-Correlated Single Photon Counting Measurements; [e] The hydrogen evolution rate (HER) was measured with 25 mg of the samples in 8.3 mL water, 8.3 mL triethylamine, 8.3 mL methanol in presence of 3 wt. % platinum as a co-catalyst; [f] No hydrogen evolved during a typical 5 h run.

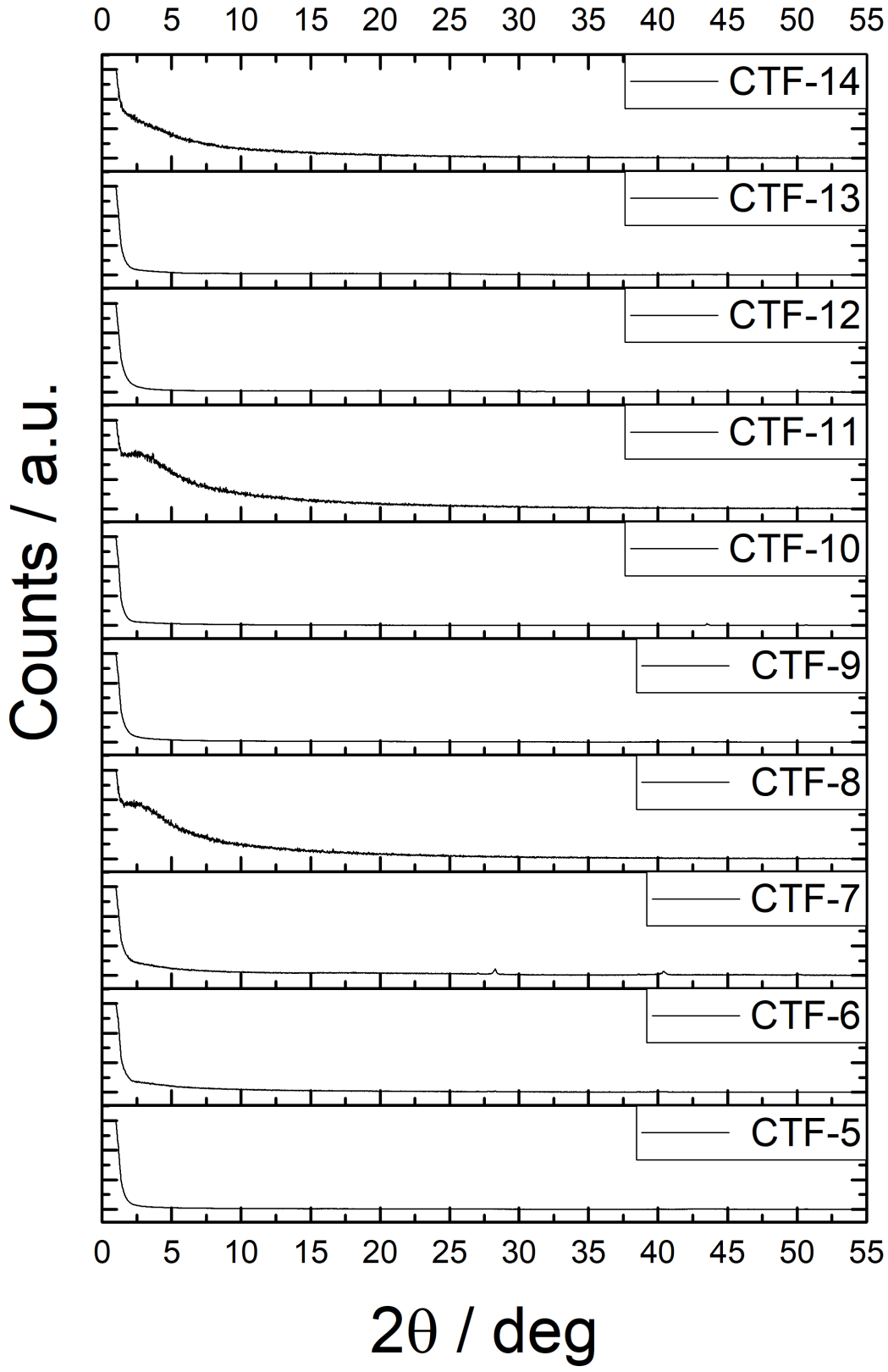

Figure S-19: Normalised PXRD spectra for the polymers CTF-5 to CTF-14.

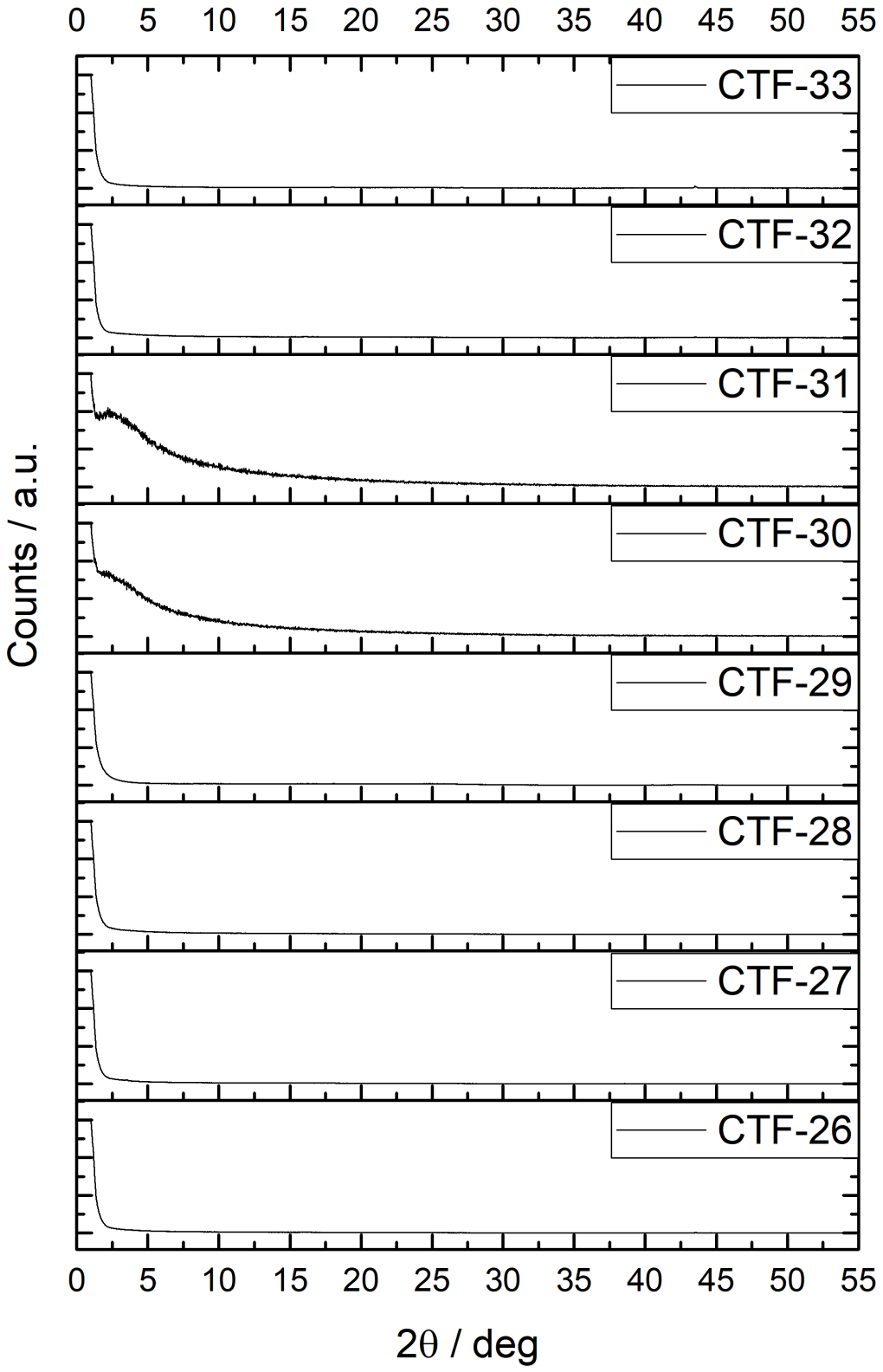

Figure S-20: Normalised PXRD spectra for the polymers CTF-26 to CTF-33.

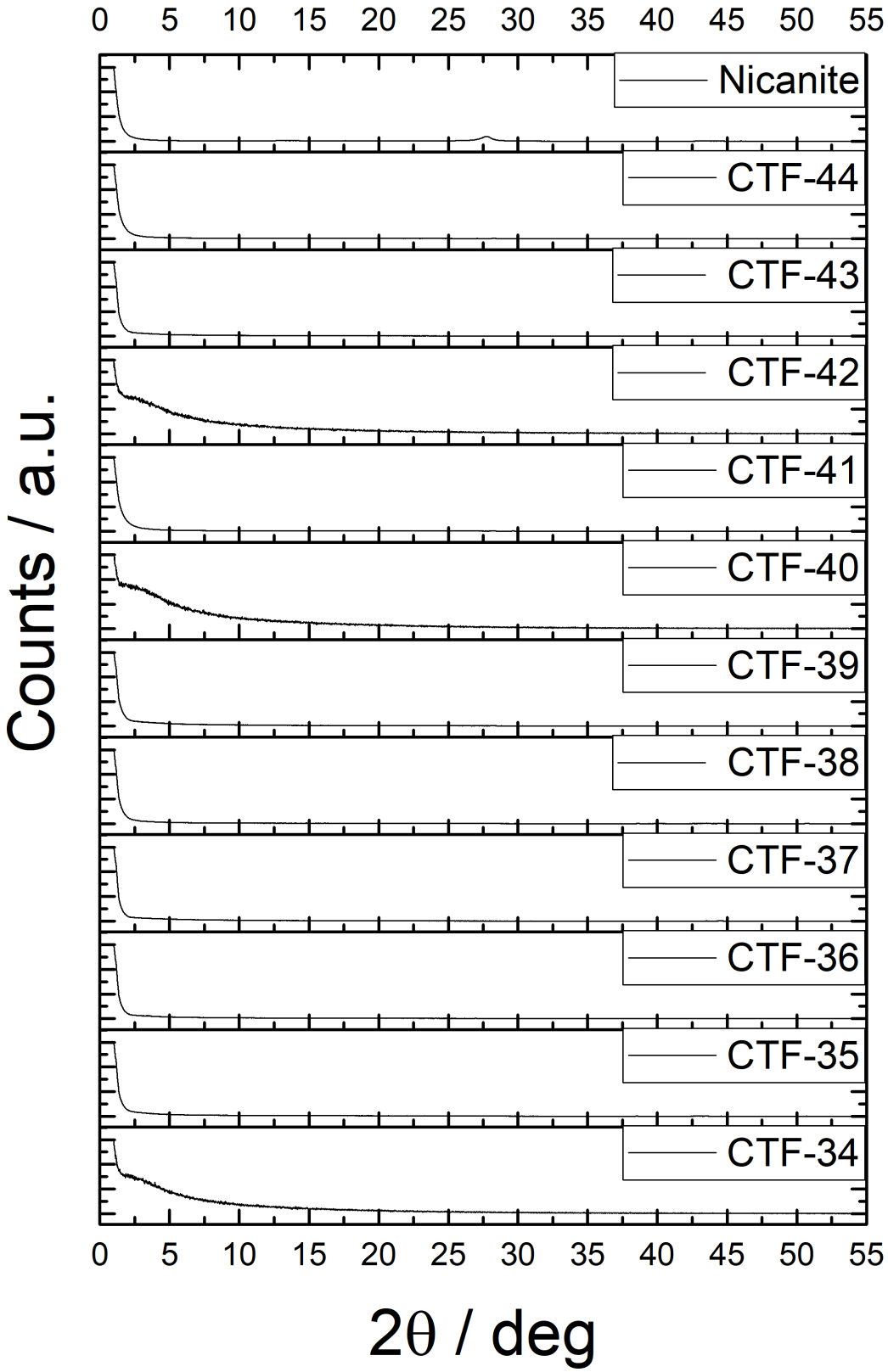

Figure S-21: Normalised PXRD spectra for the polymers CTF-34 to CTF-44 and Nicanite.

Table S-3: Overview of the contact angles against water for the polymers CTF-5 to CTF-44 and comparison literature known polymers CTF-2 and commercially available carbon nitride (Nicanite).

Polymer	Contact angle (°) against water	Polymer	Contact angle (°) against water
CTF-5	80 ± 1	**CTF-27**	72 ± 2
CTF-6	77 ± 5	**CTF-28**	59 ± 2
CTF-7	67 ± 3	**CTF-29**	65 ± 2
CTF-8	80 ± 5	**CTF-30**	swelling
CTF-9	95 ± 1	**CTF-31**	swelling
CTF-10	90 ± 4	**CTF-32**	swelling
CTF-11	68 ± 2	**CTF-33**	56 ± 3
CTF-12	70 ± 3	**CTF-34**	swelling
CTF-13	68 ± 3	**CTF-35**	91 ± 1
CTF-14	55 ± 7	**CTF-36**	swelling
CTF-15	swelling	**CTF-37**	swelling
CTF-16	swelling	**CTF-38**	86 ± 4
CTF-17	swelling	**CTF-39**	78 ± 4
CTF-18	swelling	**CTF-40**	swelling
CTF-19	68 ± 3	**CTF-41**	59 ± 7
CTF-20	87 ± 5	**CTF-42**	swelling
CTF-21	73 ± 8	**CTF-43**	swelling
CTF-22	81 ± 3	**CTF-44**	61 ± 5
CTF-23	64 ± 6		
CTF-24	66 ± 4	**CTF-2**	swelling
CTF-25	106 ± 1	**CTF-3 Suzuki**	56 ± 3
CTF-26	66 ± 5	**Nicanite**	swelling

The contact angles were measured in at least three points with three measurements, compared to the instrument standard and determined with the Young Laplace shape. The polymer disc was pressed at 10 tons with a pellet press usually used for KBr in IR experiments.

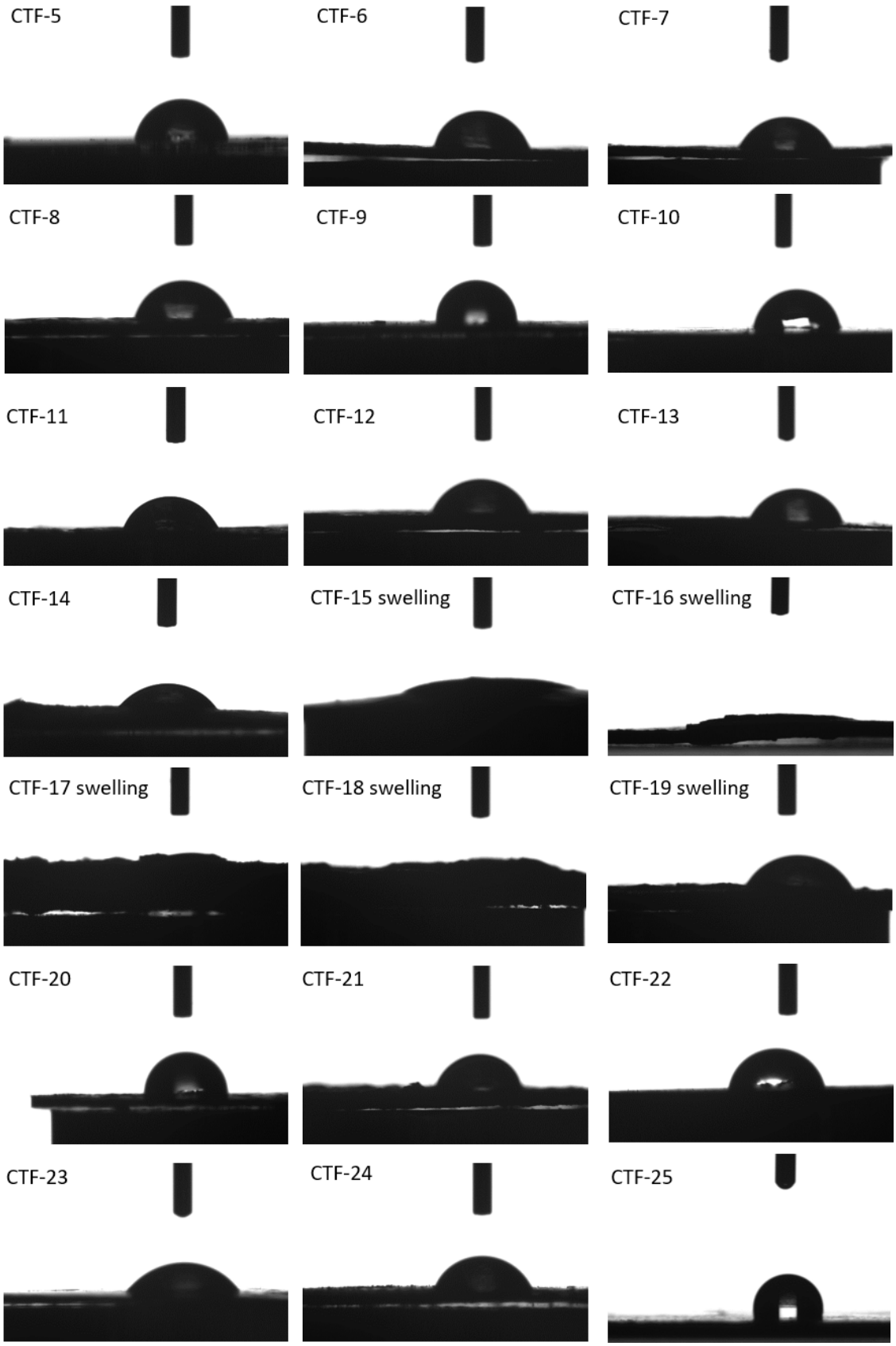

Figure S-22: Contact angle images from water for the polymers CTF-5 to CTF-25. For materials that swell, the picture is taken 20 seconds after the drop is deposited onto the polymer surface.

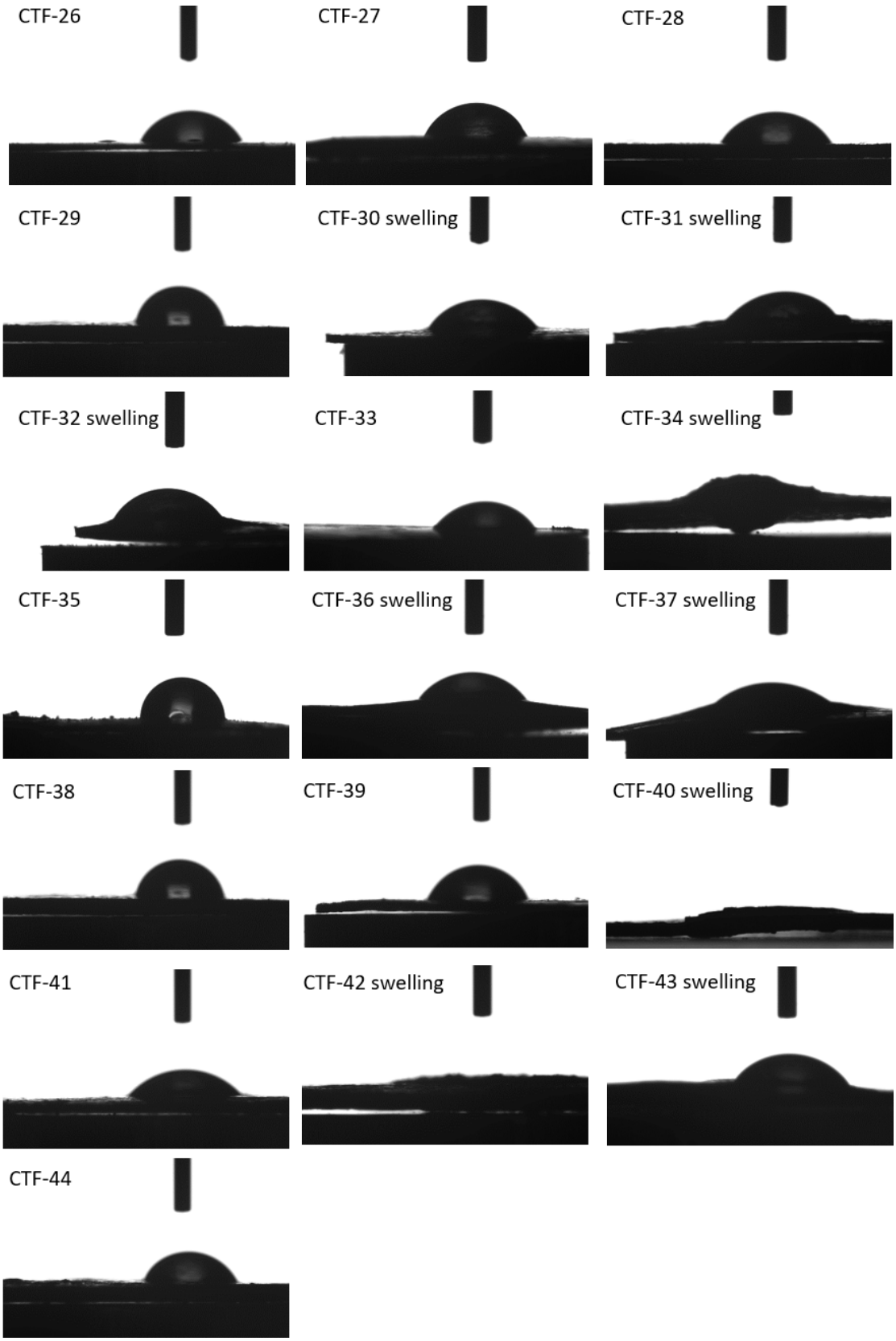

Figure S-23: Contact angle images from water for the polymers CTF-26 to CTF-44. For materials that swell, the picture is taken 20 seconds after the drop is deposited onto the polymer surface.

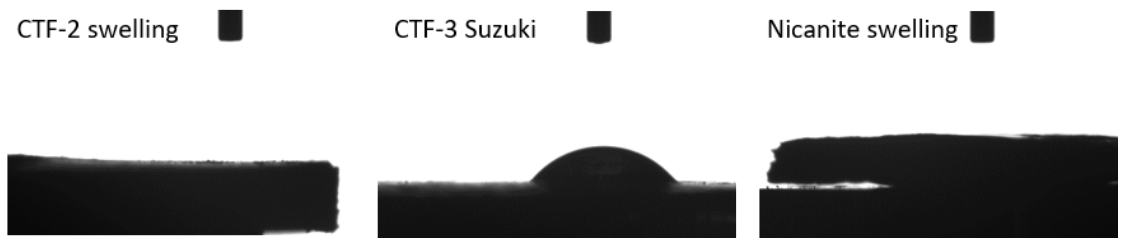

Figure S-24: Contact angle images from water for the polymers CTF-2 and CTF-3 Suzuki, and commercially available Nicanite. For materials that swell, the picture is taken 20 seconds after the drop is deposited onto the polymer surface.

Table S-4: Overview of the light obscuration from water/TEA/MeOH (1:1:1) and water for the polymers CTF-5 to CTF-44 and comparison to CTF-2 and commercially available Nicanite.

Polymer	Transmission H_2O/MeOH/TEA (%)[a]	Transmission H_2O (%)[a]	Polymer	Transmission H_2O/MeOH/TEA (%)[a]	Transmission H_2O (%)[a]
CTF-5	5.4	35.3	**CTF-27**	4.6	8.9
CTF-6	42.8	60.1	**CTF-28**	19.1	27.9
CTF-7	15.1	48.0	**CTF-29**	16.9	34.0
CTF-8	1.5	6.2	**CTF-30**	4.5	3.9
CTF-9	2.9	29.0	**CTF-31**	5.0	3.9
CTF-10	4.9	23.4	**CTF-32**	11.1	8.6
CTF-11	31.3	33.8	**CTF-33**	21.7	28.8
CTF-12	40.4	50.8	**CTF-34**	0.8	83.0
CTF-13	6.8	24.5	**CTF-35**	8.4	28.7
CTF-14	51.4	64.4	**CTF-36**	3.6	3.1
CTF-15	0.8	85.2	**CTF-37**	11.3	61.8
CTF-16	5.6	21.6	**CTF-38**	3.8	12.7
CTF-17	5.7	73.0	**CTF-39**	2.2	20.0
CTF-18	31.4	39.7	**CTF-40**	41.9	13.3
CTF-19	53.3	58.0	**CTF-41**	12.1	23.4
CTF-20	6.2	35.3	**CTF-42**	35.2	72.8
CTF-21	52.2	51.2	**CTF-43**	1.9	3.5
CTF-22	3.7	54.7	**CTF-44**	34.0	57.2
CTF-23	25.5	65.6			
CTF-24	59.4	77.6	**CTF-2**	9.5	83.0
CTF-25	20.1	42.7	**CTF-3 Suzuki**	26.8	57.0
CTF-26	24.2	51.3	**Nicanite**	16.8	11.4

[a]The transmission was calculated as an average of 0.4 µm steps in the range of 4-30 mm.

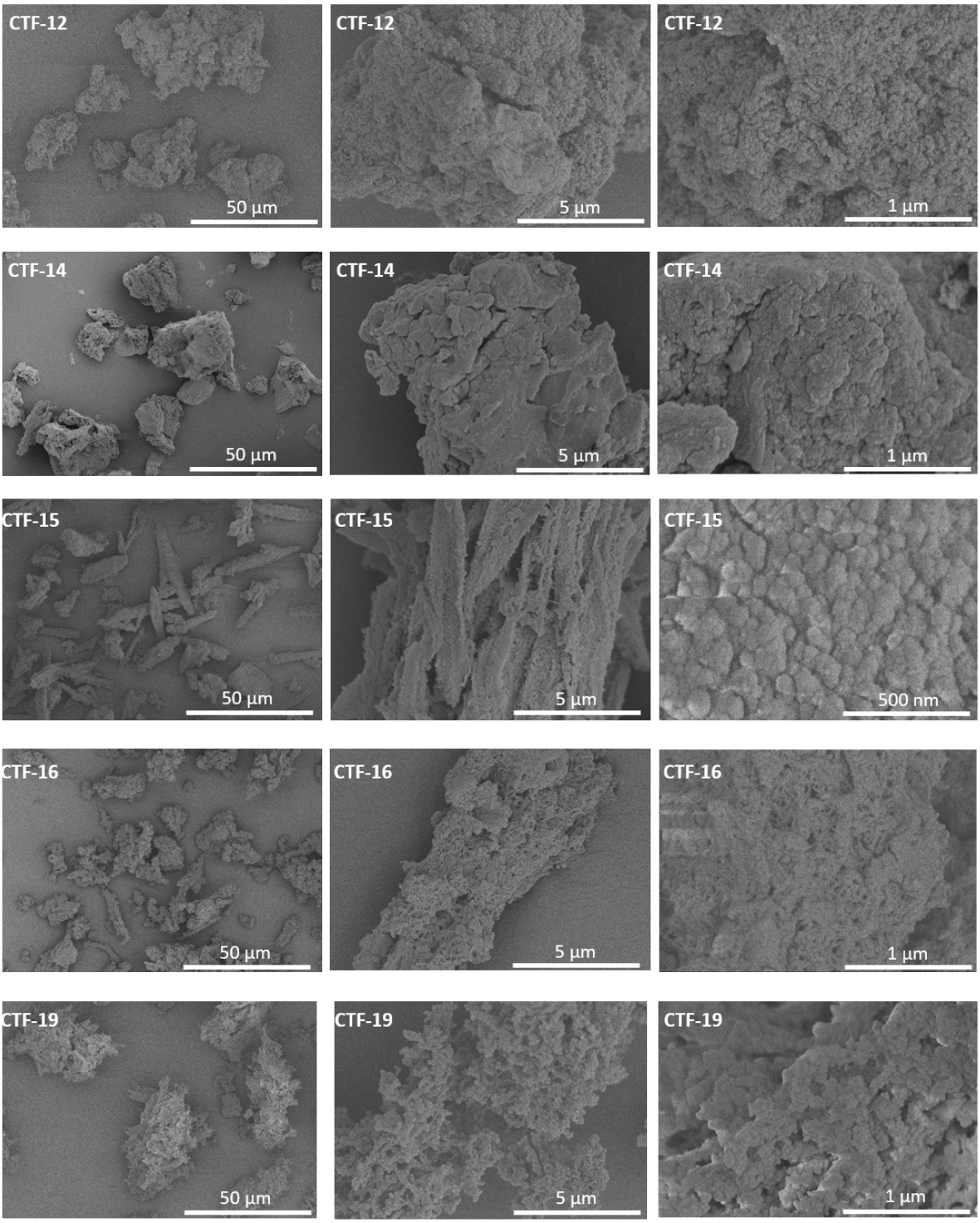

Figure S-25: SEM pictures of polymers CTF-12, CTF-14, CTF-15, CTF-16, and CTF-19.

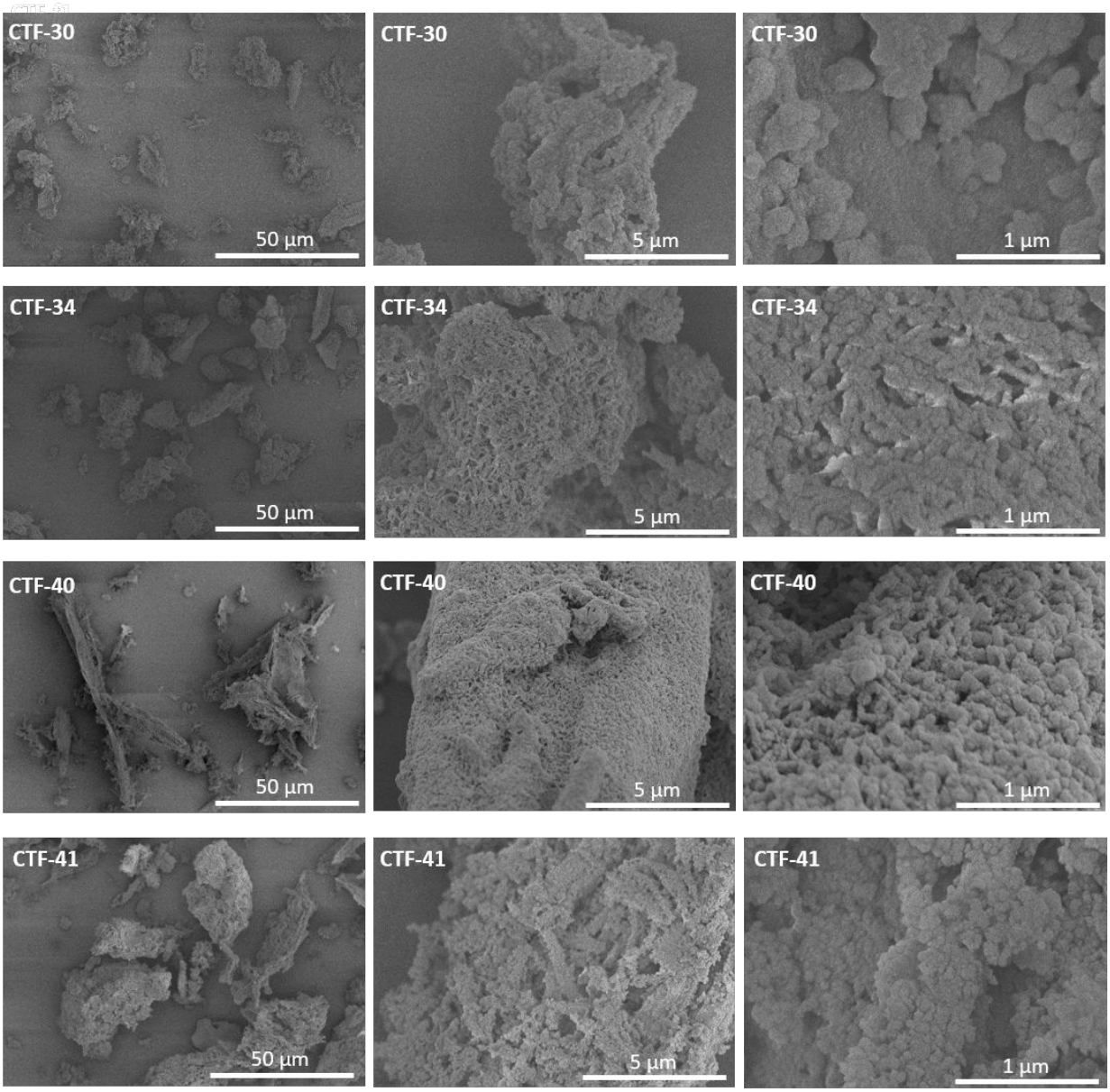

Figure S-26: SEM pictures of polymers CTF-30, CTF-34, CTF-40, and CTF-41.

4. Time-Correlated Single Photon Counting Experiments

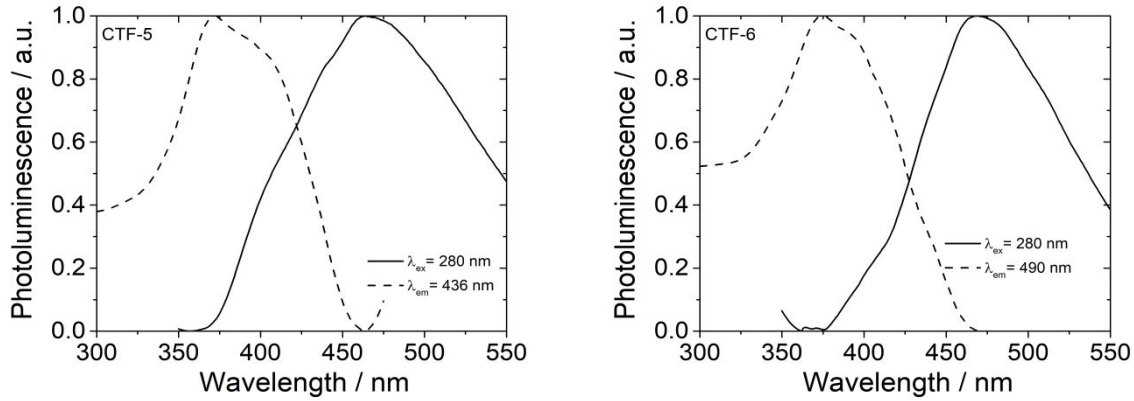

Figure S-27: Excitation and emission photoluminescence spectra of CTF-5 and CTF-6.

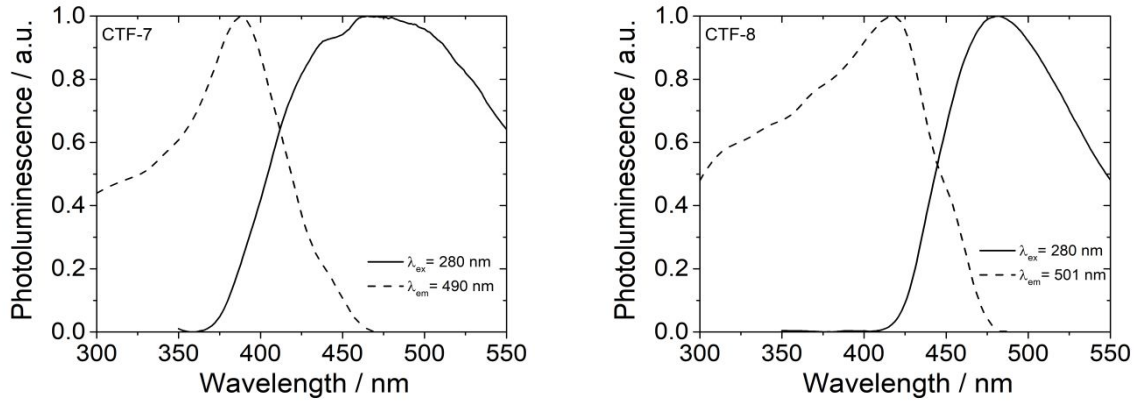

Figure S-28: Excitation and emission photoluminescence spectra of CTF-7 and CTF-8.

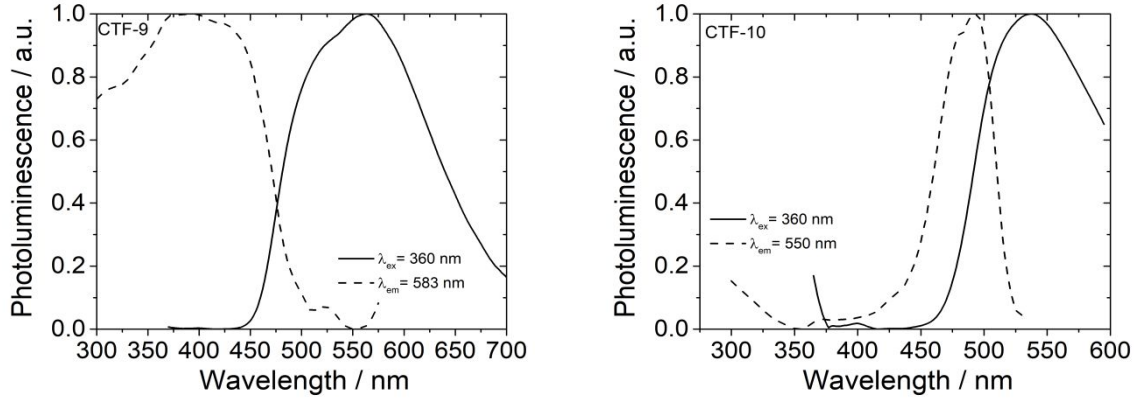

Figure S-29: Excitation and emission photoluminescence spectra of CTF-9 and CTF-10.

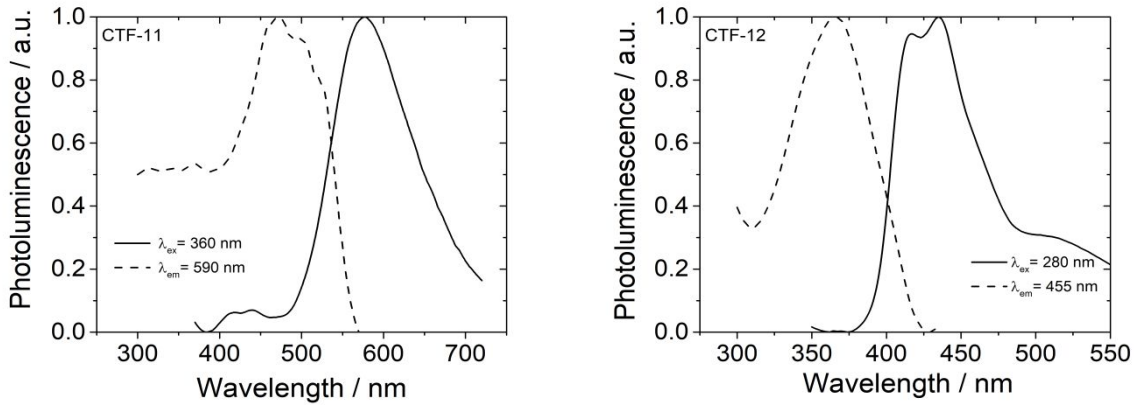

Figure S-30: Excitation and emission photoluminescence spectra of CTF-11 and CTF-12.

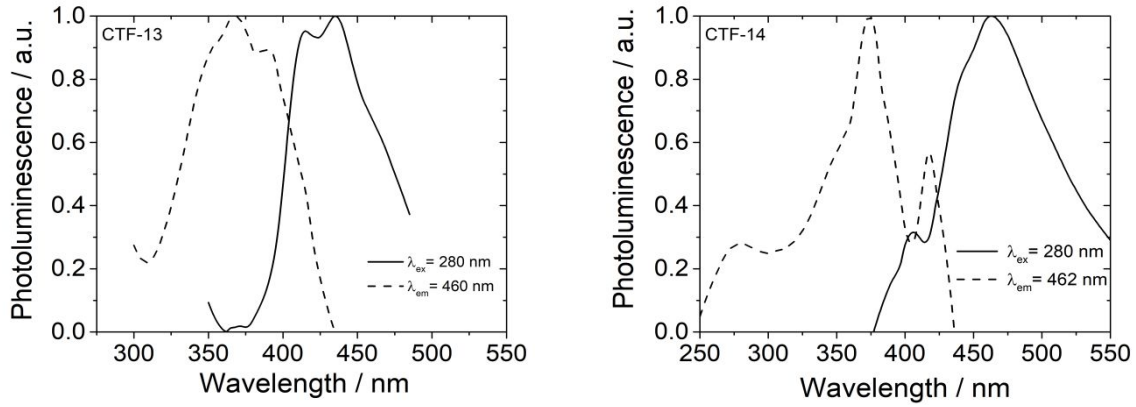

Figure S-31: Excitation and emission photoluminescence spectra of CTF-13 and CTF-14.

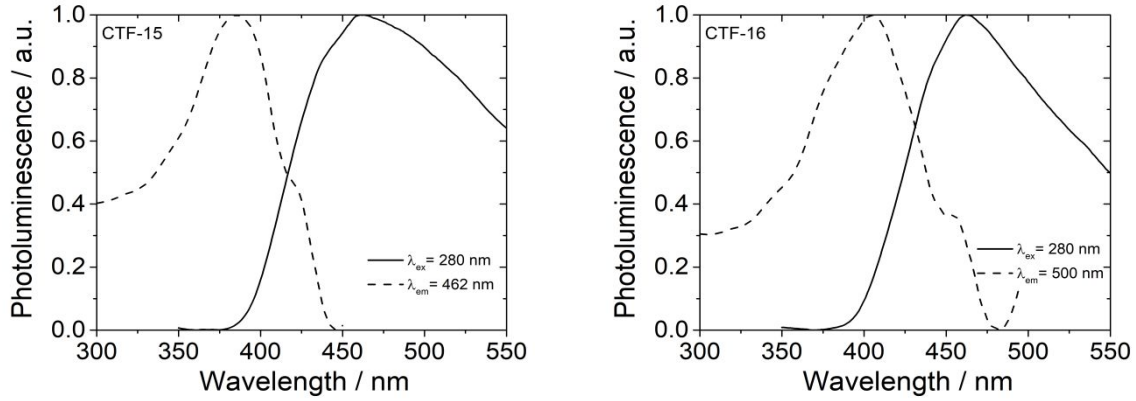

Figure S-32: Excitation and emission photoluminescence spectra of CTF-15 and CTF-16.

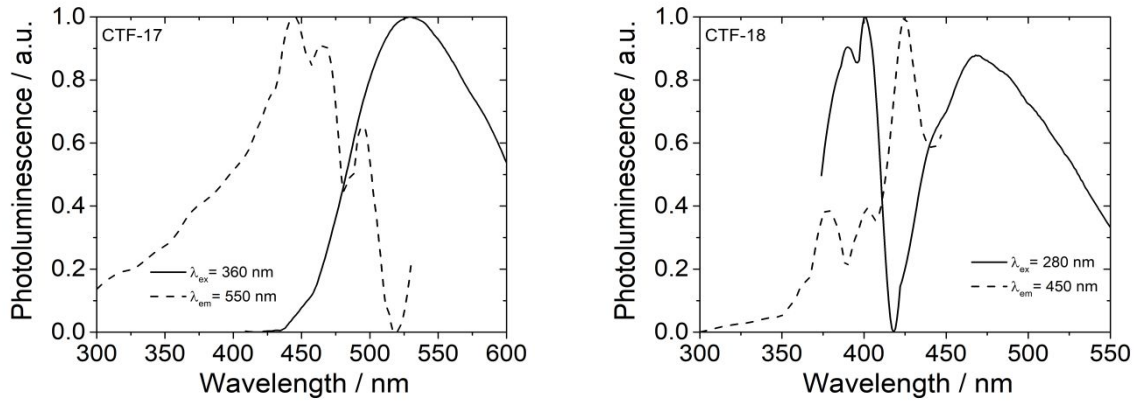

Figure S-33: Excitation and emission photoluminescence spectra of CTF-17 and CTF-18.

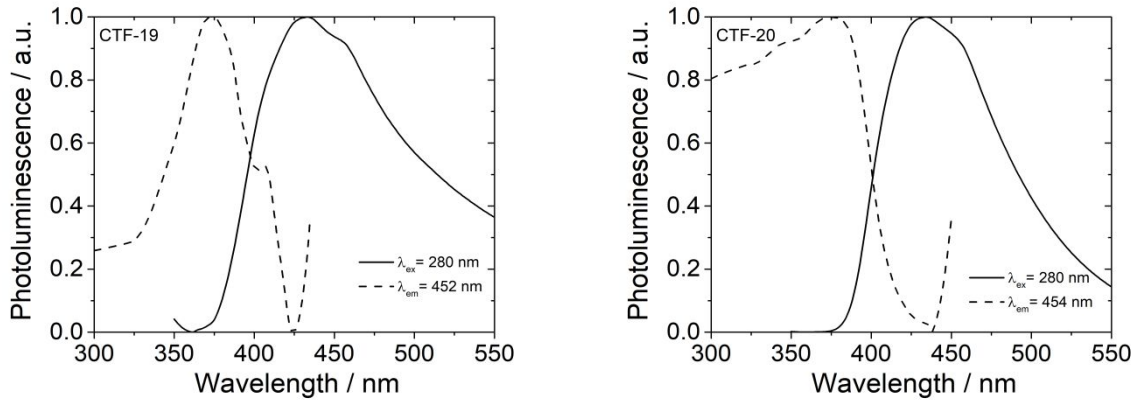

Figure S-34: Excitation and emission photoluminescence spectra of CTF-19 and CTF-20.

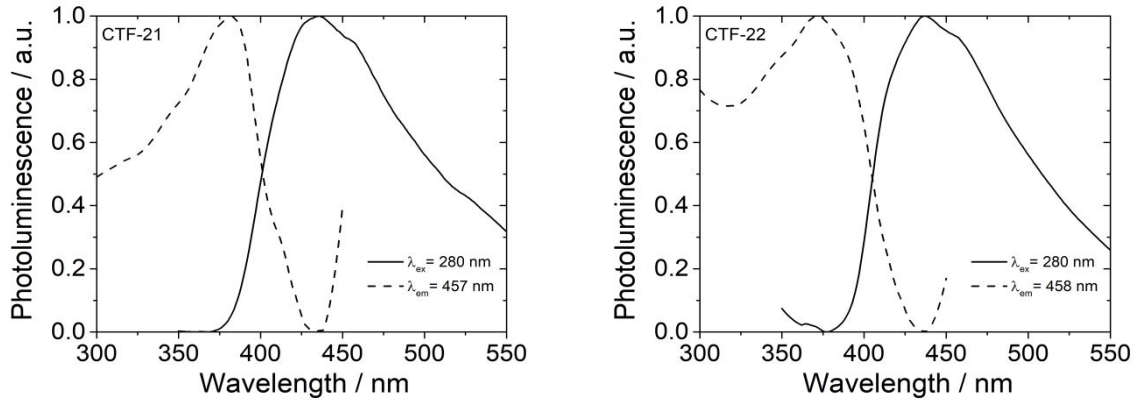

Figure S-35: Excitation and emission photoluminescence spectra of CTF-21 and CTF-22.

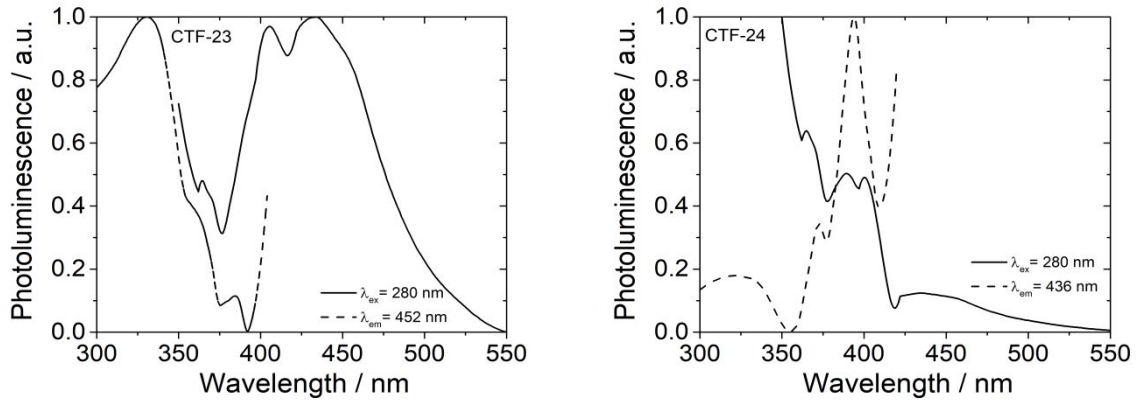

Figure S-36: Excitation and emission photoluminescence spectra of CTF-23 and CTF-24.

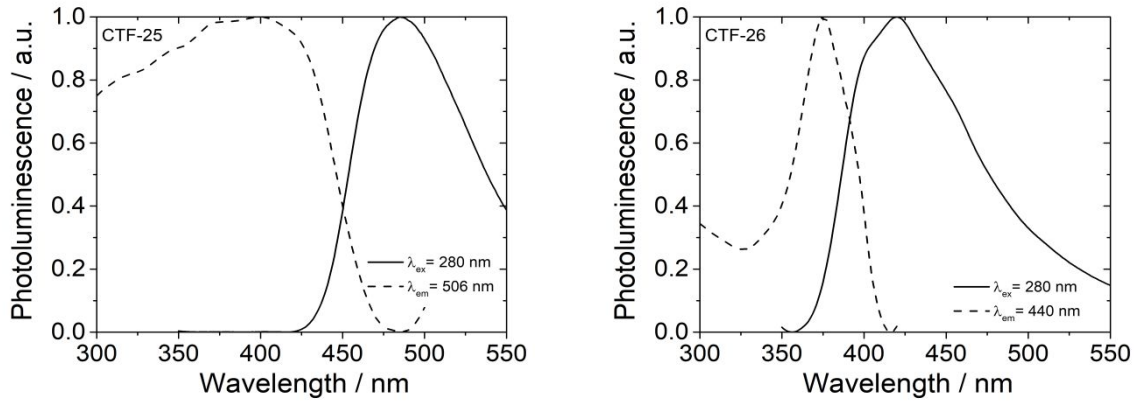

Figure S-37: Excitation and emission photoluminescence spectra of CTF-25 and CTF-26.

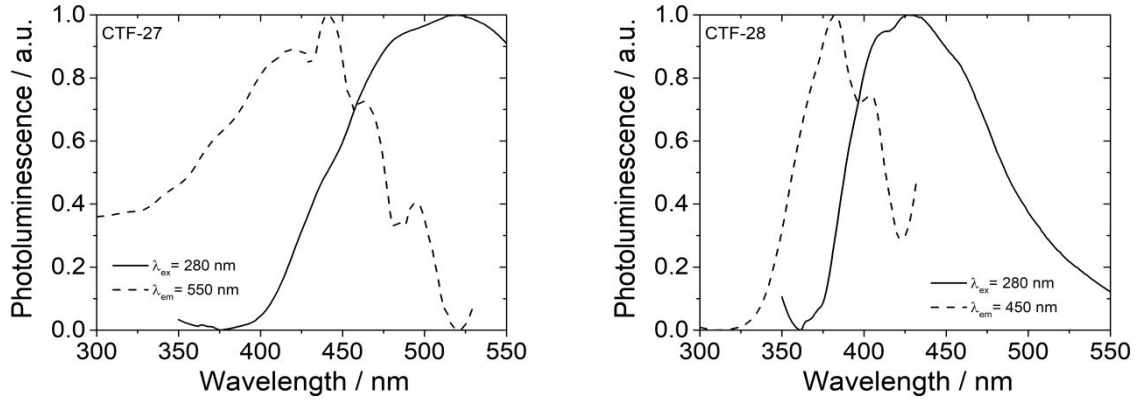

Figure S-38: Excitation and emission photoluminescence spectra of CTF-27 and CTF-28.

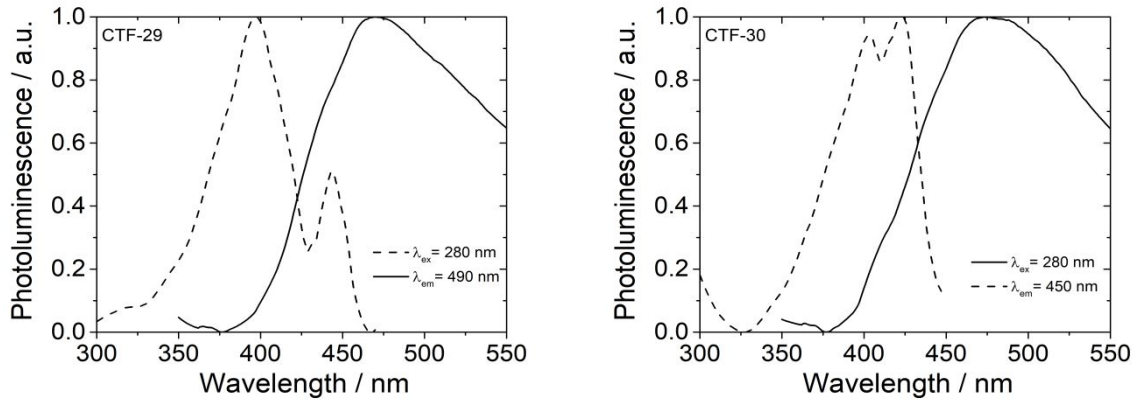

Figure S-39: Excitation and emission photoluminescence spectra of CTF-29 and CTF-30.

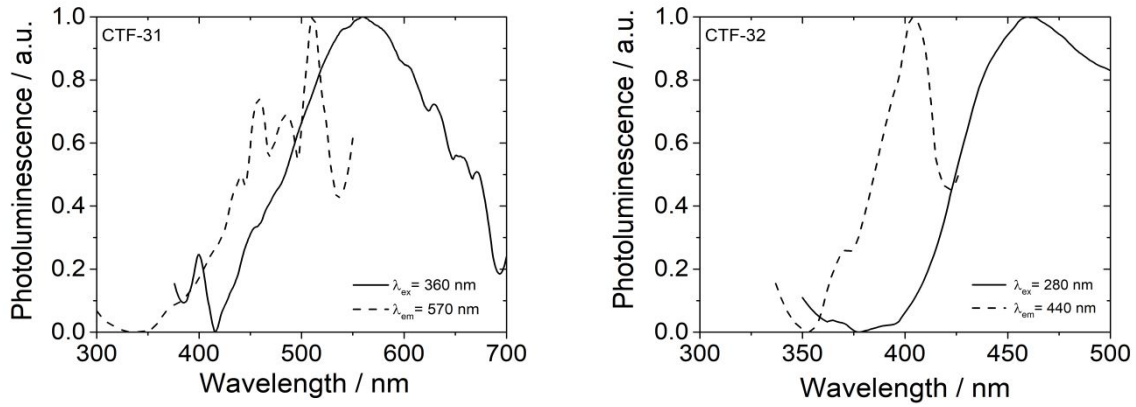

Figure S-40: Excitation and emission photoluminescence spectra of CTF-31 and CTF-32.

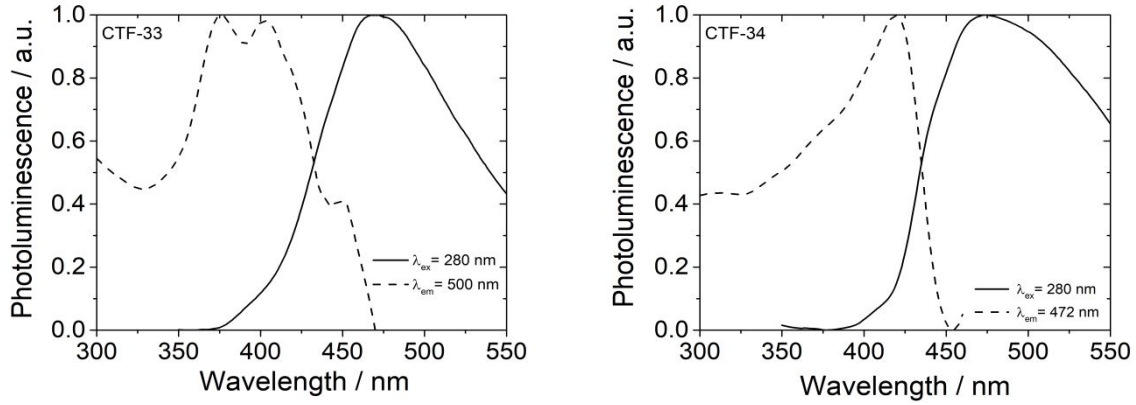

Figure S-41: Excitation and emission photoluminescence spectra of CTF-33 and CTF-34.

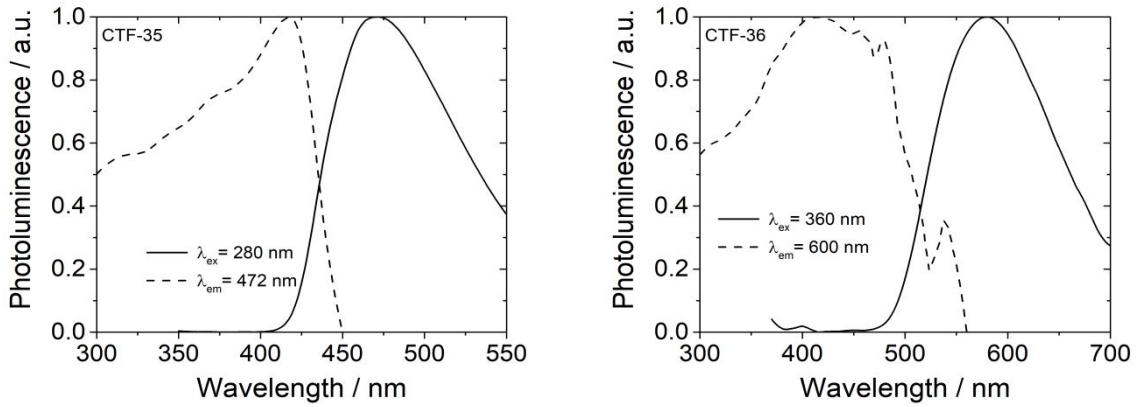

Figure S-42: Excitation and emission photoluminescence spectra of CTF-35 and CTF-36.

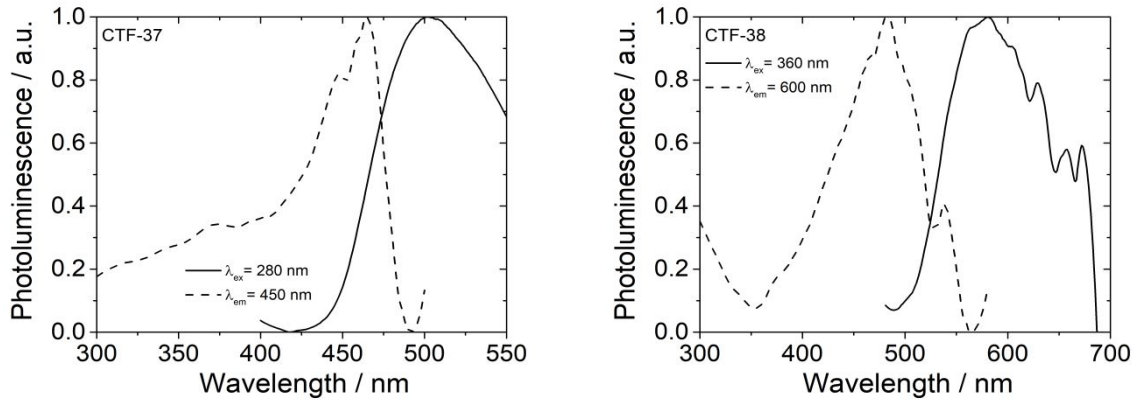

Figure S-43: Excitation and emission photoluminescence spectra of CTF-37 and CTF-38.

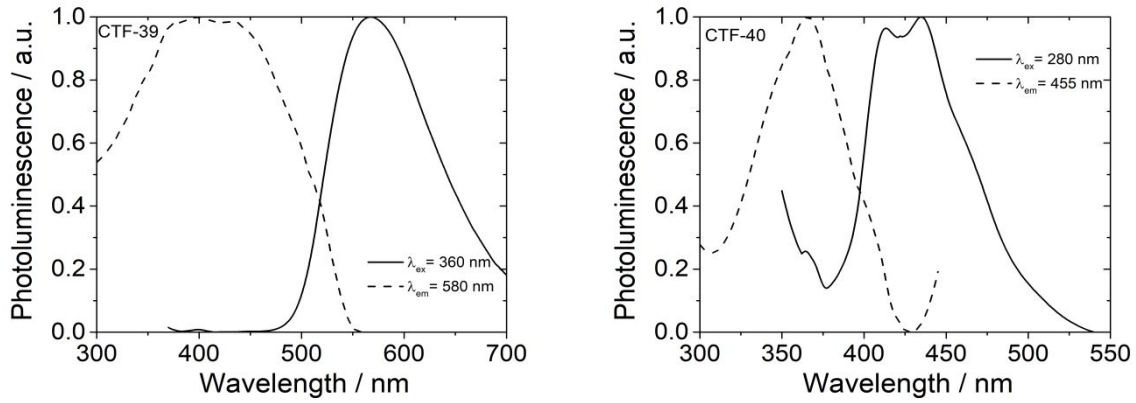

Figure S-44: Excitation and emission photoluminescence spectra of CTF-39 and CTF-40.

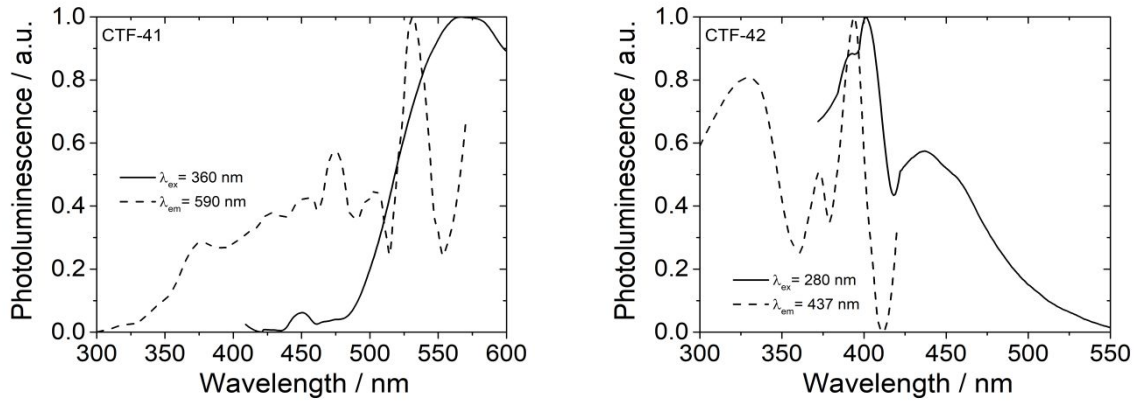

Figure S-45: Excitation and emission photoluminescence spectra of CTF-41 and CTF-42.

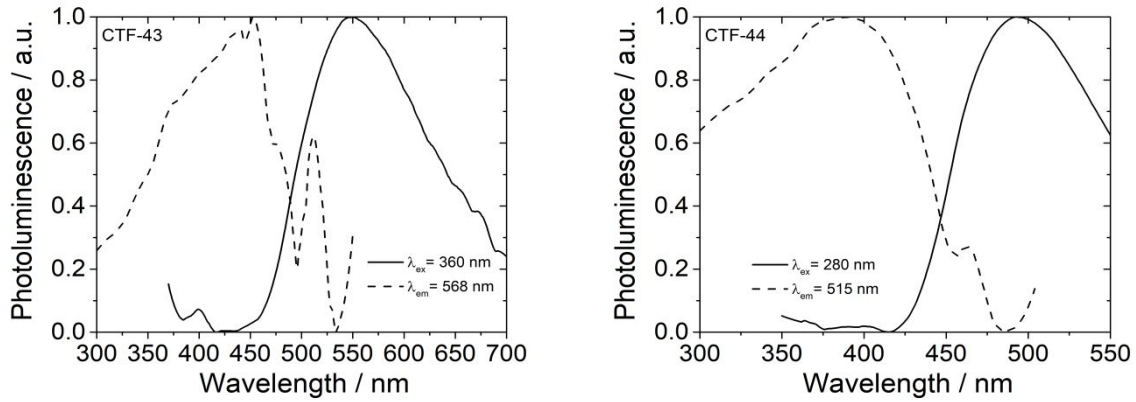

Figure S-46: Excitation and emission photoluminescence spectra of CTF-43 and CTF-44.

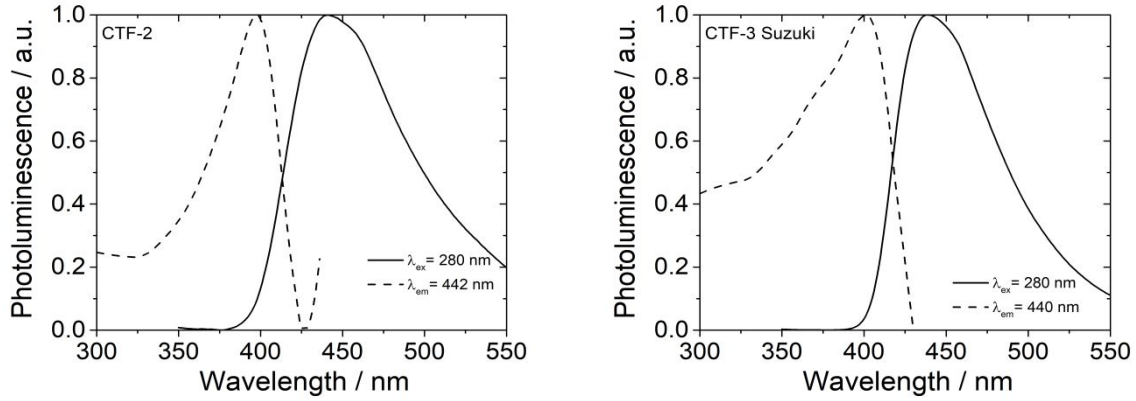

Figure S-47: Excitation and emission photoluminescence spectra of CTF-2 and CTF-3 Suzuki.

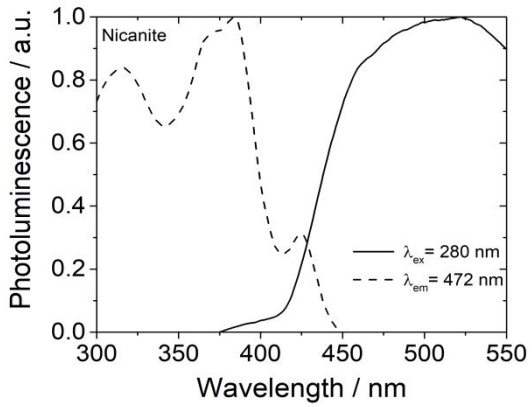

Figure S-48: Excitation and emission photoluminescence spectra of Nicanite.

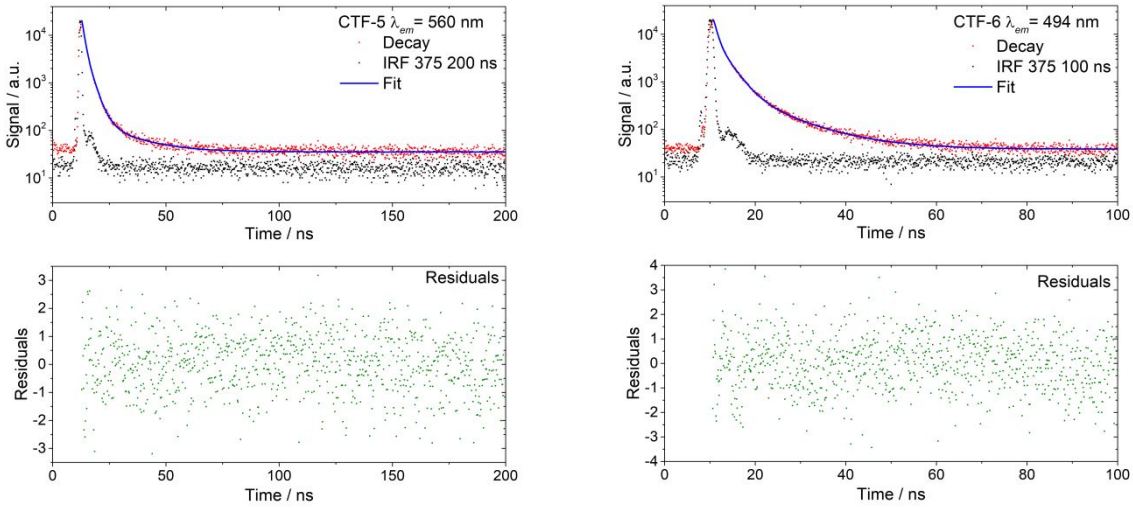

Figure S-49: Time-correlated single-photon counting measurement of CTF-5 and CTF-6 in the solid state.

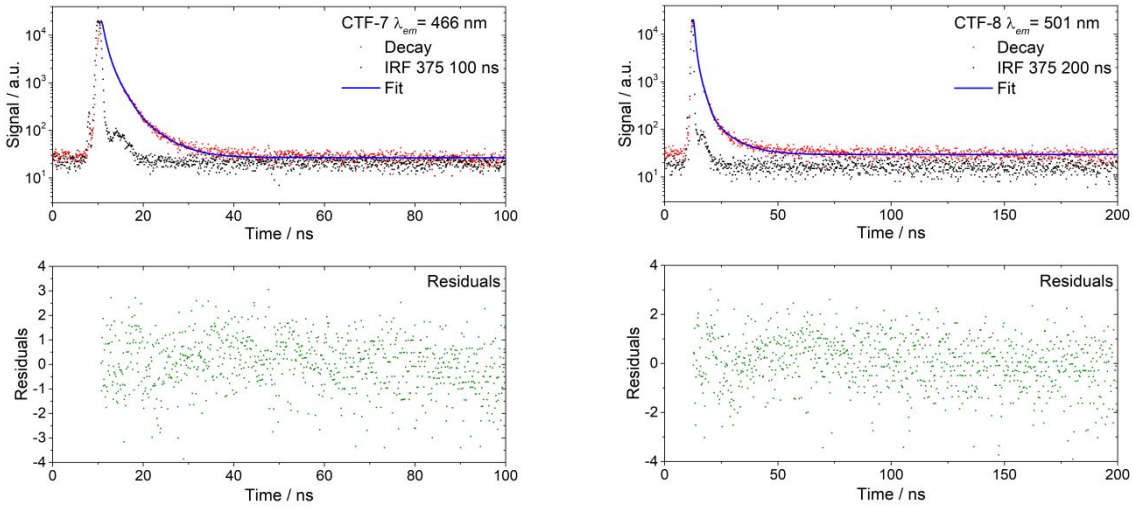

Figure S-50: Time-correlated single-photon counting measurement of CTF-7 and CTF-8 in the solid state.

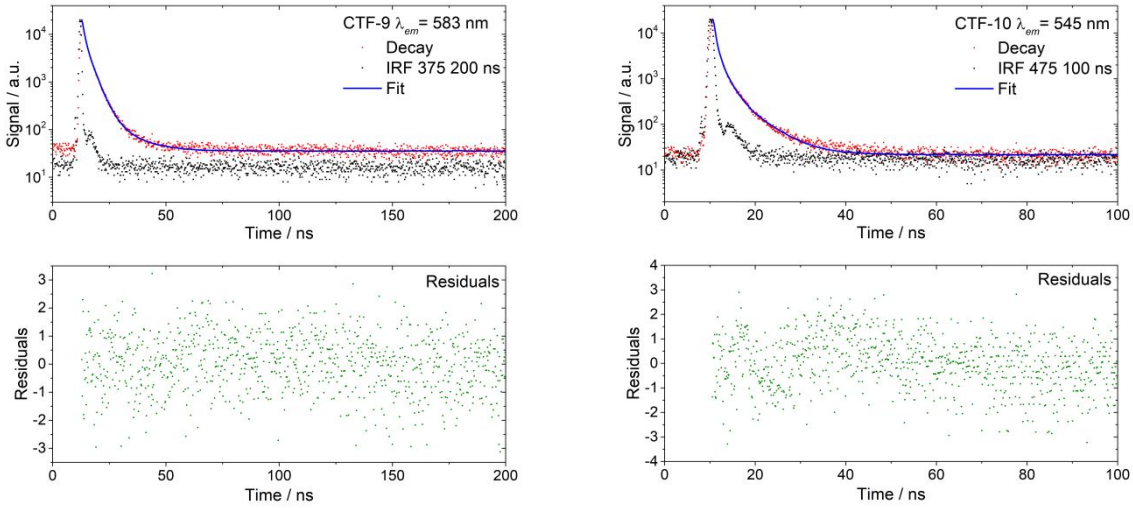

Figure S-51: Time-correlated single-photon counting measurement of CTF-9 and CTF-10 in the solid state.

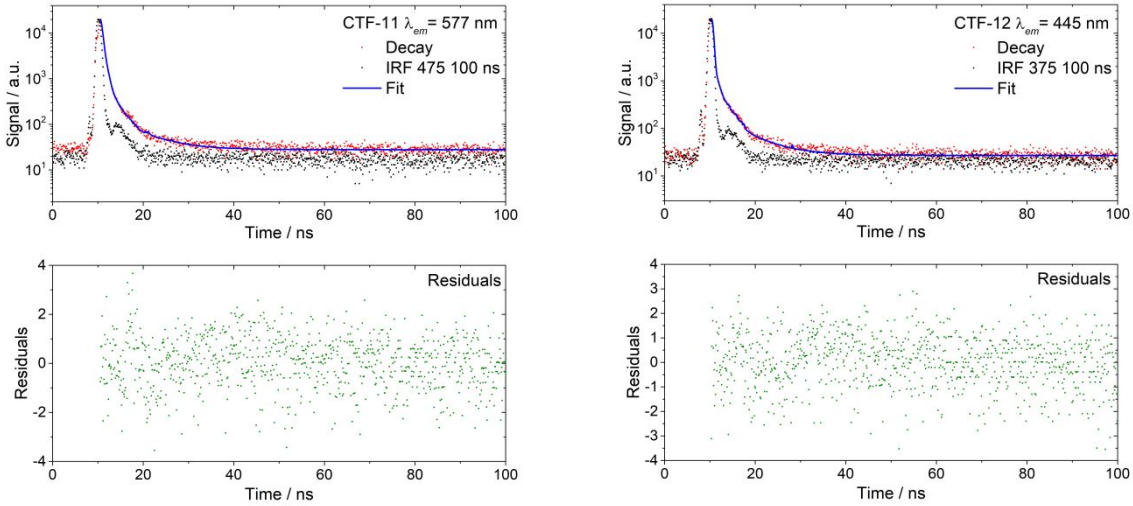

Figure S-52: Time-correlated single-photon counting measurement of CTF-11 and CTF-12 in the solid state.

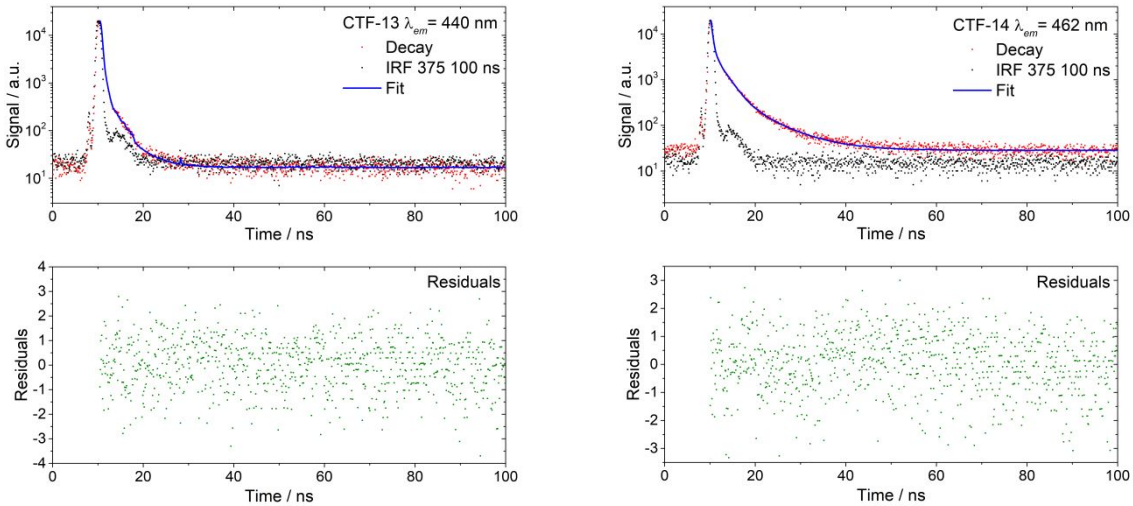

Figure S-53: Time-correlated single-photon counting measurement of CTF-13 and CTF-14 in the solid state.

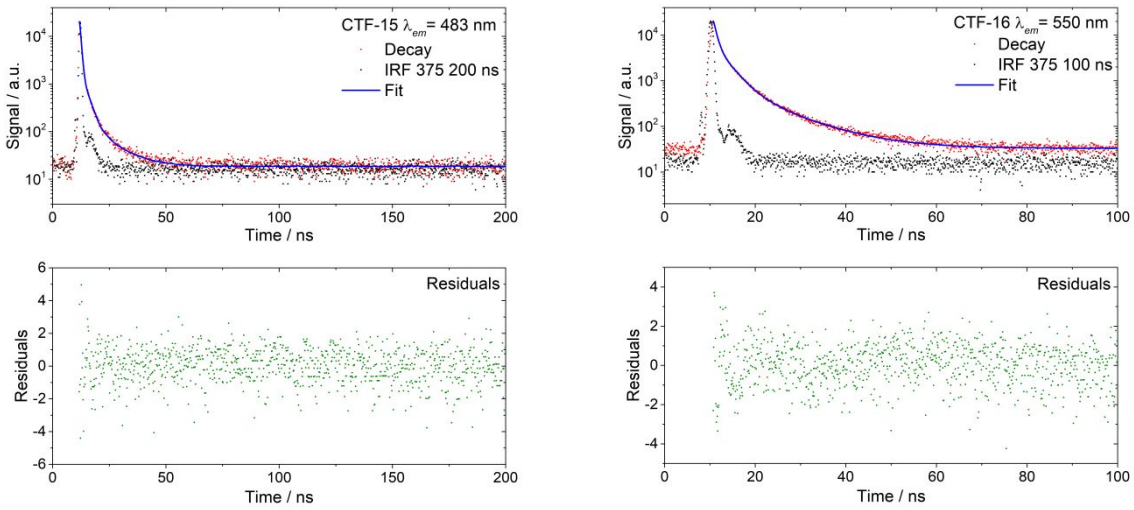

Figure S-54: Time-correlated single-photon counting measurement of CTF-15 and CTF-16 in the solid state.

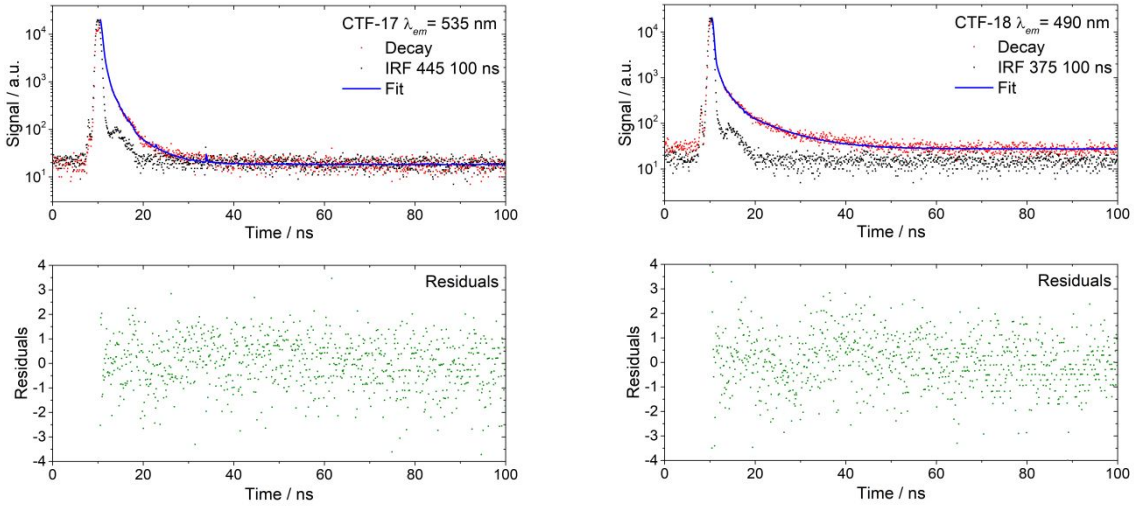

Figure S-55: Time-correlated single-photon counting measurement of CTF-17 and CTF-18 in the solid state.

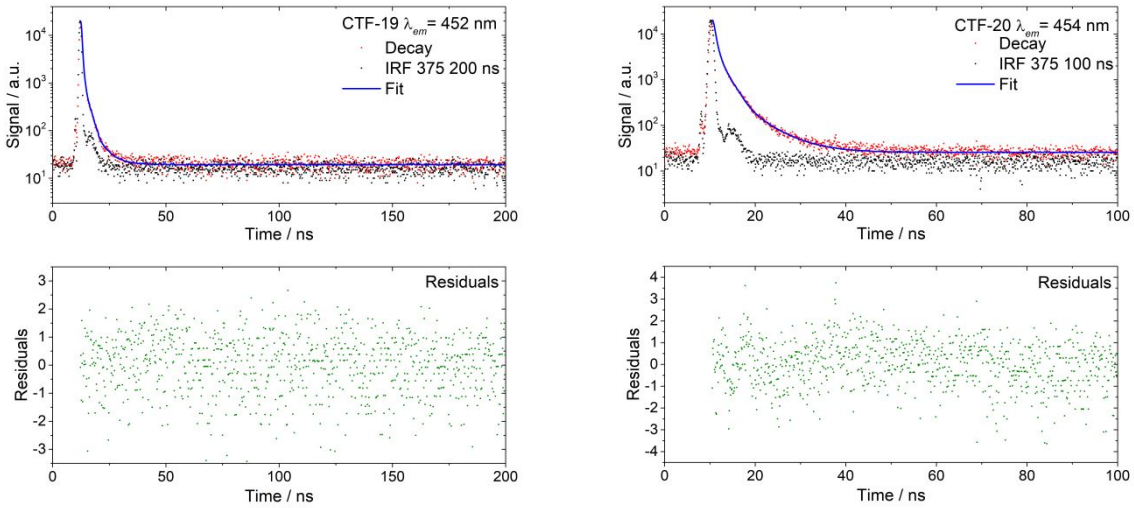

Figure S-56: Time-correlated single-photon counting measurement of CTF-19 and CTF-20 in the solid state.

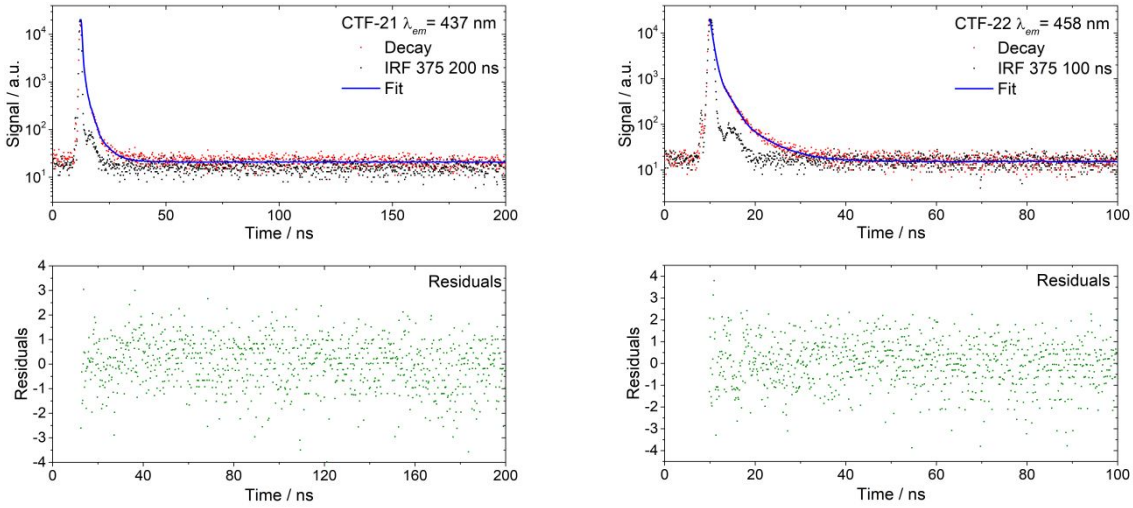

Figure S-57: Time-correlated single-photon counting measurement of CTF-21 and CTF-22 in the solid state.

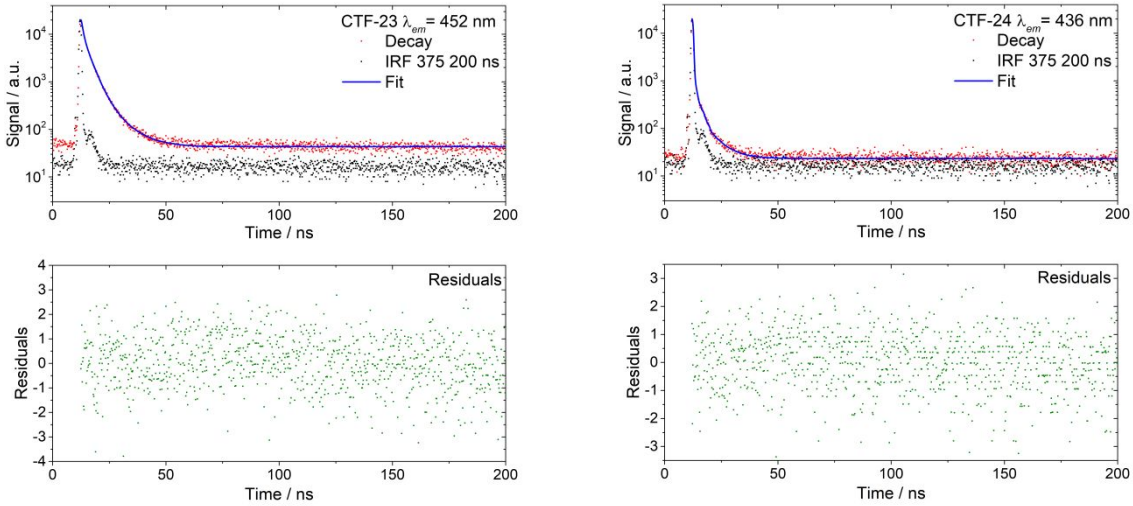

Figure S-58: Time-correlated single-photon counting measurement of CTF-23 and CTF-24 in the solid state.

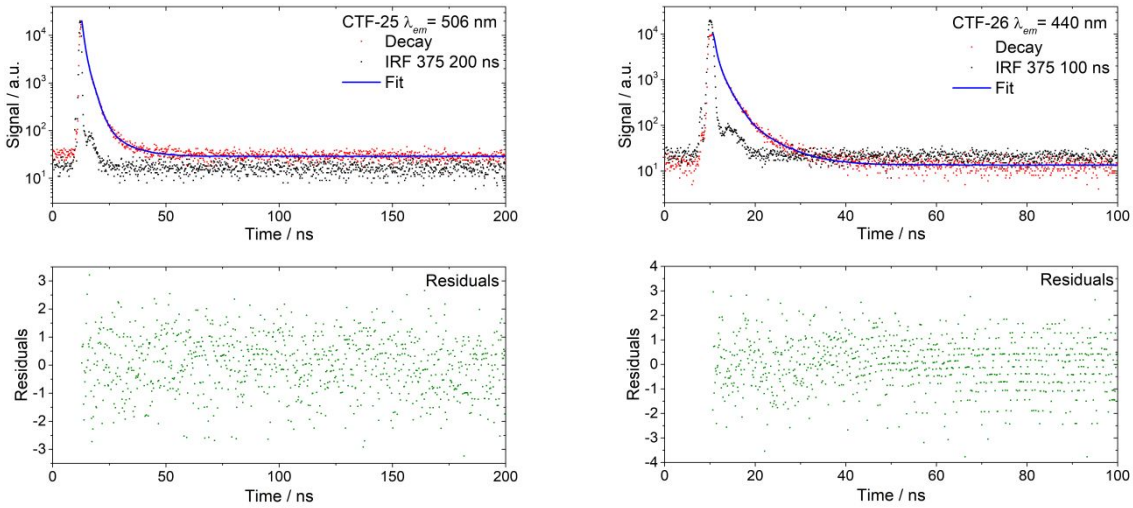

Figure S-59: Time-correlated single-photon counting measurement of CTF-25 and CTF-26 in the solid state.

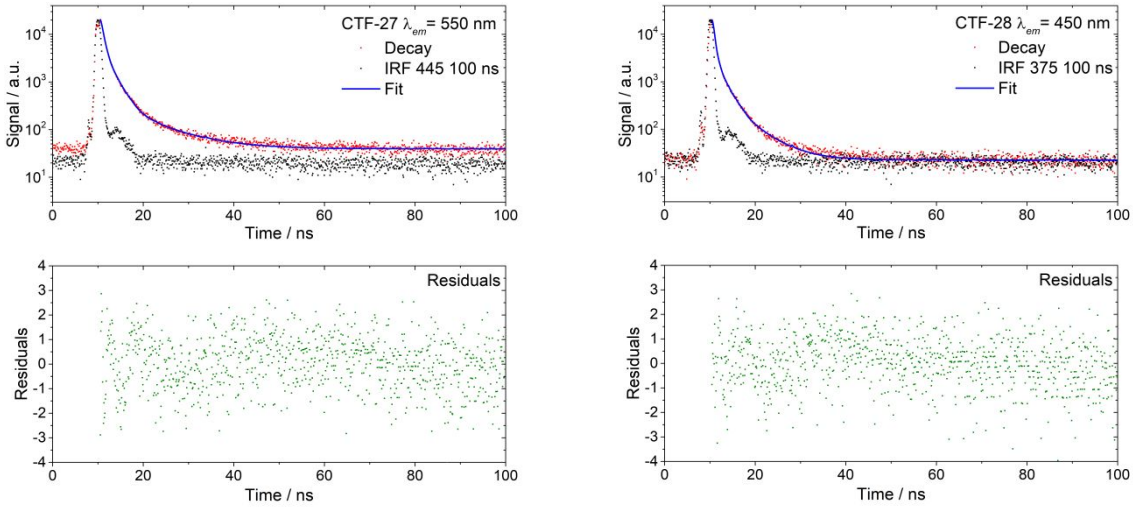

Figure S-60: Time-correlated single-photon counting measurement of CTF-27 and CTF-28 in the solid state.

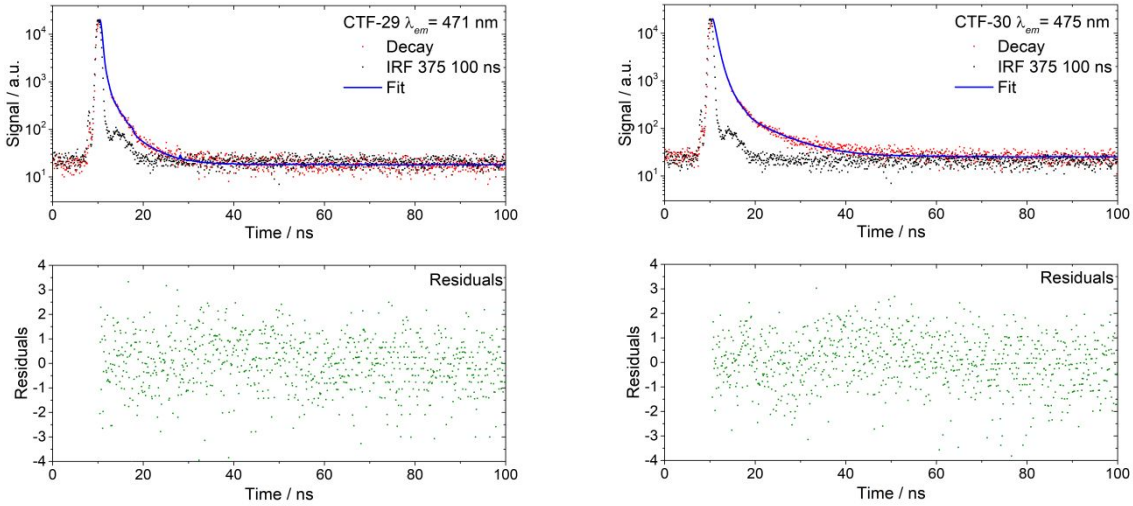

Figure S-61: Time-correlated single-photon counting measurement of CTF-29 and CTF-30 in the solid state.

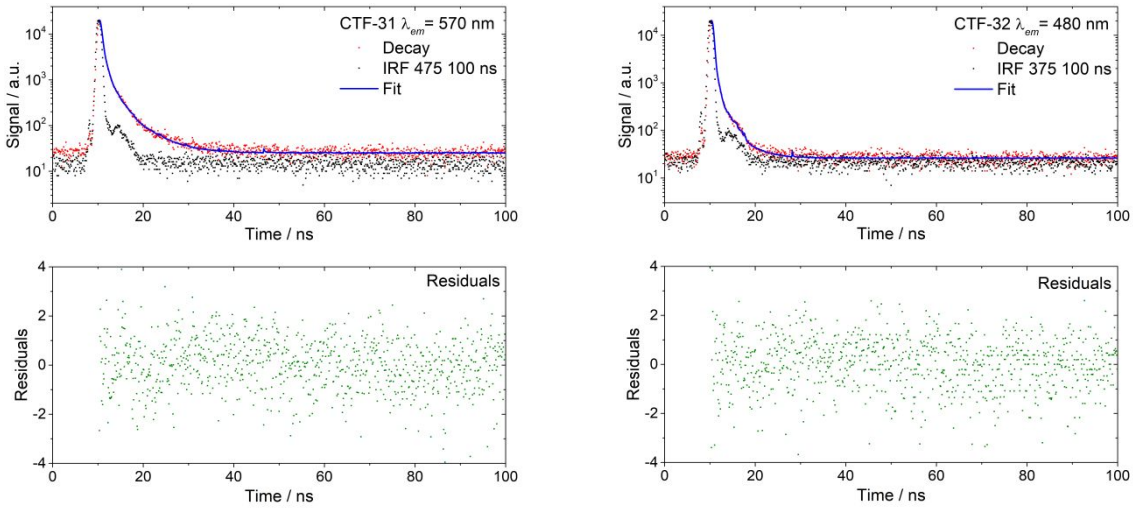

Figure S-62: Time-correlated single-photon counting measurement of CTF-31 and CTF-32 in the solid state.

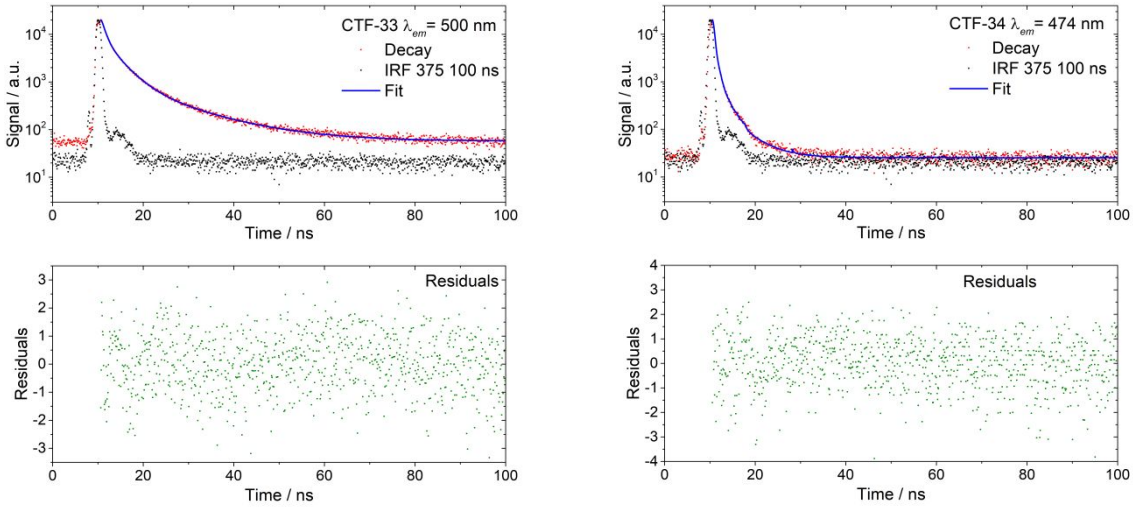

Figure S-63: Time-correlated single-photon counting measurement of CTF-33 and CTF-34 in the solid state.

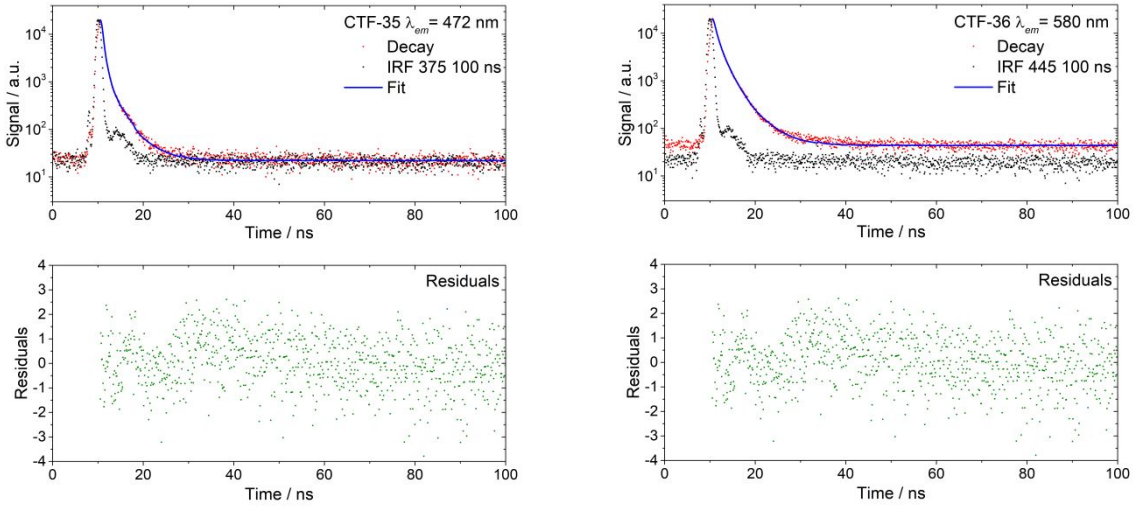

Figure S-64: Time-correlated single-photon counting measurement of CTF-35 and CTF-36 in the solid state.

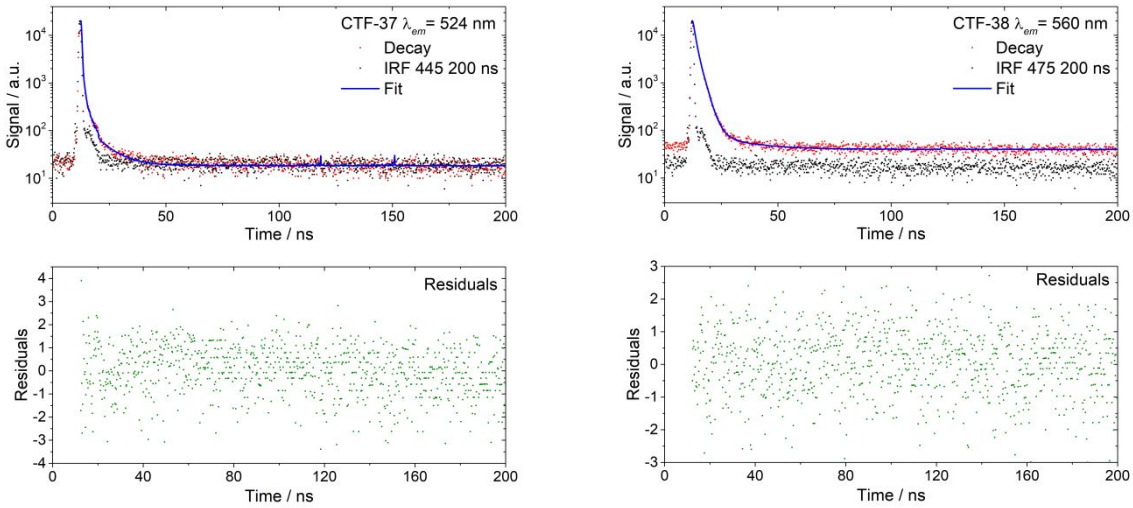

Figure S-65: Time-correlated single-photon counting measurement of CTF-37 and CTF-38 in the solid state.

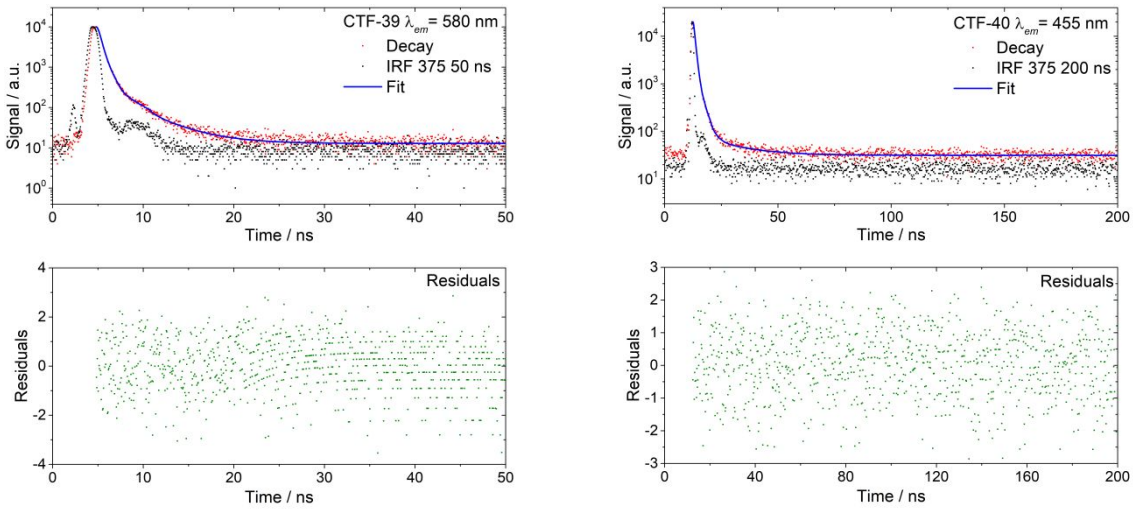

Figure S-66: Time-correlated single-photon counting measurement of CTF-39 and CTF-40 in the solid state.

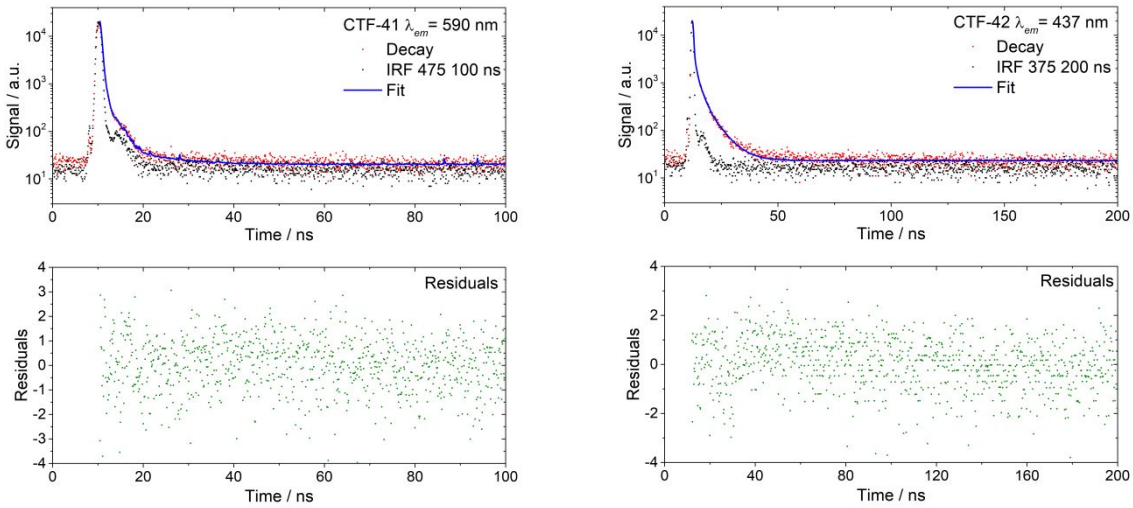

Figure S-67: Time-correlated single-photon counting measurement of CTF-41 and CTF-42 in the solid state.

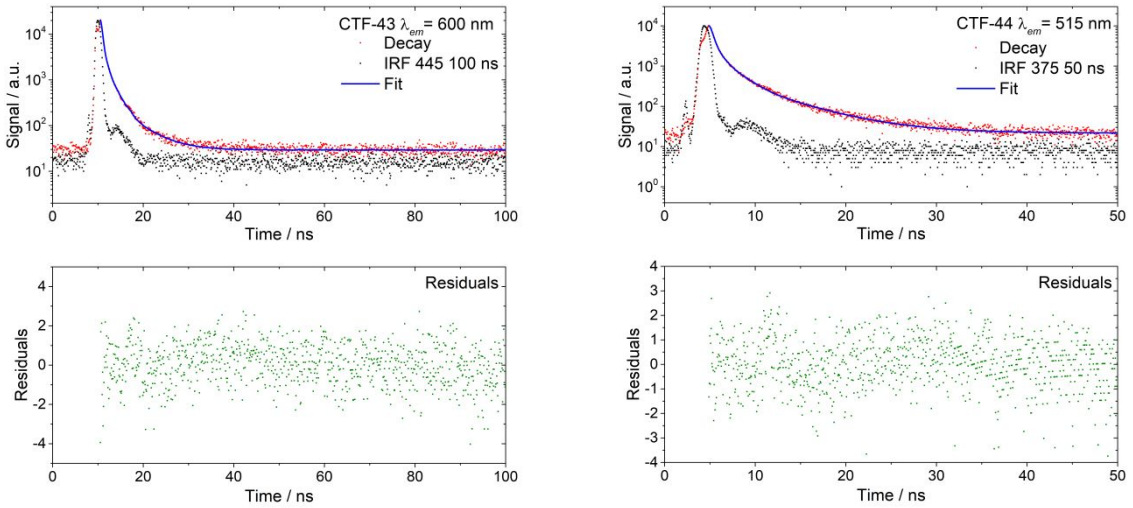

Figure S-68: Time-correlated single-photon counting measurement of CTF-43 and CTF-44 in the solid state.

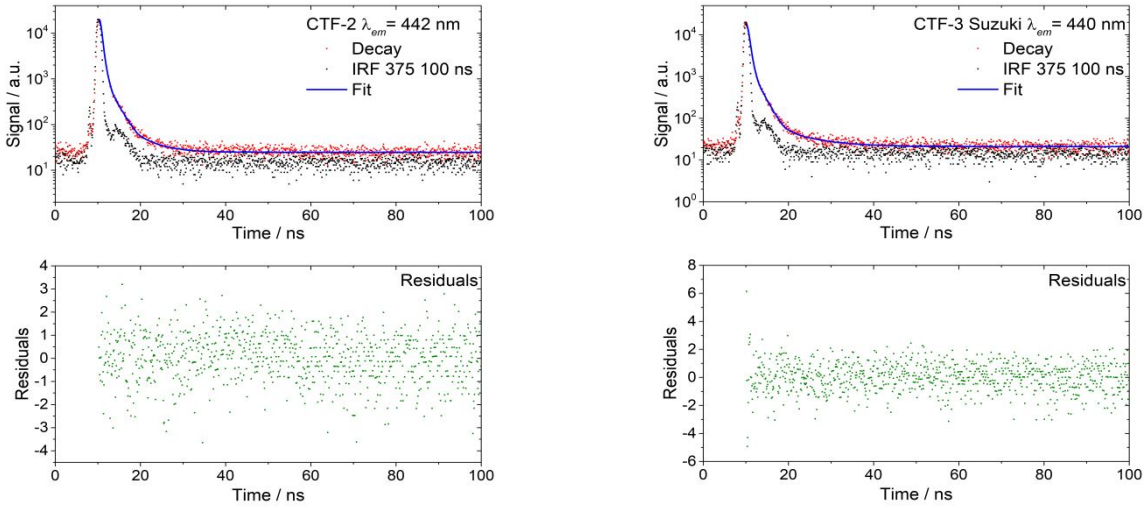

Figure S-69: Time-correlated single-photon counting measurement of CTF-2 and CTF-3 Suzuki in the solid state.

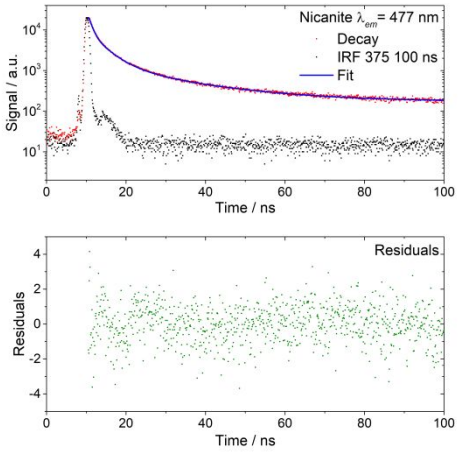

Figure S-70: Time-correlated single-photon counting measurement of Nicanite in the solid state.

Table S-5: Time-correlated single-photon counting results.

Polymer	$\lambda_{excitation}$ / nm	$\lambda_{emission}$ / nm	τ1 / ns	τ2 / ns	τ3 / ns	χ^2	B1 / %	B2 / %	B3 / %	τ_{avg}[a] / ns
CTF-5	375	560	1.142	2.872	15.488	1.047	61.861	33.881	4.259	2.339
CTF-6	375	494	0.758	2.666	10.251	1.146	40.822	45.382	13.797	2.934
CTF-7	375	466	0.491	1.427	4.662	1.194	40.809	48.093	11.098	1.404
CTF-8	375	501	0.518	1.72	8.198	1.134	57.54	36.433	6.027	1.419
CTF-9	375	583	1.007	3.206	10.313	1.029	41.277	53.324	5.399	2.682
CTF-10	475	545	0.231	1.199	5.125	1.154	49.96	38.225	11.815	1.179
CTF-11	475	577	0.2	0.83	6.478	1.131	65.882	31.045	3.073	0.589
CTF-12	375	445	0.08	1.163	6.289	1.152	90.531	6.96	2.509	0.311
CTF-13	375	440	0.134	0.734	3.984	1.138	81.106	16.192	2.702	0.335
CTF-14	375	462	0.31	2.086	7.258	1.2	59.405	29.232	11.362	1.619
CTF-15	375	483	0.586	2.371	9.478	1.205	82.092	13.292	4.615	1.234
CTF-16	375	550	0.674	2.852	10.19	1.198	47.665	36.278	16.057	2.992
CTF-17	445	535	0.166	0.963	4.734	1.026	74.296	22.161	3.543	0.504
CTF-18	375	490	0.089	1.219	8.032	1.141	84.437	10.441	5.123	0.614
CTF-19	375	452	0.308	1.189	4.678	1.102	80.045	16.781	3.174	0.595
CTF-20	375	454	0.428	1.682	5.757	1.137	54.383	35.59	10.027	1.409
CTF-21	375	437	0.203	1.061	4.583	1.031	78.261	18.448	3.291	0.505
CTF-22	375	458	0.514	1.455	5.445	1.158	75.201	19.805	4.994	0.947
CTF-23	375	452	0.764	2.986	7.853	1.108	30.179	55.907	13.914	2.993
CTF-24	375	436	0.116	1.198	6.123	1.077	92.702	4.844	2.454	0.316
CTF-25	375	506	0.818	2.36	8.583	1.044	57.462	38.87	3.669	1.702
CTF-26	375	440	0.381	1.589	5.803	1.132	46.557	43.92	9.523	1.428
CTF-27	445	550	0.554	1.823	8.817	1.174	58.242	34.21	7.548	1.612
CTF-28	375	450	0.324	1.393	5.196	1.111	63.916	27.236	8.848	1.046
CTF-29	375	471	0.189	0.911	4.685	1.192	77.384	18.891	3.725	0.493
CTF-30	375	475	0.529	1.148	7.222	1.181	37.359	55.259	7.382	1.365
CTF-31	475	570	0.211	1.003	4.888	1.159	63.86	29.03	7.11	0.773
CTF-32	375	480	0.11	0.764	3.773	1.14	83.953	13.943	2.104	0.278
CTF-33	375	500	0.928	3.43	12.742	1.054	37.448	42.437	20.115	4.366
CTF-34	375	474	0.191	0.948	4.618	1.06	68.385	27.272	4.342	0.59
CTF-35	375	472	0.25	0.894	3.693	1.194	62.148	31.625	6.227	0.668

[a] Fluorescence life-times for all polymers obtained from fitting time-correlated single photon counting decays to a sum of three exponentials, which yield τ_1, τ_2, and τ_3 according to $\sum_{i=1}^{n}(A + B_i \exp(-t/\tau_i))$. τ_{AVG} is the weighted average lifetime calculated as $\sum_{i=1}^{n} B_i \tau_i$.

Table S-6: Time-correlated single-photon counting results.

Polymer	$\lambda_{excitation}$ / nm	$\lambda_{emission}$ / nm	τ1 / ns	τ2 / ns	τ3 / ns	χ^2	B1 / %	B2 / %	B3 / %	τ_{avg}[a] / ns
CTF-35	375	472	0.25	0.894	3.693	1.194	62.148	31.625	6.227	0.668
CTF-36	445	580	0.389	1.419	3.917	1.126	26.29	56.652	17.057	1.574
CTF-37	445	524	0.048	0.939	7.663	1.149	98.253	1.444	0.303	0.084
CTF-38	475	560	1.019	2.377	15.791	1.044	46.548	51.536	1.916	2.002
CTF-39	375	580	0.271	0.737	3.762	1.206	52.775	40.395	6.83	0.698
CTF-40	375	455	0.814	2.299	15.847	1.154	85.442	12.382	2.176	1.325
CTF-41	475	590	0.172	0.782	7.348	1.205	86.567	12.441	0.992	0.319
CTF-42	375	437	0.152	1.341	5.647	1.165	74.744	15.562	9.695	0.87
CTF-43	445	600	0.191	1.131	4.875	1.145	67.309	26.732	5.959	0.721
CTF-44	375	515	0.307	1.394	5.686	1.095	49.69	32.689	17.62	1.61
CTF-2	375	442	0.953	4.042	19.018	1.153	31.375	37.636	30.989	7.714
CTF-3 Suzuki	375	440	0.444	1.511	7.669	1.128	75.605	21.982	2.413	0.444
Nicanite	375	477	0.379	1.140	4.785	1.110	75.717	21.019	3.264	0.683

[a] Fluorescence life-times for all polymers obtained from fitting time-correlated single photon counting decays to a sum of three exponentials, which yield τ_1, τ_2, and τ_3 according to $\sum_{i=1}^{n}(A + B_i \exp(-t/\tau_i))$. τ_{AVG} is the weighted average lifetime calculated as $\sum_{i=1}^{n} B_i \tau_i$.

5. Hydrogen evolution of polymers

Table S-7: Overview of the hydrogen evolution rates for illumination λ > 420 nm and measured area on the high-throughput gas chromatograph.

Sample	H_2 Evolved / µmol g^{-1} h^{-1} for Xe-lamp λ > 420 nm[1]	H_2 Evolved / a.u. for the solar simulator (HT)[2]	H_2 Evolved / µmol g^{-1} h^{-1} for the solar simulator on the HT-setup[3]
CTF-5	20 ± 2	663066 ± 83700	1023 ± 129
CTF-6	8 ± 1	264636 ± 83700	408 ± 129
CTF-7	20 ± 6	366196 ± 83700	565 ± 129
CTF-8	371 ± 39	787848 ± 83700	1215 ± 129
CTF-9	63 ± 3	521594 ± 83700	805 ± 129
CTF-10	1412 ± 63	1879770 ± 37429	2900 ± 58
CTF-11	1151 ± 29	1203520 ± 37429	1857 ± 58
CTF-12	1515 ± 66	1307910 ± 37429	2018 ± 58
CTF-13	72 ± 3	256851 ± 83700	396 ± 129
CTF-14	16 ± 2	158550 ± 83700	245 ± 129
CTF-15	2946 ± 381	2236820 ± 19003	3451 ± 31
CTF-16	1354 ± 133	913453 ± 37429	1409 ± 58
CTF-17	537 ± 30	711724 ± 83700	1098 ± 129
CTF-18	5 ± 1	26453 ± 83700	41 ± 129
CTF-19	1158 ± 78	1047180 ± 37429	1616 ± 58
CTF-20	87 ± 2	1278732 ± 83700	1973 ± 129
CTF-21	550 ± 28	1094090 ± 83700	1688 ± 129
CTF-22	413 ± 39	1233540 ± 83700	1903 ± 129
CTF-23	5 ± 1	211 ± 83700	0
CTF-24	0	52 ± 83700	0
CTF-25	548 ± 97	1180854 ± 37429	1822 ± 58
CTF-26	67 ± 1	708920 ± 83700	1094 ± 129
CTF-27	911 ± 37	1846820 ± 83700	2849 ± 129
CTF-28	119 ± 2	523284 ± 83700	807 ± 129
CTF-29	571 ± 37	1701600 ± 83700	2625 ± 129
CTF-30	1561 ± 150	1732470 ± 83700	2673 ± 129
CTF-31	650 ± 45	932254 ± 83700	1438 ± 129
CTF-32	1041 ± 70	2106120 ± 37429	3249 ± 129
CTF-33	260 ± 20	1174570 ± 83700	1812 ± 129
CTF-34	2373 ± 25	2102950 ± 19003	3245 ± 31
CTF-35	600 ± 22	1623260 ± 83700	2504 ± 129
CTF-36	160 ± 13	556118 ± 83700	858 ± 129
CTF-37	507 ± 33	824017 ± 83700	1271 ± 129
CTF-38	150 ± 15	873549 ± 83700	1348 ± 129
CTF-39	1151 ± 75	1404440 ± 37429	2167 ± 58
CTF-40	33 ± 3	138843 ± 83700	214 ± 129
CTF-41	0	397 ± 83700	0
CTF-42	100 ± 2	261811 ± 83700	404 ± 129
CTF-43	652 ± 45	1526450 ± 83700	2355 ± 129
CTF-44	44 ± 1	442557 ± 83700	683 ± 129
CTF-2	358 ± 21	1325510 ± 83700	2045 ± 129
CTF-3 Suzuki	158 ± 46	1043881 ± 83700	1611 ± 129
Nicanite	59 ± 3	678971 ± 83700	1047 ± 129

[1]25 mg polymer, 8.3 mL water, 8.3 mL triethylamine, 8.3 mL methanol and 3 wt. % Pt on the manual setup for 5 h and the standard error is given for the determined slope in the linear region of the evolution. [2]5 mg sample, 1.7 mL water, 1.7 mL triethylamine, 1.7 mL water and 3 wt. % for 2 h.

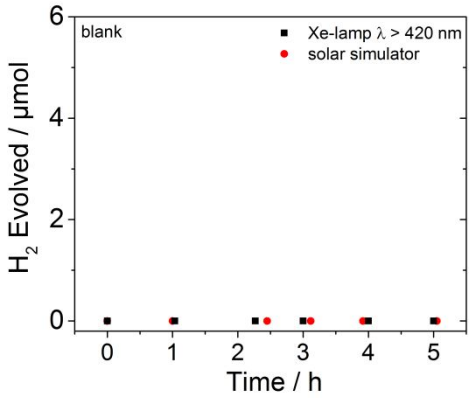

Figure S-71: Hydrogen evolution experiments in the absence of photocatalyst from 8.3 mL water, 8.3 mL triethylamine, 8.3 mL methanol and 3 wt. % Pt under visible light irradiation (300 W Xe light source, λ > 420 nm, kinetic measurements) and solar light (1 Sun, high-throughput)

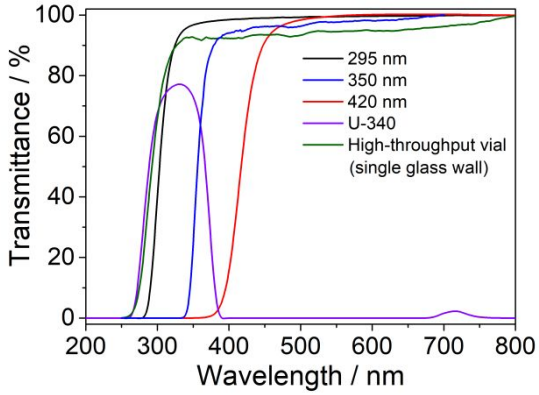

Figure S-72: Transmittance spectra of the filters used in kinetic measurements and the high-throughput vials.

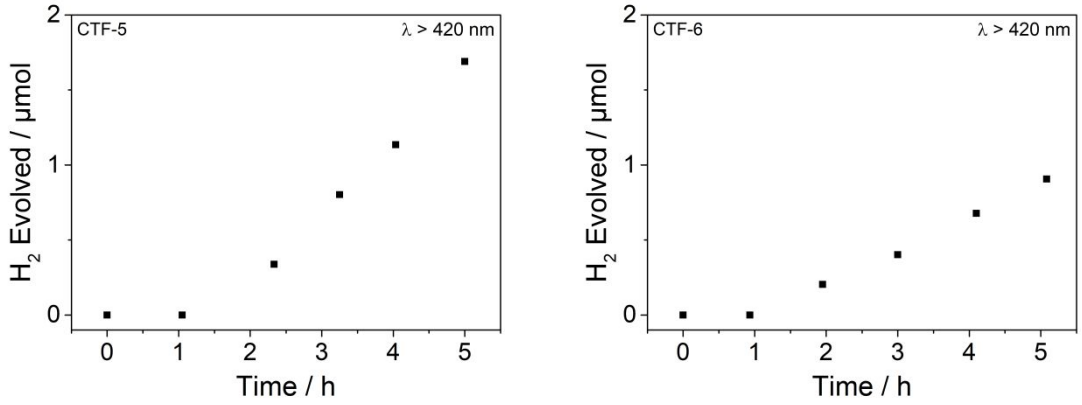

Figure S-73: Hydrogen evolution of CTF-5 (25 mg) and CTF-6 (25 mg) from 8.3 mL water, 8.3 mL triethylamine, 8.3 mL methanol and 3 wt. % Pt under visible light irradiation (300 W Xe light source, λ > 420 nm).

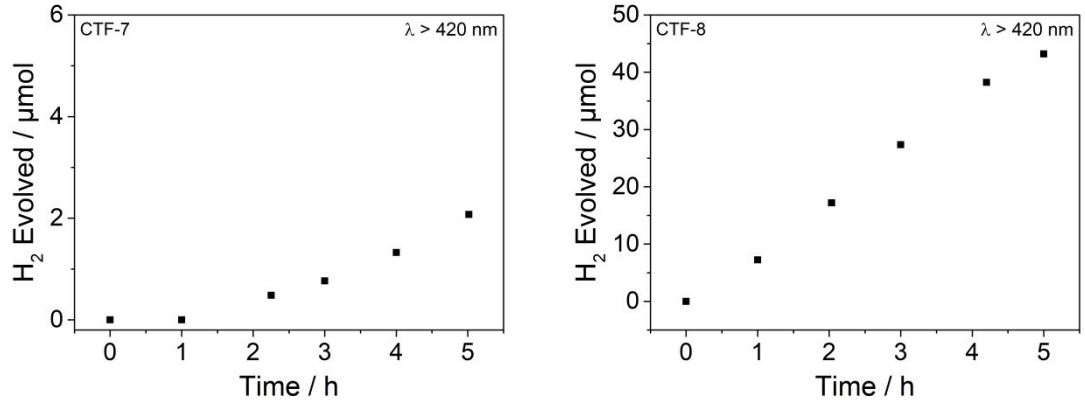

Figure S-74: Hydrogen evolution of CTF-7 (25 mg) and CTF-8 (25 mg) from 8.3 mL water, 8.3 mL triethylamine, 8.3 mL methanol and 3 wt. % Pt under visible light irradiation (300 W Xe light source, $\lambda > 420$ nm).

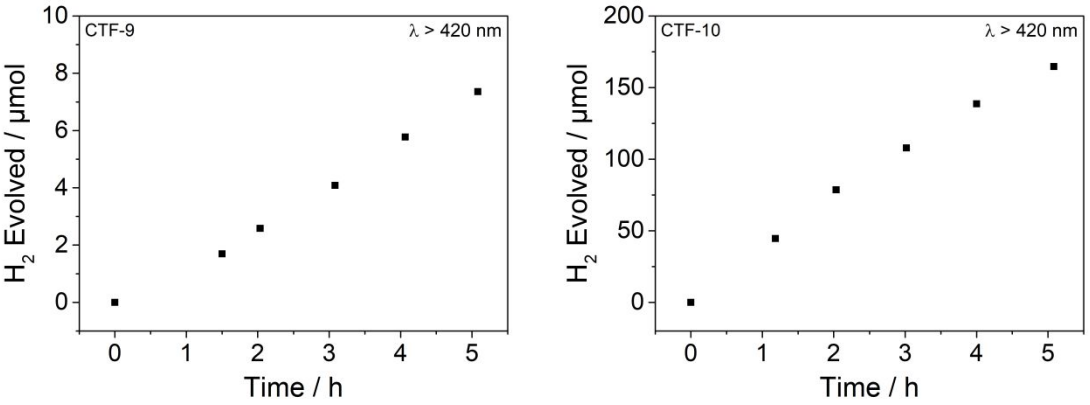

Figure S-75: Hydrogen evolution of CTF-9 (25 mg) and CTF-10 (25 mg) from 8.3 mL water, 8.3 mL triethylamine, 8.3 mL methanol and 3 wt. % Pt under visible light irradiation (300 W Xe light source, $\lambda > 420$ nm).

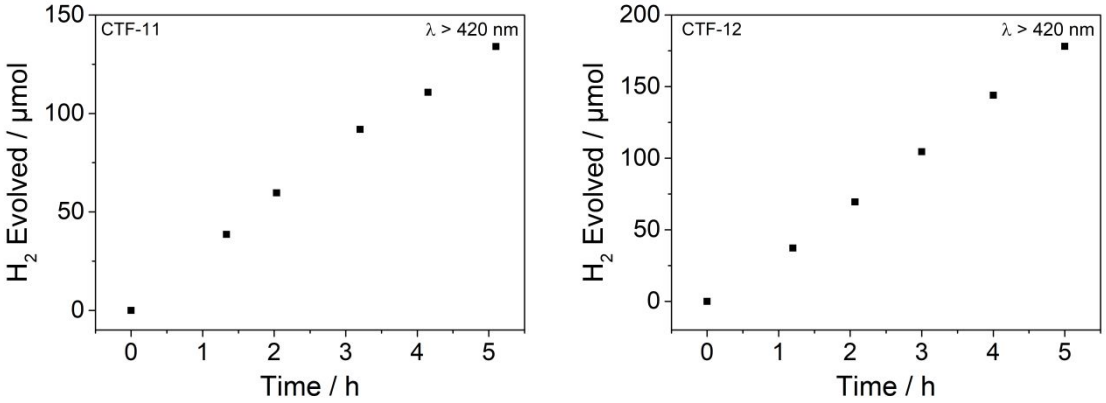

Figure S-76: Hydrogen evolution of CTF-11 (25 mg) and CTF-12 (25 mg) from 8.3 mL water, 8.3 mL triethylamine, 8.3 mL methanol and 3 wt. % Pt under visible light irradiation (300 W Xe light source, $\lambda > 420$ nm).

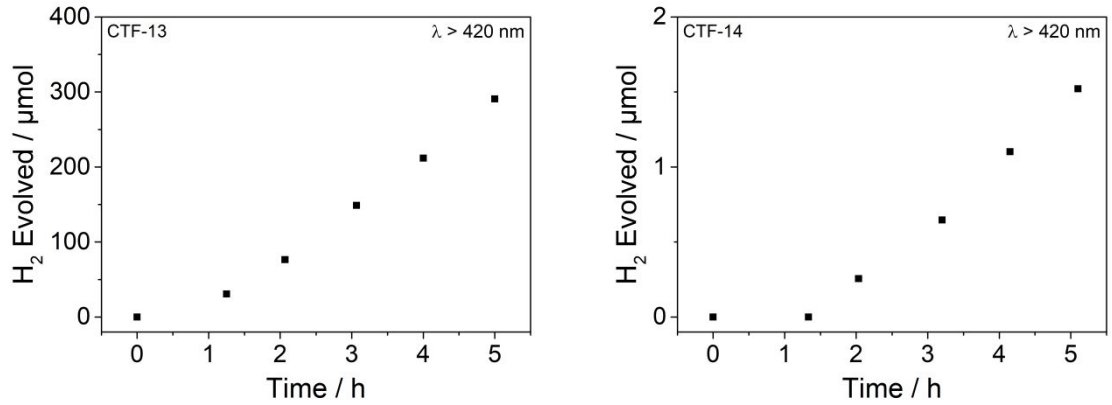

Figure S-77: Hydrogen evolution of CTF-13 (25 mg) and CTF-14 (25 mg) from 8.3 mL water, 8.3 mL triethylamine, 8.3 mL methanol and 3 wt. % Pt under visible light irradiation (300 W Xe light source, $\lambda > 420$ nm).

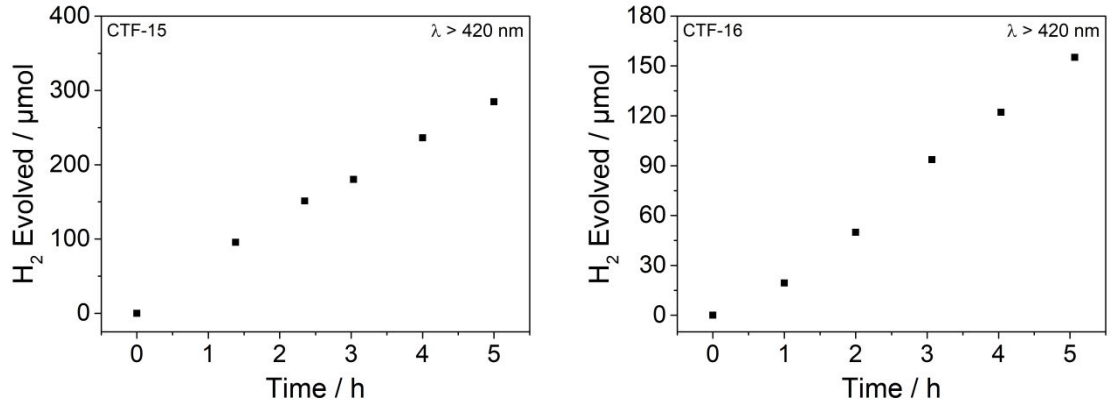

Figure S-78: Hydrogen evolution of CTF-15 (25 mg) and CTF-16 (25 mg) from 8.3 mL water, 8.3 mL triethylamine, 8.3 mL methanol and 3 wt. % Pt under visible light irradiation (300 W Xe light source, $\lambda > 420$ nm).

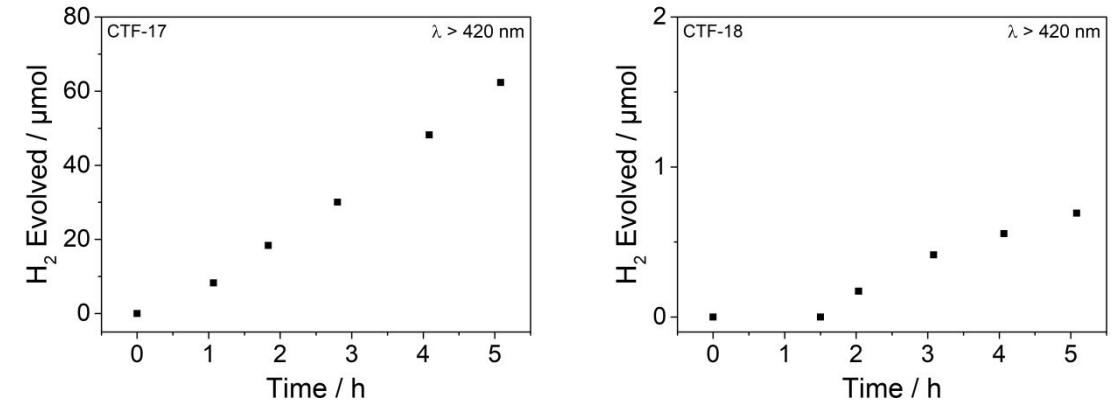

Figure S-79: Hydrogen evolution of CTF-17 (25 mg) and CTF-18 (25 mg) from 8.3 mL water, 8.3 mL triethylamine, 8.3 mL methanol and 3 wt. % Pt under visible light irradiation (300 W Xe light source, $\lambda > 420$ nm).

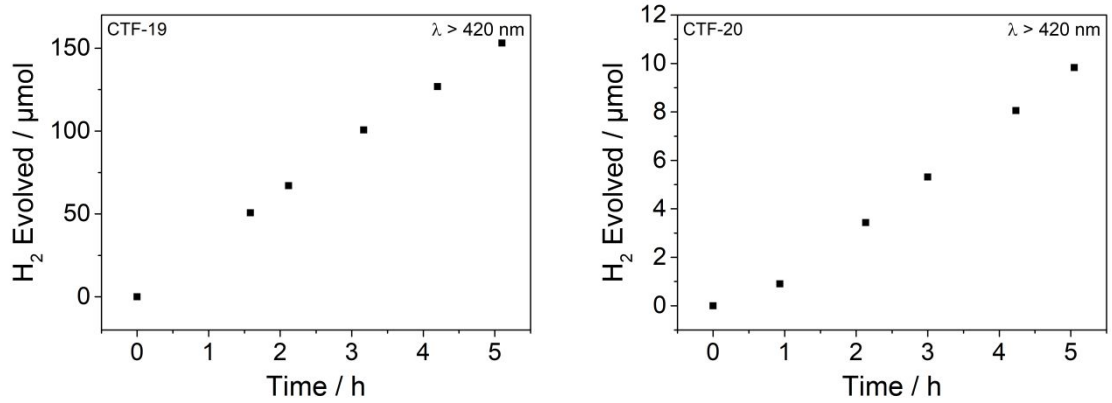

Figure S-80: Hydrogen evolution of CTF-19 (25 mg) and CTF-20 (25 mg) from 8.3 mL water, 8.3 mL triethylamine, 8.3 mL methanol and 3 wt. % Pt under visible light irradiation (300 W Xe light source, $\lambda > 420$ nm).

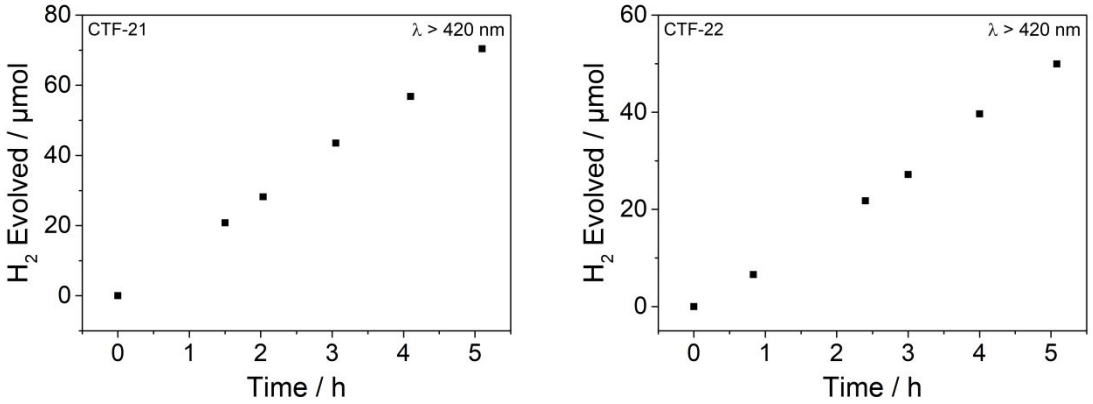

Figure S-81: Hydrogen evolution of CTF-21 (25 mg) and CTF-22 (25 mg) from 8.3 mL water, 8.3 mL triethylamine, 8.3 mL methanol and 3 wt. % Pt under visible light irradiation (300 W Xe light source, $\lambda > 420$ nm).

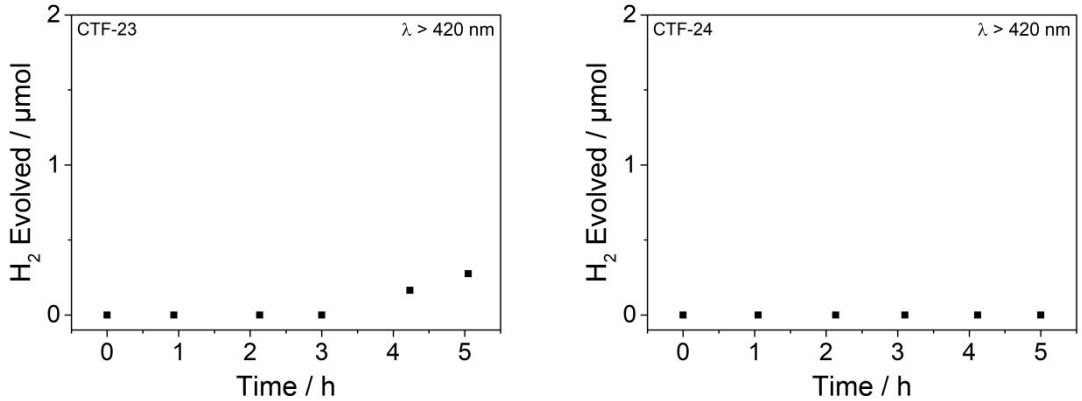

Figure S-82: Hydrogen evolution of CTF-23 (25 mg) and CTF-24 (25 mg) from 8.3 mL water, 8.3 mL triethylamine, 8.3 mL methanol and 3 wt. % Pt under visible light irradiation (300 W Xe light source, $\lambda > 420$ nm).

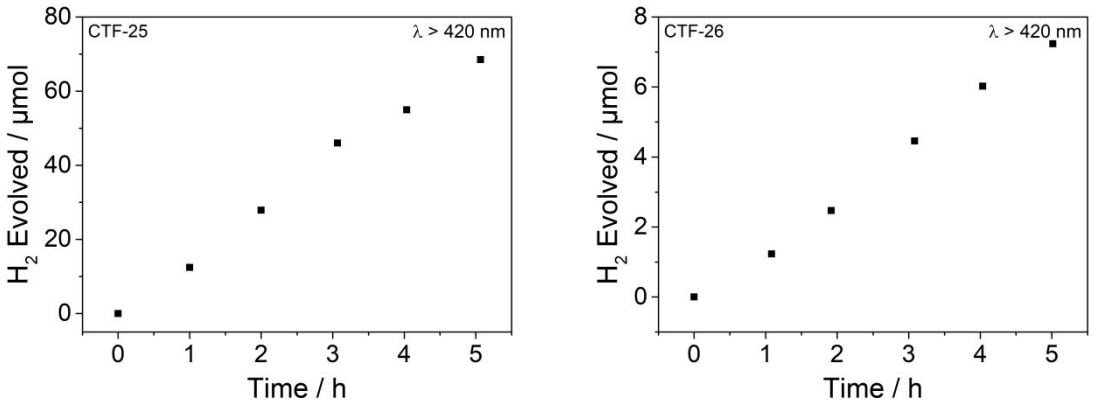

Figure S-83: Hydrogen evolution of CTF-25 (25 mg) and CTF-26 (25 mg) from 8.3 mL water, 8.3 mL triethylamine, 8.3 mL methanol and 3 wt. % Pt under visible light irradiation (300 W Xe light source, $\lambda > 420$ nm).

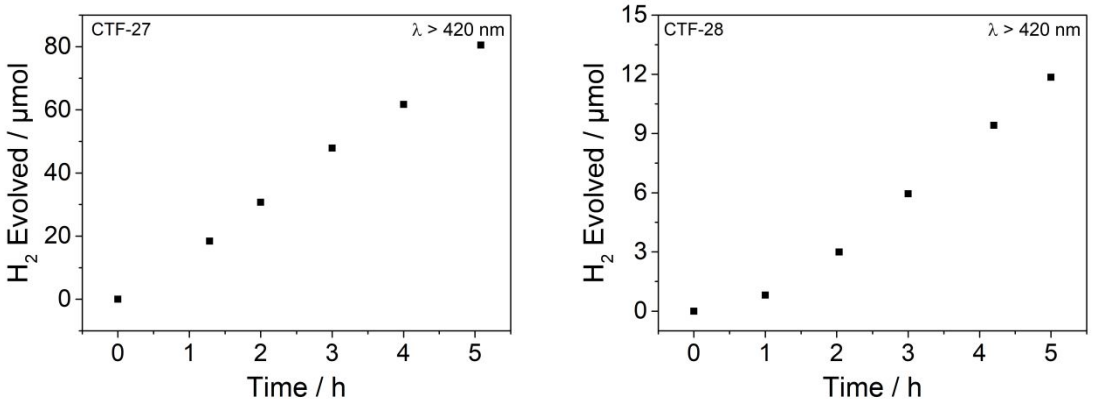

Figure S-84: Hydrogen evolution of CTF-27 (25 mg) and CTF-28 (25 mg) from 8.3 mL water, 8.3 mL triethylamine, 8.3 mL methanol and 3 wt. % Pt under visible light irradiation (300 W Xe light source, $\lambda > 420$ nm).

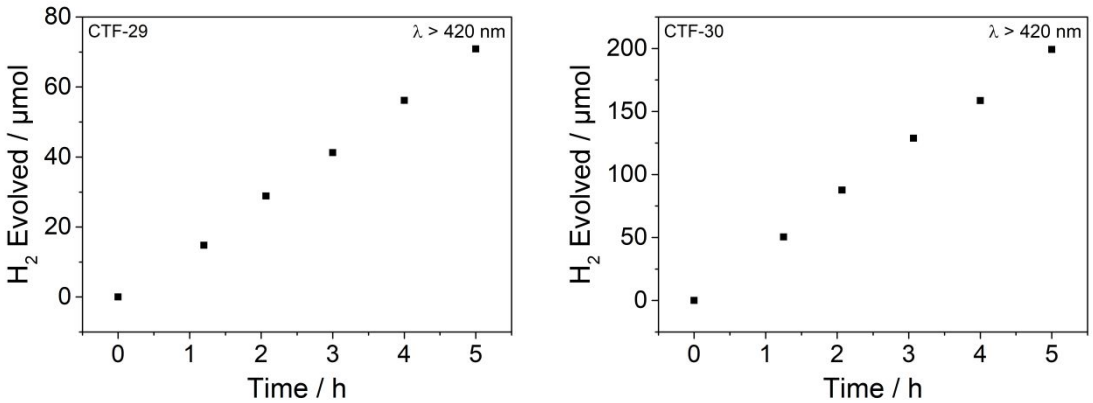

Figure S-85: Hydrogen evolution of CTF-29 (25 mg) and CTF-30 (25 mg) from 8.3 mL water, 8.3 mL triethylamine, 8.3 mL methanol and 3 wt. % Pt under visible light irradiation (300 W Xe light source, $\lambda > 420$ nm).

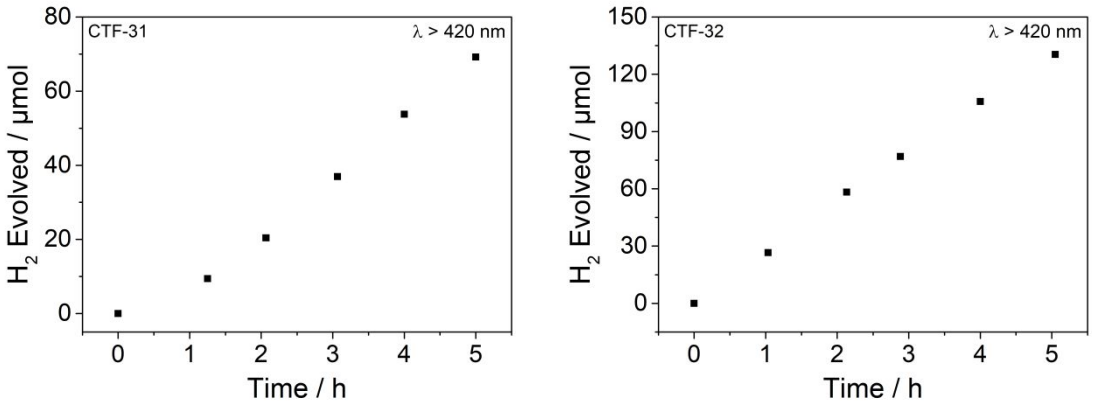

Figure S-86: Hydrogen evolution of CTF-31 (25 mg) and CTF-32 (25 mg) from 8.3 mL water, 8.3 mL triethylamine, 8.3 mL methanol and 3 wt. % Pt under visible light irradiation (300 W Xe light source, $\lambda > 420$ nm).

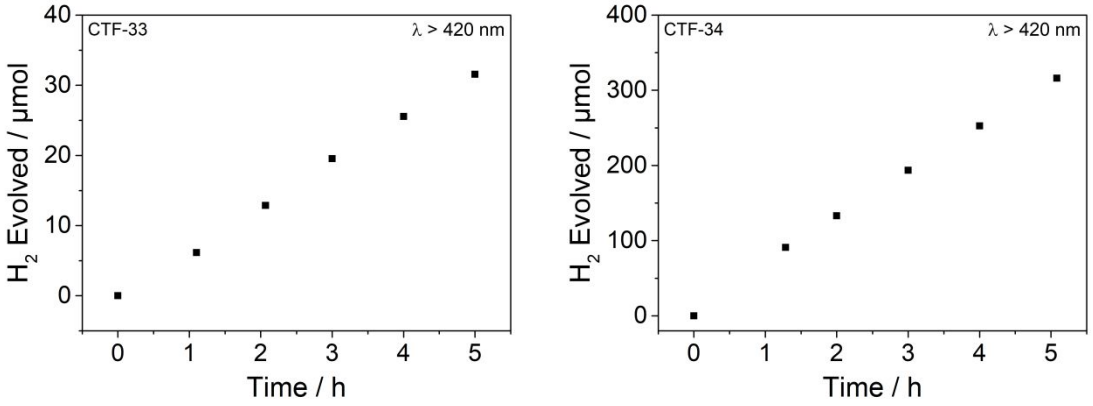

Figure S-87: Hydrogen evolution of CTF-33 (25 mg) and CTF-34 (25 mg) from 8.3 mL water, 8.3 mL triethylamine, 8.3 mL methanol and 3 wt. % Pt under visible light irradiation (300 W Xe light source, $\lambda > 420$ nm).

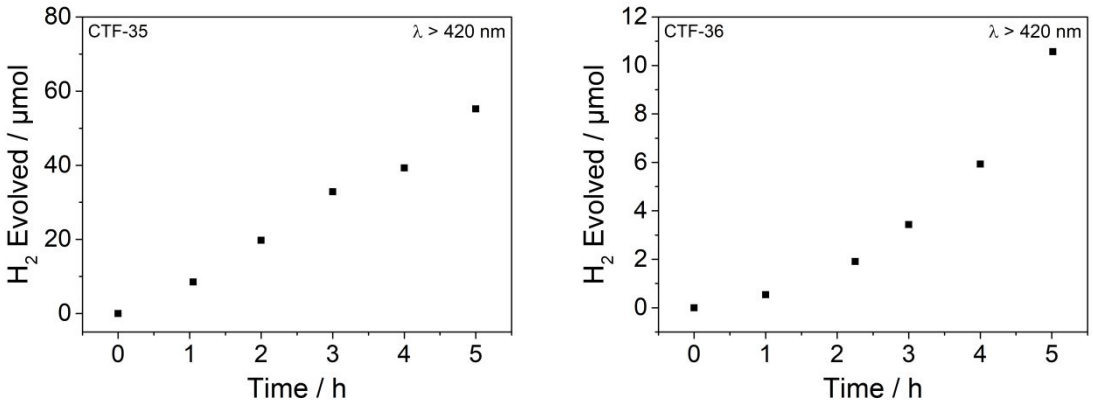

Figure S-88: Hydrogen evolution of CTF-35 (25 mg) and CTF-36 (25 mg) from 8.3 mL water, 8.3 mL triethylamine, 8.3 mL methanol and 3 wt. % Pt under visible light irradiation (300 W Xe light source, $\lambda > 420$ nm).

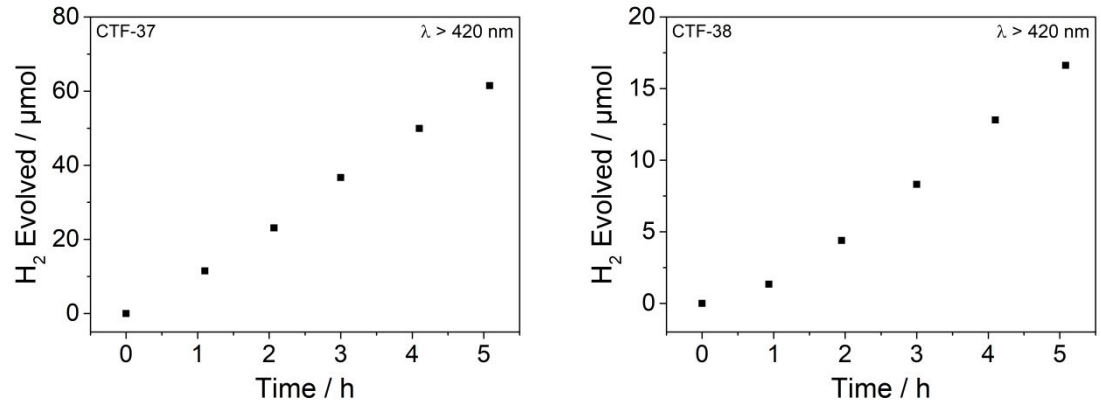

Figure S-89: Hydrogen evolution of CTF-37 (25 mg) and CTF-38 (25 mg) from 8.3 mL water, 8.3 mL triethylamine, 8.3 mL methanol and 3 wt. % Pt under visible light irradiation (300 W Xe light source, λ > 420 nm).

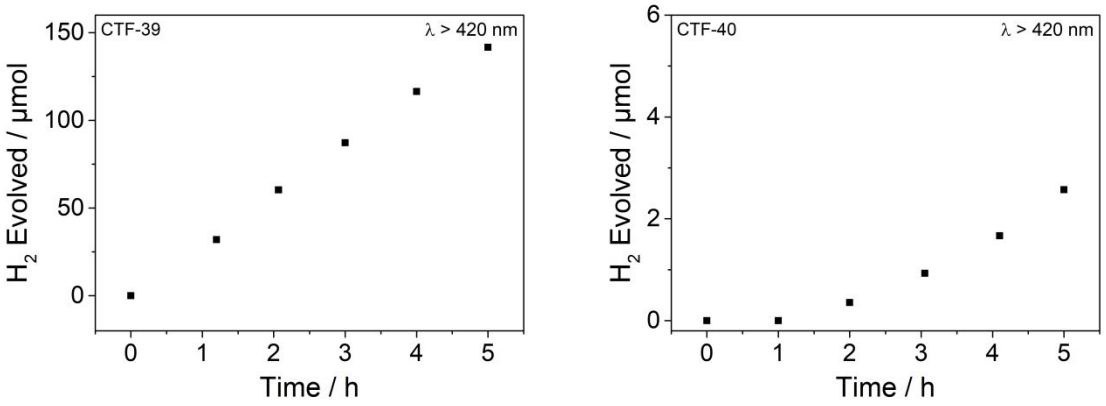

Figure S-90: Hydrogen evolution of CTF-39 (25 mg) and CTF-40 (25 mg) from 8.3 mL water, 8.3 mL triethylamine, 8.3 mL methanol and 3 wt. % Pt under visible light irradiation (300 W Xe light source, λ > 420 nm).

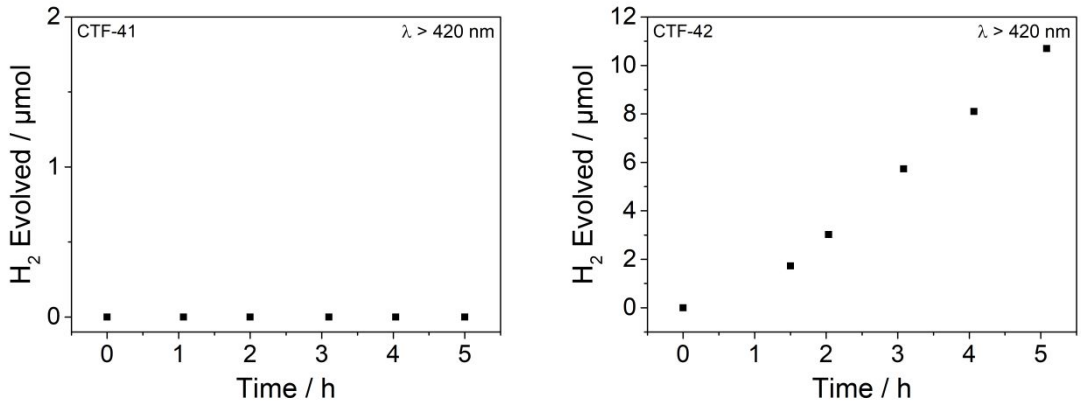

Figure S-91: Hydrogen evolution of CTF-41 (25 mg) and CTF-42 (25 mg) from 8.3 mL water, 8.3 mL triethylamine, 8.3 mL methanol and 3 wt. % Pt under visible light irradiation (300 W Xe light source, λ > 420 nm).

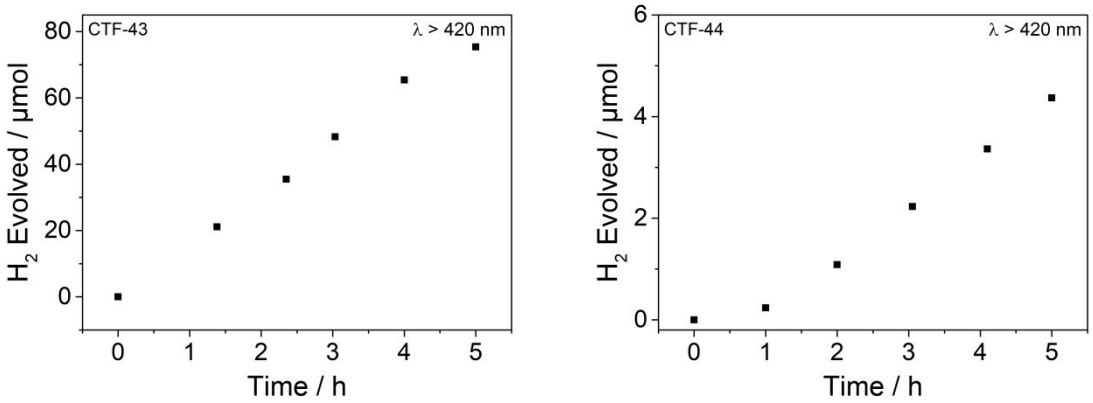

Figure S-92: Hydrogen evolution of CTF-43 (25 mg) and CTF-44 (25 mg) from 8.3 mL water, 8.3 mL triethylamine, 8.3 mL methanol and 3 wt. % Pt under visible light irradiation (300 W Xe light source, $\lambda > 420$ nm).

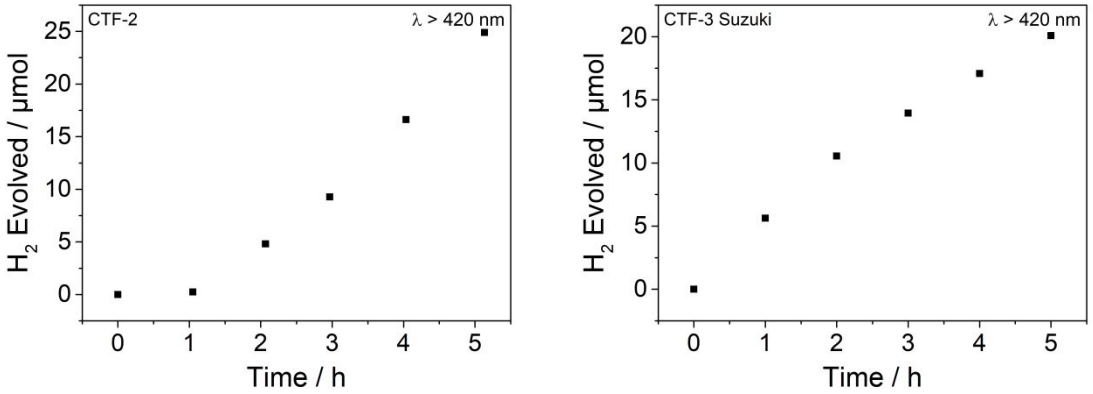

Figure S-93: Hydrogen evolution of CTF-2 (25 mg) and CTF-3 Suzuki (25 mg) from 8.3 mL water, 8.3 mL triethylamine, 8.3 mL methanol and 3 wt. % Pt under visible light irradiation (300 W Xe light source, $\lambda > 420$ nm).

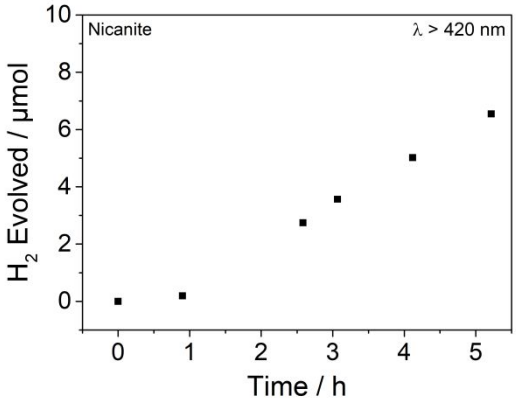

Figure S-94: Hydrogen evolution of commercial carbon nitride (25 mg) from 8.3 mL water, 8.3 mL triethylamine, 8.3 mL methanol and 3 wt. % Pt under visible light irradiation (300 W Xe light source, $\lambda > 420$ nm).

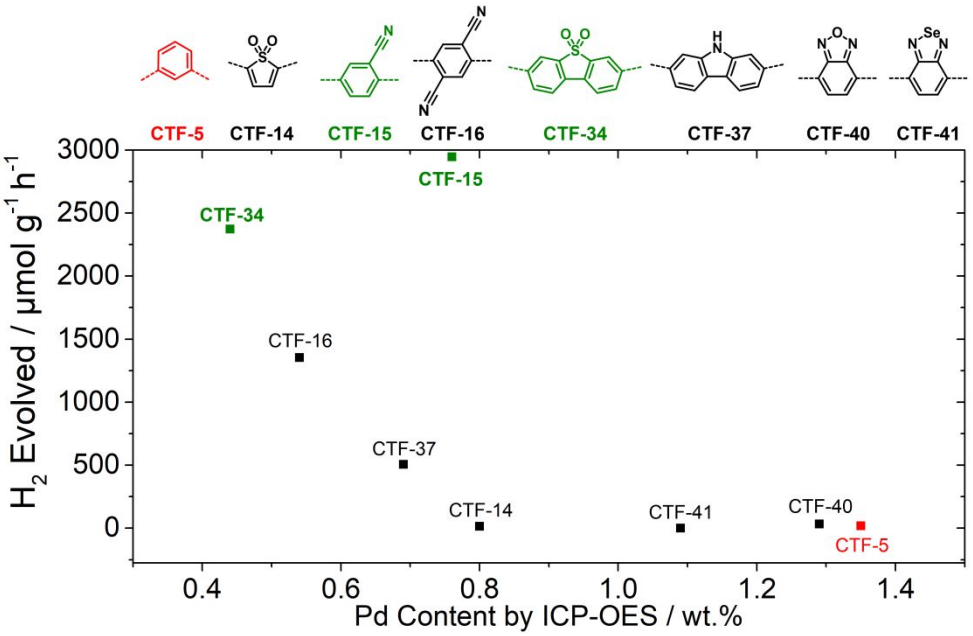

Figure S-95: Diagram of Pd content in the polymer, as determined by ICP-OES, against the hydrogen evolution rate under visible light (300 W Xe light source, $\lambda > 420$ nm, 25 mg catalyst, water/TEA/MeOH 1:1:1).

Table S-8: Table of Pd content in the polymers, as determined by ICP-OES.

Sample	Pd content by ICP-OES / wt. %
CTF-5	1.35
CTF-14	0.80
CTF-15	0.76
CTF-16	0.54
CTF-34	0.44
CTF-37	0.69
CTF-40	1.29
CTF-41	1.09

Conditions: 20 mg of samples were microwave digested using aqua regia. The resulting solutions were run on the ICP-OES instrument calibrated with yttrium internal standard and palladium calibration standards at 340 nm.

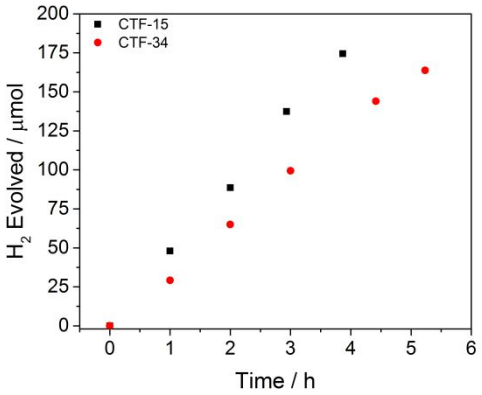

Figure S-96: Hydrogen evolution of as synthesized CTF-15 and CTF-34 (25 mg) from a 1:1:1 mixture of water/triethylamine/methanol under visible light irradiation (300 W Xe light source, $\lambda > 420$ nm) without additional co-catalysts.

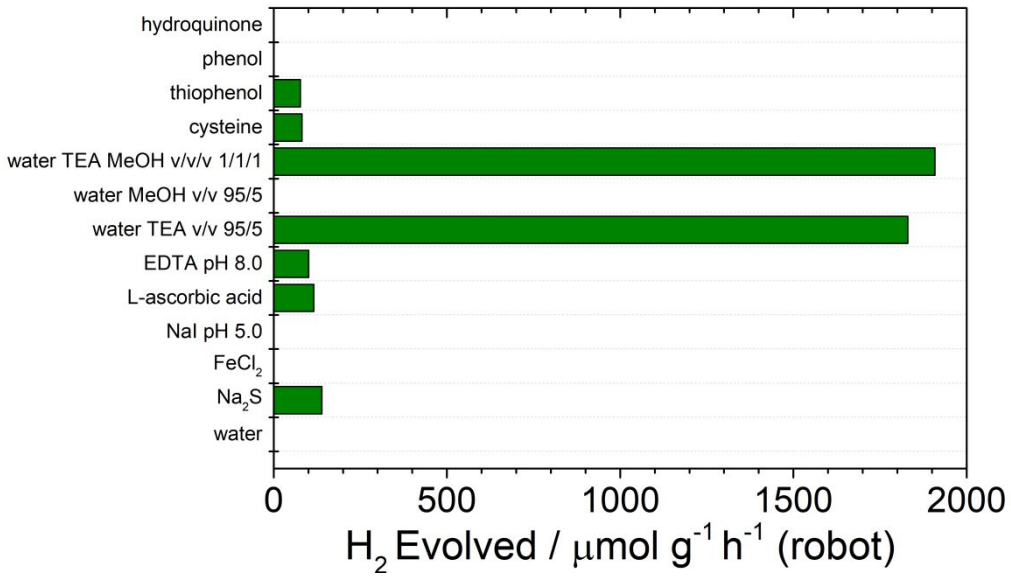

Figure S-97: Scavenger screening for CTF-15 under solar simulator irradiation (2 hours) on the high-throughput setup. Na_2S, $FeCl_2$, NaI pH 5.0, ascorbic acid, EDTA pH 8.0, cysteine, thiophenol, phenol, and hydroquinone were used with a concentration of 0.2 M.

Table S-9: Conversion of the scavenger screening for CTF-15.

Scavenger	Peak area HT / a.u.	Hydrogen evolution / µmol g^{-1} h^{-1}
No scavenger (pure water)	7	0
Na_2S	180131	139
$FeCl_2$	808	1
NaI pH 5.0	68	0
L-Ascorbic acid	215089	165
EDTA sodium salt pH 8.0	130726	100
Water/TEA v/v 95/5	2371991	1830
Water/MeOH v/v 95/5	496	1
Water/TEA/MeOH v/v/v 1/1/1	2475132	1910
Cystein	105912	82
Thiophenol	100049	77
Phenol	27	0
Hydroquinone	437	0

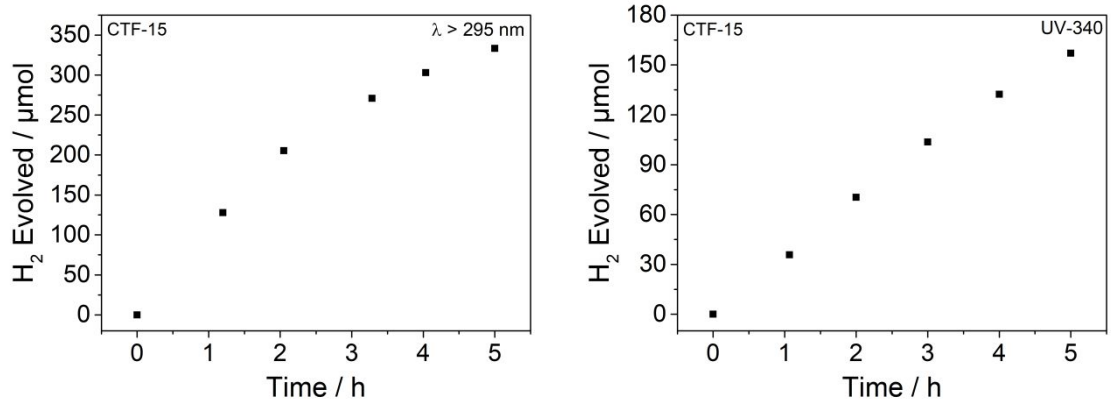

Figure S-98: Hydrogen evolution of CTF-15 (25 mg) from 8.3 mL water, 8.3 mL triethylamine, 8.3 mL methanol and 3 wt. % Pt under UV-visible light irradiation (λ > 295 nm, left) and UV-light (UV-340, right).

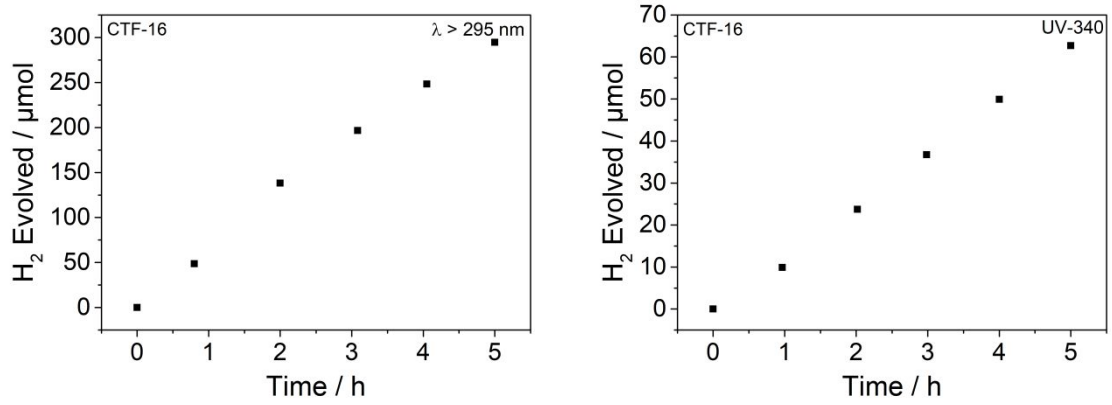

Figure S-99: Hydrogen evolution of CTF-16 (25 mg) from 8.3 mL water, 8.3 mL triethylamine, 8.3 mL methanol and 3 wt. % Pt under broad-band irradiation (300 W Xe light source, λ > 295 nm, left) and UV-light (300 W Xe light source, UV-340 filter, right).

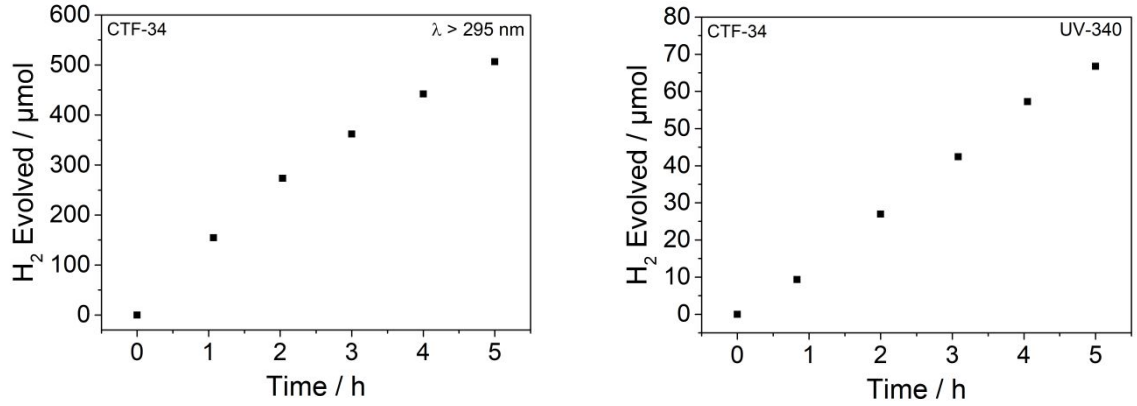

Figure S-100: Hydrogen evolution of CTF-34 (25 mg) from 8.3 mL water, 8.3 mL triethylamine, 8.3 mL methanol and 3 wt. % Pt under broad-band irradiation (300 W Xe light source, λ > 295 nm, left) and UV-light (300 W Xe light source, UV-340 filter, right).

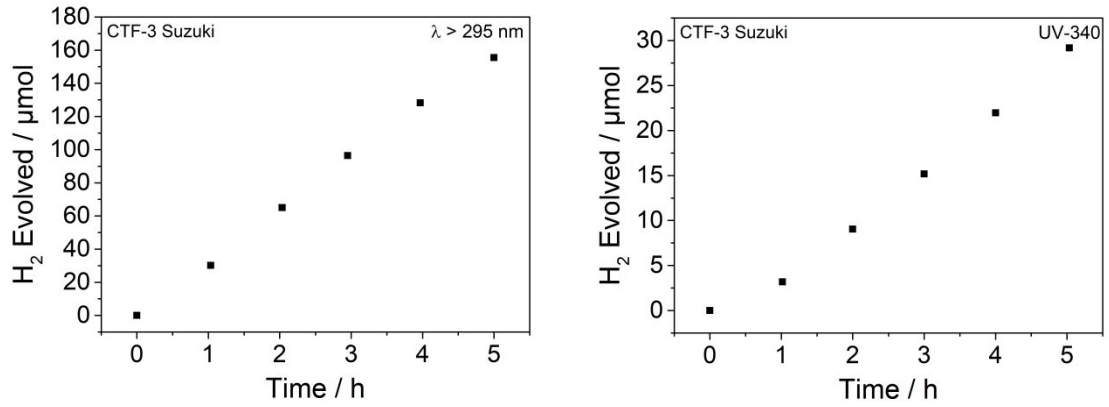

Figure S-101: Hydrogen evolution of CTF-3 Suzuki (25 mg) from 8.3 mL water, 8.3 mL triethylamine, 8.3 mL methanol and 3 wt. % Pt under broad-band irradiation (300 W Xe light source, λ > 295 nm, left) and UV-light (300 W Xe light source, UV-340 filter, right).

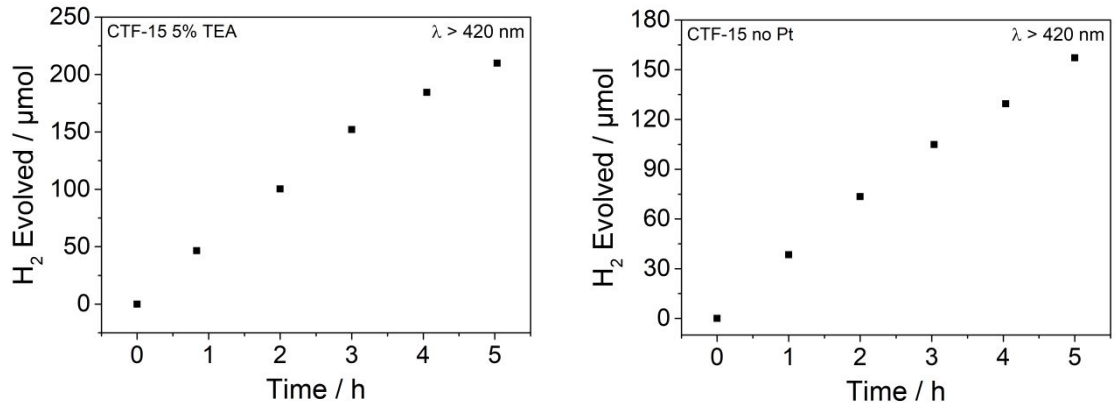

Figure S-102: Hydrogen evolution of CTF-15 (25 mg) from 25 mL water with 5 vol. % TEA under visible light irradiation (300 W Xe light source, $\lambda > 420$ nm, left) and CTF-15 (25 mg) from 8.3 mL water, 8.3 mL triethylamine, 8.3 mL methanol without platinum co-catalyst (300 W Xe light source, $\lambda > 420$ nm, right).

Table S-10: Overview of hydrogen evolution rates for further filters and scavengers with 3 wt% platinum co-catalyst.

Sample	H_2 Evolved / µmol g^{-1} h^{-1}	Light source and cut-off filter used	Scavenger
CTF-15	2622 ± 1268[a] / 4026 ± 244[b]	Xe LS 300 W λ > 295 nm	Water/TEA/MeOH
CTF-15	1274 ± 178	Xe LS 300 W UV-340	Water/TEA/MeOH
CTF-16	2383 ± 381	Xe LS 300 W λ > 295 nm	Water/TEA/MeOH
CTF-16	509 ± 39	Xe LS 300 W UV-340	Water/TEA/MeOH
CTF-34	4013 ± 1288[a] / 5384 ± 363[b]	Xe LS 300 W λ > 295 nm	Water/TEA/MeOH
CTF-34	552 ± 61	Xe LS 300 W UV-340	Water/TEA/MeOH
CTF-3 Suzuki	1270 ± 10	Xe LS 300 W λ > 295 nm	Water/TEA/MeOH
CTF-3 Suzuki	254 ± 54	Xe LS 300 W UV-340	Water/TEA/MeOH
CTF-15	1690 ± 467	Xe LS 300 W λ > 420 nm	Water/5 vol% TEA
CTF-15 no Pt	1242 ± 208	Xe LS 300 W λ > 420 nm	Water/TEA/MeOH
CTF-15	55 ± 5[c]	Xe LS 300 W λ > 420 nm	Ascorbic acid 0.2 M
CTF-15	100 ± 13	Xe LS 300 W λ > 350 nm	Ascorbic acid 0.2 M
CTF-15	277 ± 28	Xe LS 300 W λ > 295 nm	Ascorbic acid 0.2 M
CTF-15	50 ± 11	Solar simulator (ABA, LED system, no filter)	Ascorbic acid 0.2 M
CTF-15	122 ± 26	Xe LS 300 W λ > 420 nm	Sodium sulfide 0.2 M
CTF-15	170 ± 12	Xe LS 300 W λ > 420 nm	Sodium sulfide 0.2 M
CTF-15	224 ± 8	Xe LS 300 W λ > 295 nm	Sodium sulfide 0.2 M
CTF-15	172 ± 13[d]	Solar simulator (ABA, LED system, no filter)	Sodium sulfide 0.2 M

[a] Regression fit including standard deviation over 0-5 hours; [b] Regression fit including standard deviation over 0-2 hours; [c] Regression fit including standard deviation over 3-5 hours; [d] uncorrected result, control experiment of sodium sulfide had an evolution rate of 6 ± 1 µmol g^{-1} h^{-1} under broad-band illumination in absence a photocatalyst.

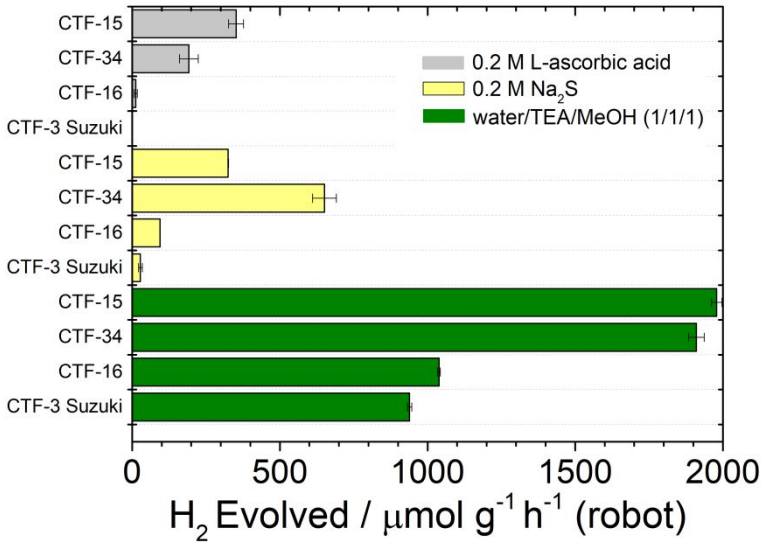

Figure S-103: Scavenger screening for hydrogen evolution: comparison of four polymers under solar irradiation (1 Sun) on the high-throughput setup.

Table S-11: Conversion of the scavenger screening for the polymers CTF-15, CTF-16, CTF-34, and CTF-3 Suzuki.

Scavenger	Peak area HT / a. u.	Hydrogen evolution rate[a] / µmol g^{-1} h^{-1}
CTF-3 Suzuki TEA water MeOH	1217313.5	939
CTF-16 TEA water MeOH	1347174.5	1039
CTF-34 TEA water MeOH	2475548.5	1910
CTF-15 TEA water MeOH	2564781	1979
CTF-3 Suzuki Na_2S	35942	28
CTF-16 Na_2S	123007	94
CTF-34 Na_2S	844368.5	651
CTF-15 Na_2S	421608	325
CTF-3 Suzuki ascorbic acid	21.5	0
CTF-16 ascorbic acid	15485.5	12
CTF-34 ascorbic acid	248990.5	192
CTF-15 ascorbic acid	456555	352

[a] Calibration using standard gas mixtures with a known concentration of H_2.

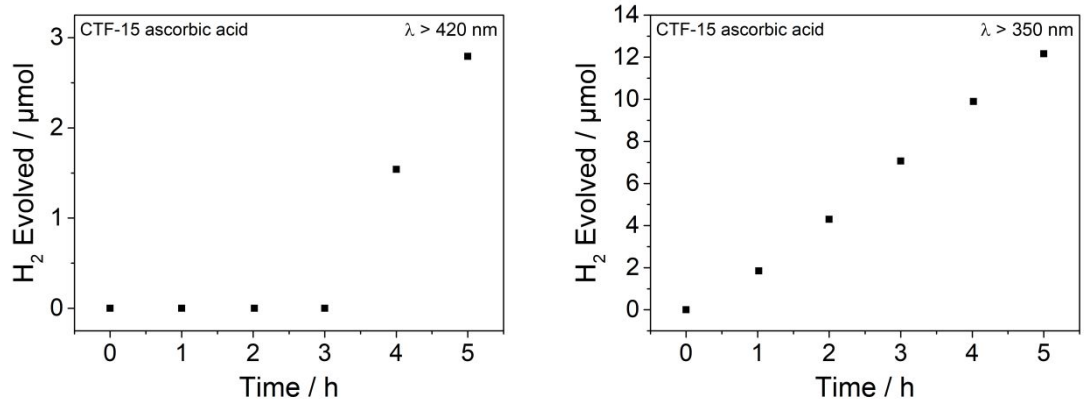

Figure S-104: Hydrogen evolution of CTF-15 (25 mg) from 25 mL 0.2 M ascorbic acid solution under visible light irradiation (300 W Xe light source, λ > 420 nm, left) and UV-visible light (300 W Xe light source, λ > 350 nm, right).

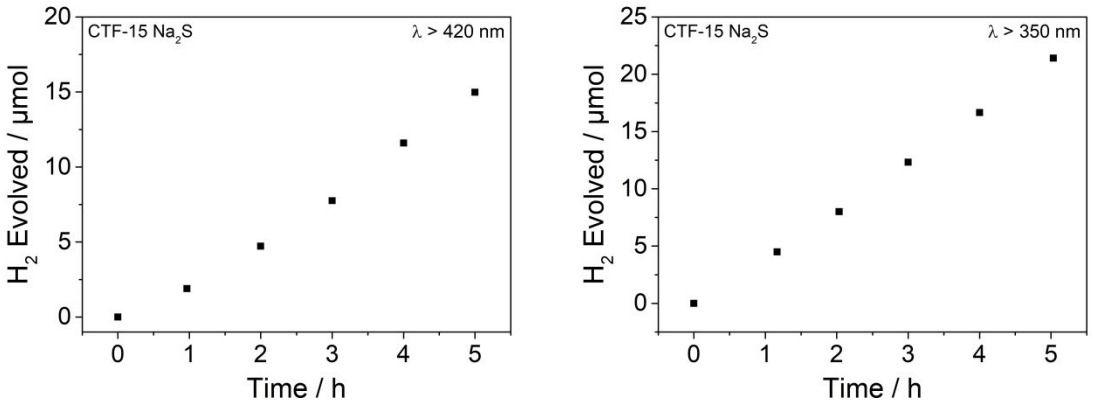

Figure S-105: Hydrogen evolution of CTF-15 (25 mg) from 25 mL 0.2 M sodium sulphide solution under visible light irradiation (300 W Xe light source, λ > 420 nm, left) and UV-visible light (300 W Xe light source, λ > 350 nm, right).

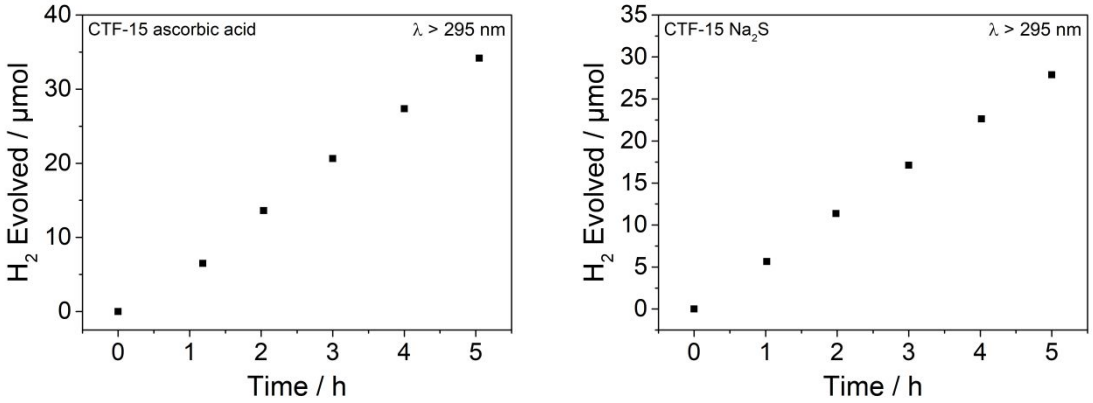

Figure S-106: Hydrogen evolution of CTF-15 (25 mg) from 25 mL 0.2 M L-ascorbic acid solution under UV-visible irradiation (300 W Xe light source, $\lambda > 295$ nm, left) CTF-15 (25 mg) from 25 mL 0.2 M sodium sulfide solution under UV-visible irradiation (300 W Xe light source, $\lambda > 295$ nm, right).

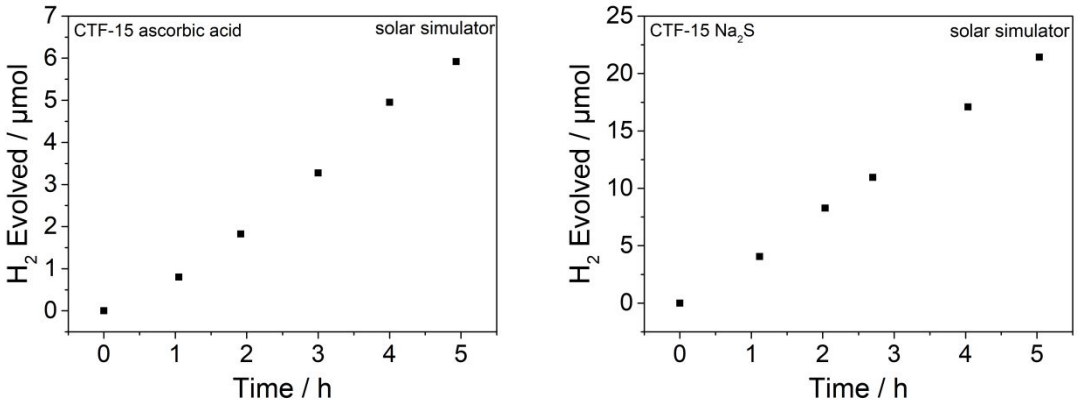

Figure S-107: Hydrogen evolution of CTF-15 (25 mg) from 25 mL 0.2 M ascorbic acid solution under solar light irradiation (1 Sun, left) CTF-15 (25 mg) from 25 mL 0.2 M sodium sulfide solution under solar light irradiation (1 Sun, right).

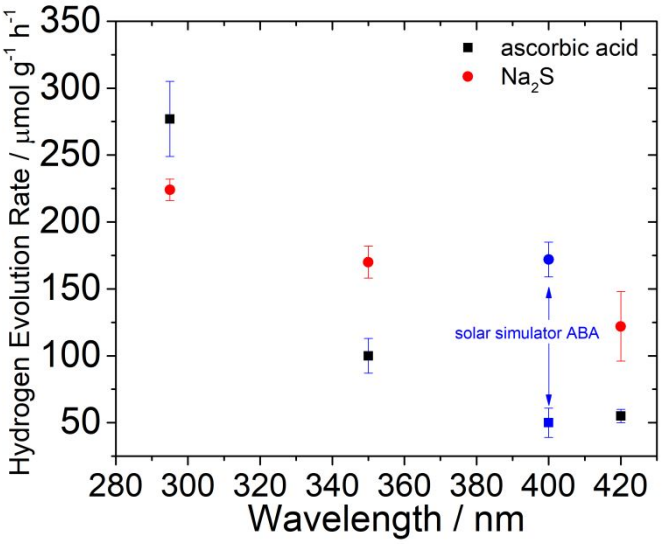

Figure S-108: Kinetic hydrogen evolution of CTF-15 (25 mg) from 25 mL scavenger solution and 3 wt. % Pt under λ > 295 nm, λ > 350 nm, λ > 420 nm (300 W Xe light source) and solar light irradiation (1 Sun, ABA).

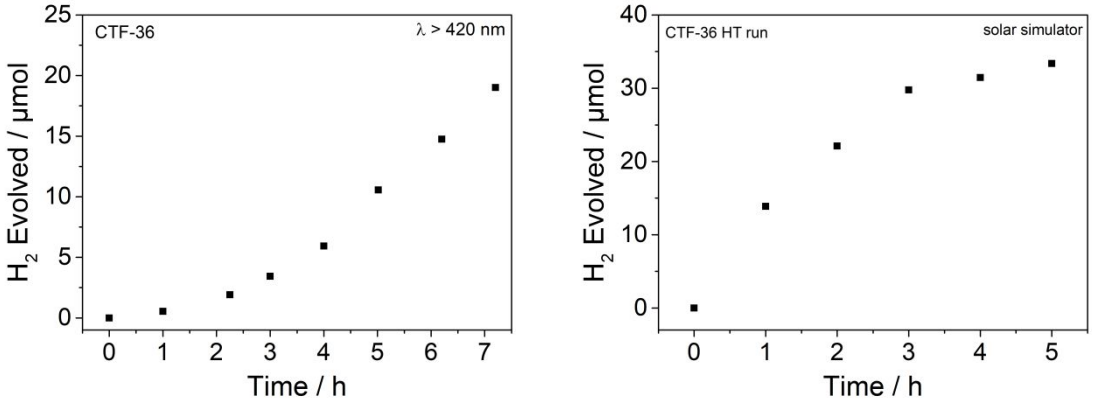

Figure S-109: Comparison of hydrogen evolution rates for CTF-36 on the manual setup and the HT setup. The measurements were carried out in water/TEA/MeOH with 3 wt. % platinum. For the kinetic measurement, 25 mg CTF-36 was used, and for the HT run, 5 mg of CTF-36 was used. The data shown in the HT run has been normalized to a quantity of 25 mg for comparison.

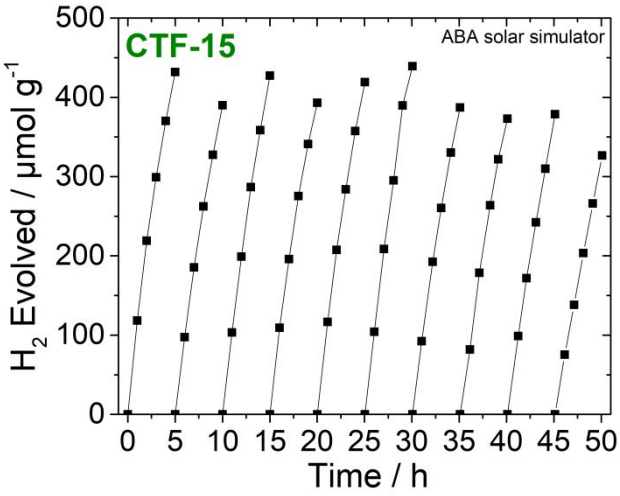

Figure S-110: Hydrogen evolution of CTF-15 (2,5-linked benzonitrile) tested in a long run under sacrificial conditions water/TEA/MeOH and 3 wt. % platinum co-catalyst under solar simulated light. The sample was reused from a previous, 50 hours run under λ > 420 nm irradiation (300 W Xe light source).

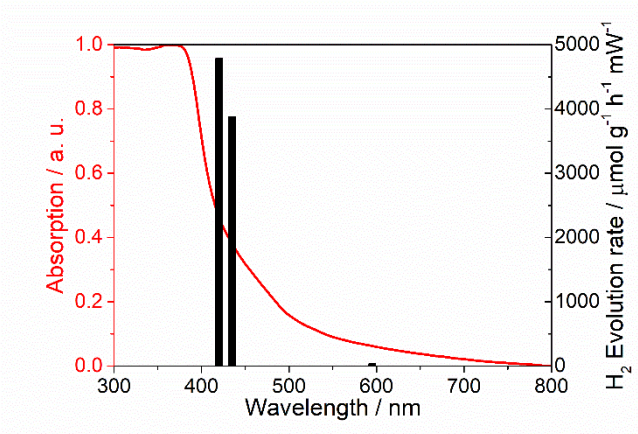

Figure S-111: UV-Vis absorption spectrum of CTF-15 (2,5-linked benzonitrile) and wavelength dependent hydrogen evolution experiments (8 mg photocatalyst, area illuminated = 7.8 cm^2) in water/TEA/MeOH with 3 wt. % platinum as co-catalyst using monochromated LEDs (420 nm, 435 nm, and 595 nm).

The photostability of CTF-15 (2,5-linked benzonitrile CTF) was tested over 50 hours under visible light illumination (λ > 420 nm, Xe light source) and showed no change of activity. The results rule out the photocatalyst as the source of hydrogen as more than 450 μmol hydrogen are evolved within in 6 hours, which is more than the amount of hydrogen present in the photocatalyst. The material was then test for further 50 hours on a solar simulator (Figure S-113), recovered and characterized. No changes in the UV-vis, photoluminescence, Raman and FT-IR spectra are observed after this extended run of a total of 100 hours. The nitrile band at 2226 cm^{-1} can still be identified in the FT-IR spectrum, which indicates that the material is very stable, although we cannot fully rule out partial hydrolysis of the nitrile groups.[3] The BET surface area of the material was slightly decreased from SA_{BET} = 383 $m^2 g^{-1}$ to 289 $m^2 g^{-1}$ after photocatalysis. This could be due to platinum particles blocking the pores, which are photodeposited onto the material during photocatalysis.

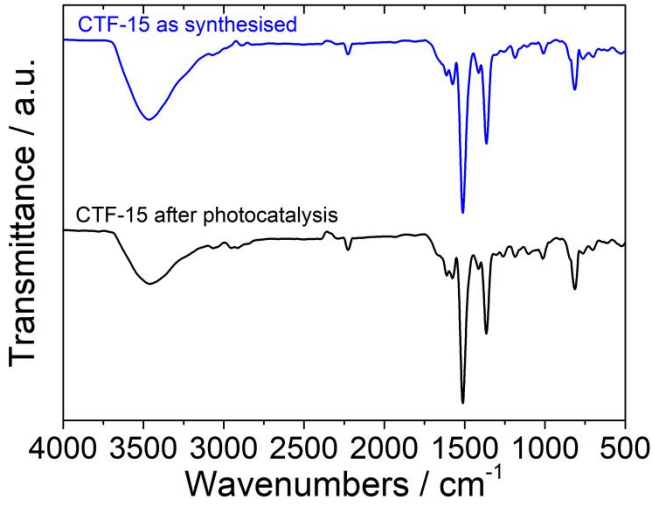

Figure S-112: FT-IR spectra for CTF-15 as synthesized and after photocatalysis for 100 hours.

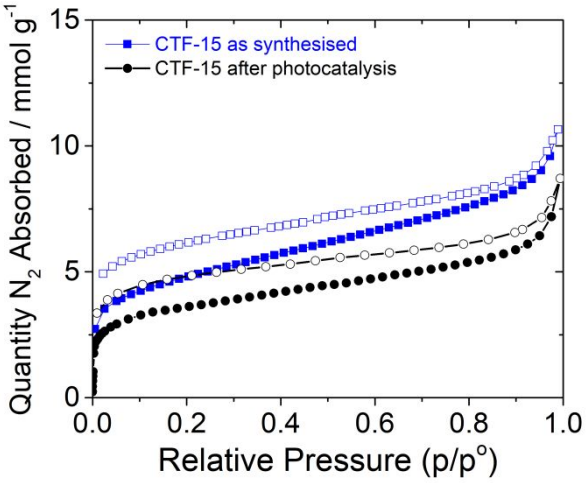

Figure S-113: Nitrogen sorption isotherms for CTF-15 as synthesized and after photocatalysis for 100 hours measured at 77.3 K and up to 1 bar (desorption curves shown as open symbols).

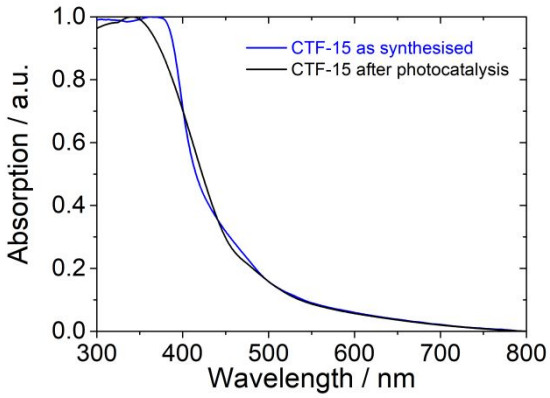

Figure S-114: Solid-state UV-Vis for CTF-15 as synthesized and after photocatalysis for 100 hours.

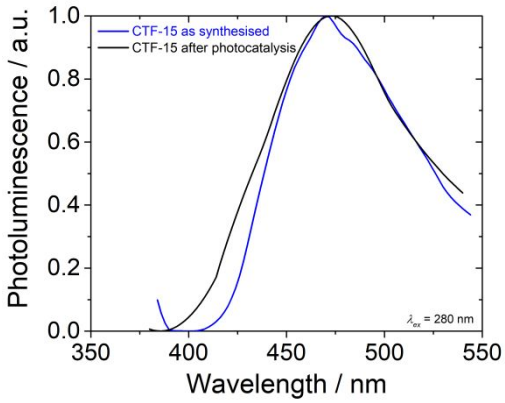

Figure S-115: Solid-state photoluminescence spectra ($\lambda_{excitation}$ = 280 nm) of CTF-15 as synthesized and after photocatalysis for 100 hours.

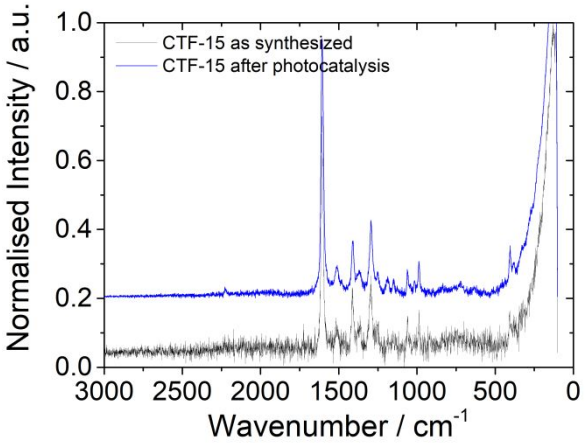

Figure S-116: Raman spectra for CTF-15 as synthesized and after photocatalysis for 100 hour measured on a CaF substrate (785 nm, 10% laser power, 100x objective).For clarity, the blue spectrum is shifted by +0.2 along the y-axis.

6. Comparison of measurements to hydrogen evolution rates on the manual setup

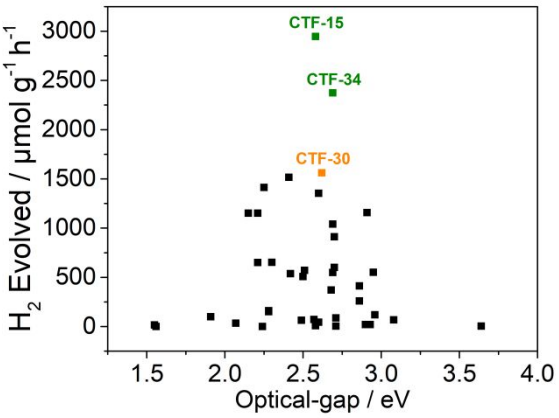

Figure S-117: Comparison of the optical-gap to the hydrogen evolution rates of CTFs form water/TEA/MeOH with 3 wt. % Pt.

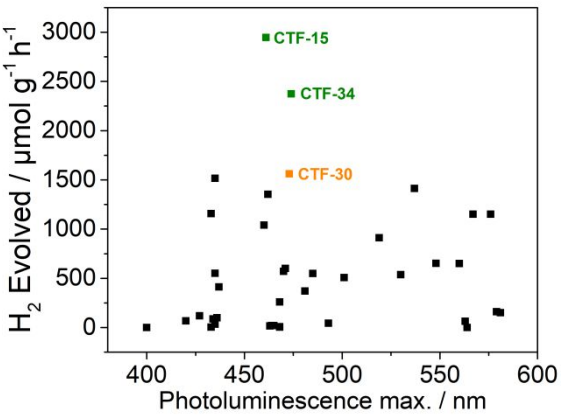

Figure S-118: Comparison of the photoluminescence to the hydrogen evolution rates of CTFs form water/TEA/MeOH with 3 wt. % Pt.

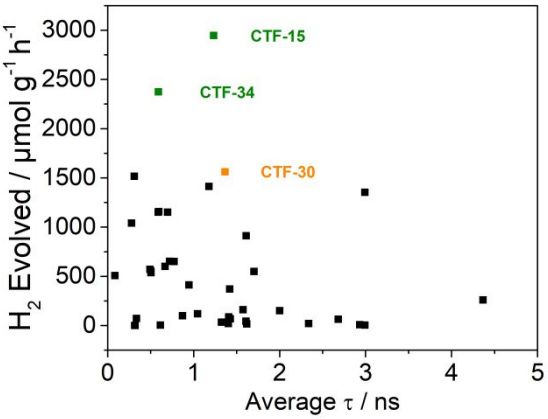

Figure S-119: Comparison of the fluorescence life-time spectroscopy (average weighted) to the hydrogen evolution rates of CTFs form water/TEA/MeOH with 3 wt. % Pt. In all cases the life-time of excited state is short with fitted average life-times ranging from 0.084 for CTF-37 (2,7-linked 9*H*-carbazole) to 4.366 ns for CTF-33 (2,6-linked pyridine).

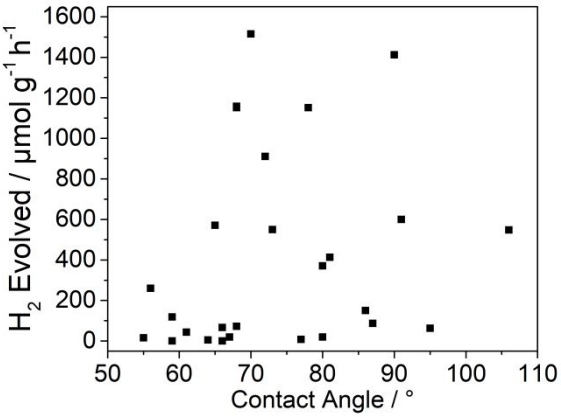

Figure S-120: Comparison of the contact angle to the hydrogen evolution rates of CTFs form water/TEA/MeOH with 3 wt. % Pt. In case of swelling, no contact angle was assigned (12 CTFs, including the three best performing hydrogen evolution catalysts CTF-15, CTF-32, and CTF-30).

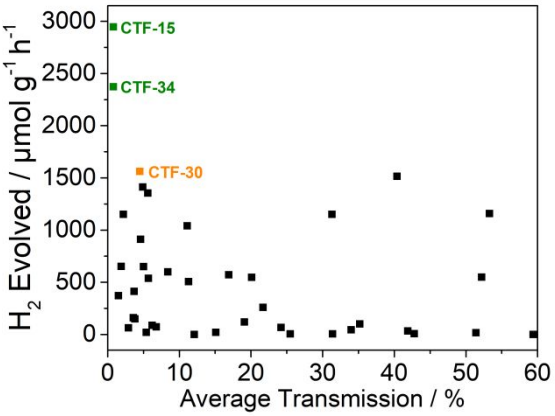

Figure S-121: Comparison of the light obscuration from water/TEA/MeOH to the hydrogen evolution rates of CTFs form water/TEA/MeOH with 3 wt. % Pt.

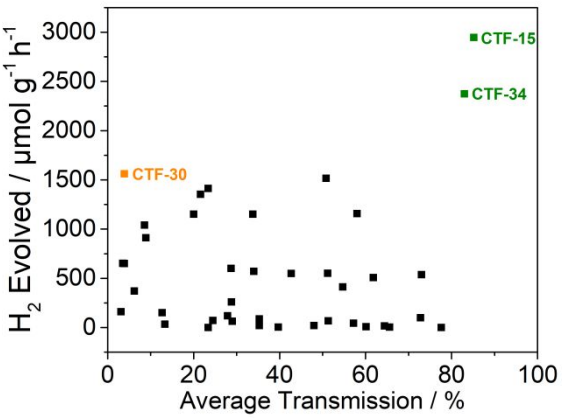

Figure S-122: Comparison of the light obscuration from water to the hydrogen evolution rates of CTFs form water/TEA/MeOH with 3 wt. % Pt.

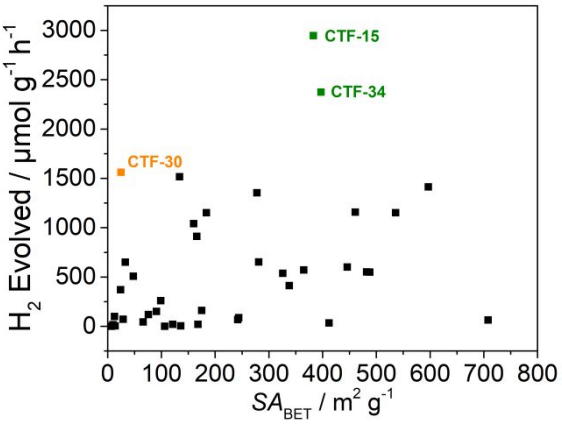

Figure S-123: Comparison of the surface area (SA_{BET}, N_2) to the hydrogen evolution rates of CTFs form water/TEA/MeOH with 3 wt. % Pt.

8. Calculations

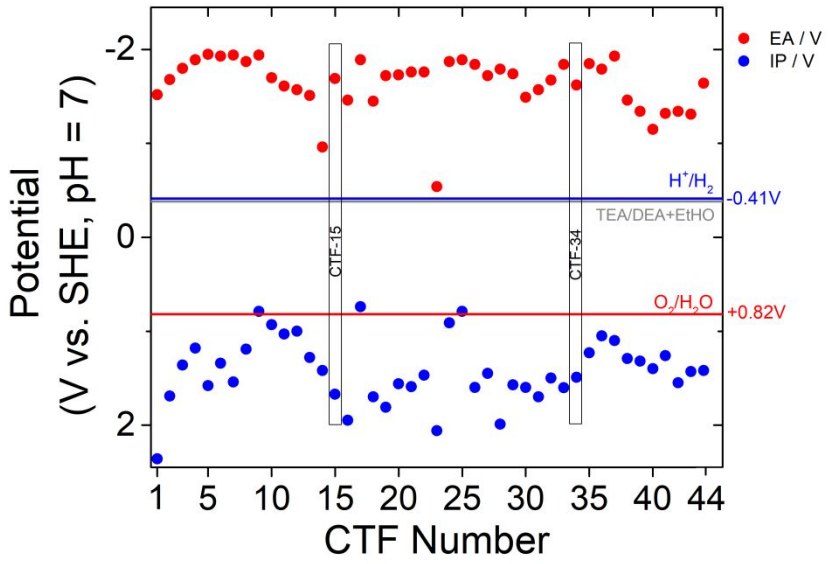

Figure S-124: Predicted values of EA and IP standard reduction potential for 40 CTFs investigated in this paper (CTF-5 to CTF-44 and comparison to CTF-1 to CTF-4 from the previous work[1]. All potentials are calculated for pH = 7 and a relative dielectric permittivity of 80.1 (water). The calculated standard reduction potentials of proton reduction (blue line), water oxidation (red line) and triethylamine oxidation (grey line) are showed for clarity.

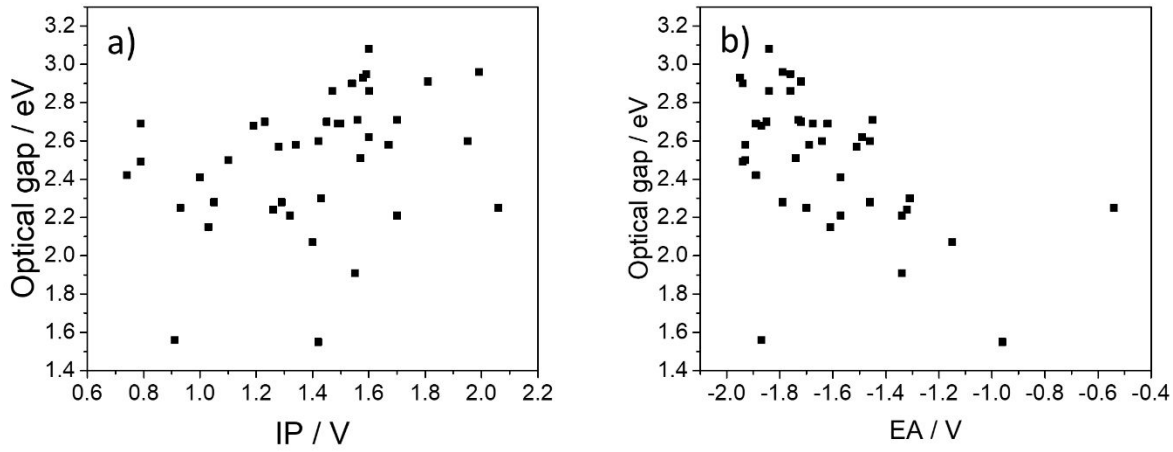

Figure S-125: Predicted values of IP a) and EA b) standard reduction potential compared to the optical gap of the CTFs.

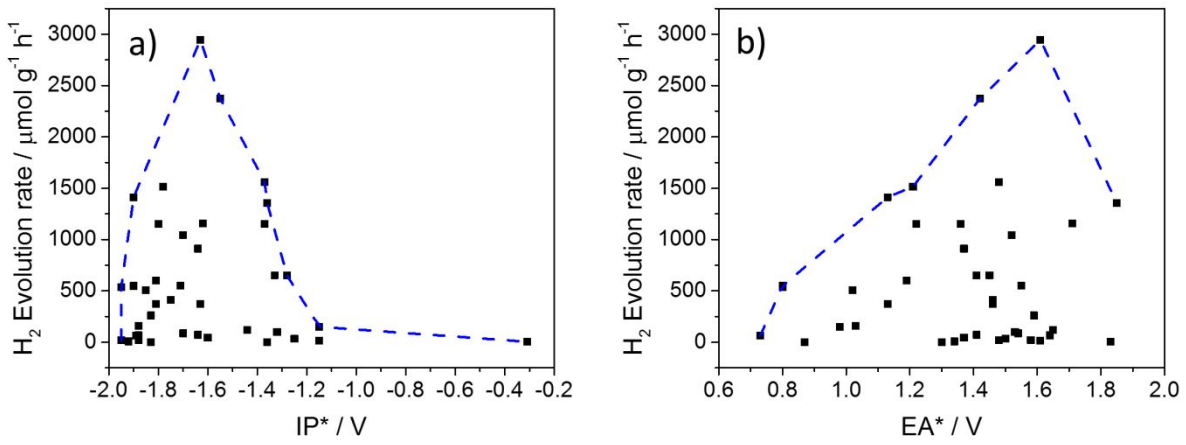

Figure S-126: Predicted values of IP* a) and EA* b) standard reduction potential compared to the hydrogen evolution rates of the CTFs. Conditions: 25 mg photocatalyst in water/TEA/MeOH and 3 wt. % platinum co-catalyst under visible light (λ > 420 nm, 300 W Xe light source).

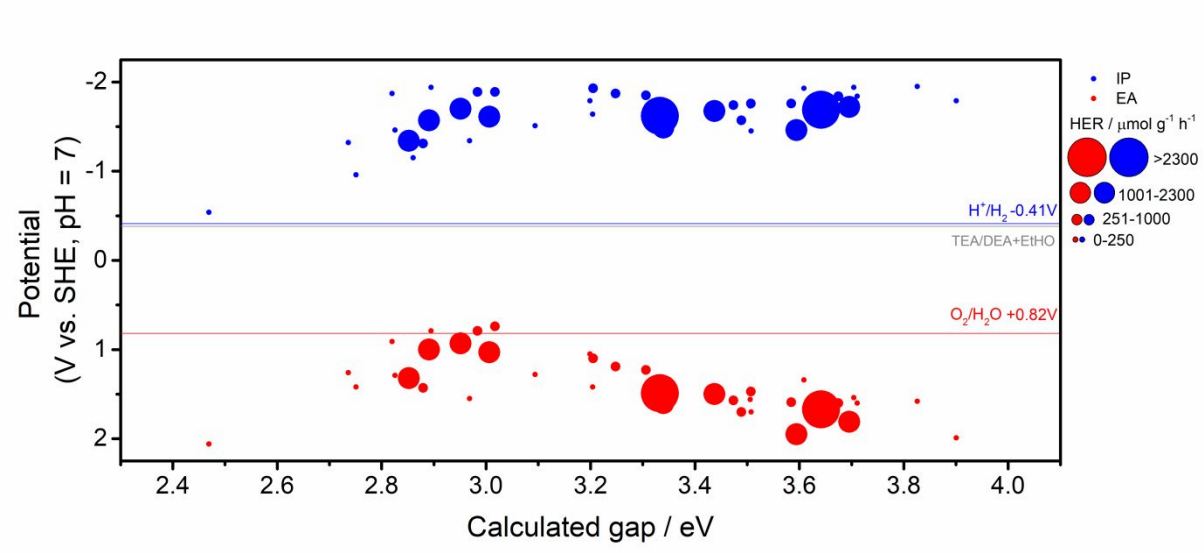

Figure S-127: Plot of the predicted values of the ionization potential (IP, blue) and electron affinity (EA, red) of the CTFs as a function of their predicted optical gap, where the circle size is proportional to the photocatalytic performance of the material. All hydrogen evolution rates were determined as linear fits of hydrogen produced over 5 hours for 25 mg photocatalyst in water/TEA/MeOH and 3 wt. % platinum co-catalyst under visible light (λ > 420 nm, 300 W Xe light source).

9. References

(1) Meier, C. B.; Sprick, R. S.; Monti, A.; Guiglion, P.; Lee, J.-S. M.; Zwijnenburg, M. A.; Cooper, A. I. Structure-Property Relationships for Covalent Triazine-Based Frameworks: The Effect of Spacer Length on Photocatalytic Hydrogen Evolution from Water. *Polymer* **2017**, *126*, 283–290.

(2) Liu, J.; Zou, J.; Yang, W.; Wu, H.; Li, C.; Zhang, B.; Peng, J.; Cao, Y. Highly Efficient and Spectrally Stable Blue-Light-Emitting Polyfluorenes Containing a Dibenzothiophene-S,S-Dioxide Unit. *Chem. Mater.* **2008**, *20*, 4499–4506.

(3) Krieble, V. K.; Noll, C. I. The Hydrolysis of Nitriles with Acids. *J. Am. Chem. Soc.* **1939**, *61*, 560–563.